Electron Spin Resonance: A Major Probe for Molecular Conductors

Claude Coulon* and Rodolphe Clérac

Centre de Recherche Paul Pascal, CNRS UPR 8641, Université Bordeaux 1, 115 Avenue Dr. A. Schweitzer, 33600 Pessac, France

Received March 9, 2004

Contents

* To whom correspondence should be addressed. Phone: (+33)-556 845650. Fax: (+33)556 845600. E-mail: coulon@crpp-bordeaux.cnrs.fr.

1. Introduction

During more than 30 years, intensive research has been devoted to organic conductors and superconductors. The main reason for this constant interest is certainly the large number of attractive results found over this long period of time. Several important steps can be emphasized. In the sixties, the synthesis of mixed valence planar platinium compounds such as $K_2Pt(CN)_4Br_{0.3}\cdot 3H_2O$ (often abbreviated as KCP)[1] revealed the importance of one-dimensional effects and the study of the first semiconducting organic salts incorporating the tetracyanoquinodimethane (TCNQ) molecule[2] demonstrated the possibility of preparing semiconducting organic solids. These materials are anion radical salts of paramagnetic TCNQ. Later, the synthesis of the tetrathiafulvalene (TTF) and other donor molecules allowed chemists to prepare both cation radical salts and charge-transfer salts incorporating cation and anion radicals in the same structure. In 1973, the synthesis of the first organic metal, TTF-TCNQ was reported.[3,4] Finally, the discovery of organic superconductivity in the tetramethyltetraselenafulvalene (TMTSF) series[5,6] was the starting point for a very active period where a large number of new materials based on TTF or TSF derivative molecules was synthesized.[7]

For each of these steps, Electron Spin Resonance (ESR) has played a major role. This can be easily understood if one realizes that ESR is observable in most of the organic conductors while very few "ordinary" metals show detectable ESR signals, even at low temperature. Indeed, this feature results principally from the electronic low dimensionality of these systems which controls the spins relaxation process.[8,9] As shown in the present review, this tendency is even reinforced by the fact that most organic molecules only contain light chemical elements for which the effect of the spin−orbit coupling on the ESR line width remains small. As a matter of fact, a commercial ESR spectrometer operating in X-band ($\approx$ 9.3 Ghz) is usually sufficient to study organic conductors, even on small single crystals. For this reason, electron spin spectroscopy is certainly a major probe to investigate the paramagnetic state of organic conductors. Moreover, the resonance signal can be still accessible when a magnetic order is present. This spectroscopy becomes hence an important tool to probe different magnetic ground states and, in particular, the antiferromagnetic (AF) state, most commonly found in organic salts. We will also see that a characteristic signature of the superconducting state can be obtained from ESR. For this reason, this

10.1021/cr030639w CCC: $48.50
Published on Web 09/16/2004

Claude Coulon was born in 1952 in Chatellerault, France. He is a graduate of the Ecole Normale Supérieure de Saint-Cloud and of the University of Paris Sud (Orsay). He got a position in the Centre National de la Recherche Scientifique in 1977 and became a Professor at the Ecole Nationale Supérieure de Chimie et Physique de Bordeaux in 1997 and at the University Bordeaux I in 1999. He received his Ph.D. degree in Bordeaux in 1982 under the supervision of Dr P. Delhaès. His doctoral work was mostly devoted to the electronic instabilities in several series of molecular conductors. In 1984, during his postdoctoral stay in the IBM Research Laboratory in San Jose (U.S.A.), he started a systematic study of the antiferromagnetic resonance of Bechgaard salts. This work was latter developed in Bordeaux and was awarded by the "Grand prix IBM France" in Material Science in 1990. He has also been involved in several research projects concerning "soft matter", including phase transitions in liquid crystals and the study of sponge phases for diluted solutions of surfactant. His current research interests are electronic properties of fullerene salts and the behavior of one-dimensional molecular magnets also called single-chain magnets.

Rodolphe Clérac, born in 1971 in Versailles (France), received his education at the University of Bordeaux 1, France. His Ph.D. work was devoted to the physical properties of molecular antiferromagnetic materials under the supervision of Prof. C. Coulon. His postdoctoral work dealt with the magnetic properties of coordination chemistry based materials with Prof. K. R. Dunbar at Michigan State University (East Lansing, Michigan, U.S.A.) and then at Texas A&M (College Station, Texas, U.S.A.). During this second part of his postdoctoral stay, he worked also with Prof. F. A. Cotton on the magnetic properties of metal–metal bonded complexes. He joined the University of Bordeaux 1 in 2000, as "Maître de Conférence". Since 2000, Prof. C. Coulon and Dr. R. Clérac have developed at the Centre de Recherche Paul Pascal (CNRS) a new research team interested in the "molecular magnetic materials" including the synthesis and physical studies of new magnetic materials based on transition metals and C_{60}. In this group, Dr. R. Clérac is working on the magnetic properties of hybrid magnetic materials (liquid crystals, gels, and nanocomposites), molecule-based magnets (including single-molecule magnets and single-chain magnets), and fullerene salts.

review will be divided into three parts: (i) a review of ESR studies in the paramagnetic state, following the main steps of the research on molecular conductors. For clarity, we will also include in this part the description of other electronic ground states for which no internal magnetic field is present. This is for example the case of diamagnetic ground states observed in Spin-Peierls phases or in TCNQ salts exhibiting triplet excitons; (ii) a presentation of the electronic resonance studies in magnetically ordered states exhibiting internal magnetic fields, in particular to describe antiferromagnetic resonance (AFMR); (iii) a short description of the ESR in superconducting states. Each of these three parts will be introduced by a brief summary of the theoretical arguments essential to understand the experimental results.

Because of the impressive number of published papers, it becomes extremely difficult, at least for ESR studies in the paramagnetic state, to give an exhaustive description of the literature. We have rather focused our review on selected topics to emphasize the information obtained from ESR. For the same reason, we have limited our report to materials where the spin is located on an organic center. Finally, we have also included data concerning fullerene salts to emphasize the analogy with other molecular conductors. A recent review is available for readers interested by a more general presentation of fullerene salts.[10]

2. Electron Paramagnetic Resonance (EPR)

2.1. Basic Ideas

The development of microwave techniques during the Second World War led in 1945 to the first observation of electron spin resonance. In 1952, the paramagnetic resonance absorption in a metal has been observed for the first time by Griswold, Kip and Kittel.[11] A typical EPR resonance absorption is shown in Figure 1a. Apart from the detailed analysis of the line-shape, three main characteristics can be deduced from this signal:

- the resonance field corresponding to the maximum of the absorption;
- the line width which should be analyzed in relation with the spin relaxation process;
- the area below the absorption signal which is proportional to the number of spins and therefore to the static (spin) susceptibility. This characteristic, not specifically obtained from the EPR (it can also be deduced by static measurements), will not be discussed in this paragraph.

We will thus successively discuss the determination of the resonance field and the theory of the line width.

2.1.1. The Resonance Condition

To deduce the resonance condition, a classical approach can be used, ignoring the relaxation process.[12] Consider an electron of angular momentum $\hbar\boldsymbol{S}$, its magnetic moment is $\mathbf{M} = -\gamma_e\hbar\mathbf{S} = -g\mu_B\mathbf{S}$ ($\mathbf{S}$ is in units of $\hbar$, γ_e is the magnetogyric ratio, μ_B is the Bohr magneton equal to $|e|\hbar/2mc$ in CGS units). For this free electron (i.e., for a spin 1/2 in a vacuum), quantum electrodynamics shows that the g factor is

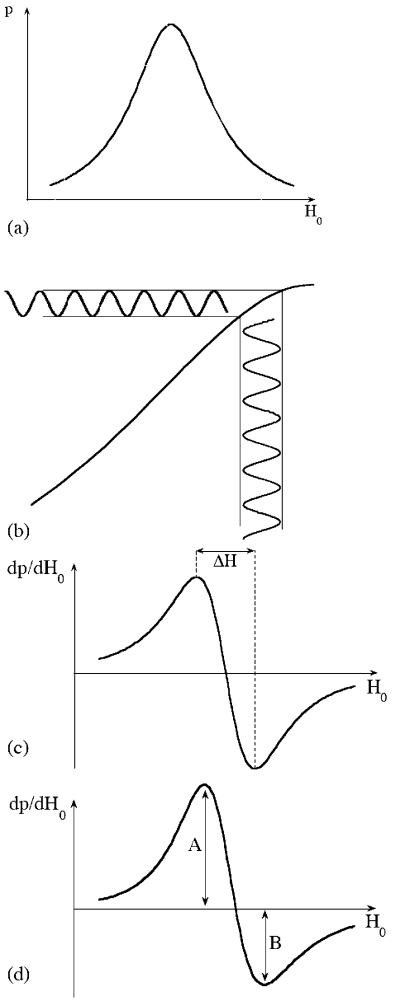

Figure 1. (a) Microwave absorption line. $\mathbf{H}_0$ is the applied magnetic field and p the microwave absorption. (b) Detection of the resonance signal using a lock-in technique: the applied field is modulated at a given frequency (x axis), the corresponding modulated signal (y axis) is then amplified. (c) Derivative of the absorption signal obtained from the lock-in technique. (d) Typical Dysonian resonance line.

2.0023. The starting point is then the dynamic equation of $\mathbf{S}$ in an applied magnetic field $\mathbf{H}$:

$$\hbar\frac{\mathrm{d}\mathbf{S}}{\mathrm{d}t} = \mathbf{M} \times \mathbf{H} \tag{1}$$

To realize the experimental setup, the applied field should be the sum of a static field ($\mathbf{H}_0$) applied along the z direction and of a time dependent ($\mathbf{H}_{MW}$) component applied in the plane perpendicular to z. The frequency of the microwave field for the most commonly used X-band is about 9.3 GHz. When both $\mathbf{H}_0$ and $\mathbf{H}_{MW}$ are present, eq 1 becomes

$$\frac{\mathrm{d}\mathbf{M}}{\mathrm{d}t} = -\mathbf{M} \times \gamma_e\mathbf{H} = -\mathbf{M} \times \gamma_e(\mathbf{H}_0 + \mathbf{H}_{MW}) \tag{2}$$

From this equation, it is easy to deduce that the equilibrium solution $\mathbf{M}_{eq}$ is parallel to $\mathbf{H}$, whereas the evolution of $\delta\mathbf{M} = \mathbf{M} - \mathbf{M}_{eq}$ is readily obtained assuming that $\mathbf{H}_{MW}$ is weak allowing the linearization of eq 2. Therefore, the linear response of the system is described by

$$\frac{\mathrm{d}\delta\mathbf{M}}{\mathrm{d}t} = -\delta\mathbf{M} \times \gamma_e\mathbf{H}_0 - \mathbf{M}_{eq} \times \gamma_e\mathbf{H}_{MW} \tag{3}$$

Taking $\mathbf{H}_{MW} = h\mathrm{e}^{i\omega t}\mathbf{x}$ and $\delta\mathbf{M} = \mathbf{m}\mathrm{e}^{i\omega t}$ gives

$$\frac{i\omega}{\gamma_e}m_x = -H_0 m_y \tag{4}$$

and

$$m_x = \frac{M_{eq}H_0}{H_0^2 - \frac{\omega^2}{\gamma_e^2}}h \tag{5}$$

Equation 5 shows the occurrence of a resonance when $\omega = \pm\gamma_e H_0$; or $\hbar\omega = \pm g\mu_B H_0$. This is nothing but the Larmor frequency introduced by Larmor in 1904. Equation 4 gives the polarization of the mode, i.e., gives $m_x = \pm i m_y$ at the resonance, indicating a circular polarization.

To conclude this presentation, let us mention that eq 5 allows the definition of a response function also called dynamic susceptibility

$$\chi_{xx} = \frac{m_x}{h} = \frac{M_{eq}H_0}{H_0^2 - \frac{\omega^2}{\gamma_e^2}} \tag{6}$$

As no relaxation term was introduced, this susceptibility diverges at the resonance. This means that the dynamic eq 3 has a nonvanishing solution at the resonance even when H_{MW} goes to zero. In other words, the resonance frequency can also be found as an eigenvalue of

$$\frac{\mathrm{d}\delta\mathbf{M}}{\mathrm{d}t} = -\delta\mathbf{M} \times \gamma_e\mathbf{H}_0 \tag{7a}$$

or, adopting a matricial representation, with $\delta\mathbf{M} = \mathbf{m}\mathrm{e}^{i\omega t}$, and for $\mathbf{H}_0$ parallel to z

$$\begin{pmatrix} i\omega/\gamma_e & H_0 & 0 \\ -H_0 & i\omega/\gamma_e & 0 \\ 0 & 0 & i\omega/\gamma_e \end{pmatrix}\begin{pmatrix} m_x \\ m_y \\ m_z \end{pmatrix} = 0 \tag{7b}$$

Apart from the trivial solution, $\omega = 0$ (which corresponds to m along z), we find $\omega = \pm\gamma_e H_0$ and $m_x = \pm i m_y$. This is in fact the most direct way to obtain the resonance frequency and the mode polarization. As we will see in section 3, this matricial method can be generalized to find the characteristics of the resonance in the presence of a magnetic order.

The previous conclusions can also be obtained from a quantum mechanical description. In that frame, the static magnetic field $\mathbf{H}_0$ removes the degeneracy between the Zeeman sublevels corresponding to the different m_s values. The microwave field causes transitions between these sublevels and the transition probability has a sharp maximum when the resonance condition is satisfied.

2.1.2. g-Factor Theory Applied to Molecular Conductors

In organic conductors, like in any solid, the g factor becomes a second-rank tensor. The specificity of these

Table 1. Selection of Single Crystal *g* Values along the Principal Magnetic Directions[a]

	g_{min}	g_{int}	g_{max}	ref
TCNQ	2.0020	2.0027	2.0032	82, 169b
TTF	2.0020	2.0074	2.0145	108, 115
TMTTF	2.0021	2.0090	2.0110	82
tTTF	2.0022	2.0070	2.0100	145
DMCTTF	2.0020	2.0085	2.0105	190
BCPTTF	2.0023	2.0079	2.0118	188
BEDT-TTF (a)	2.0023	2.0067	2.0116	221
(b)	2.0020	2.0065	2.0145	208
TMTSeF (c)	1.994	2.036	2.047	129
(d)	1.989	2.027	2.043	129
DMCTSeF	1.995	2.037	2.042	190

[a] In the BEDT-TTF and TMTSeF case, the weak effect of the radical environment is shown, comparing two different salts: (a) $(BEDT\text{-}TTF)_2AsF_6$, (b) $(BEDT\text{-}TTF)^{\bullet+}(Re_6Se_6Cl_9)^-\text{-}(C_3H_7ON)_2$, (c) $(TMTSeF)_2NO_3$, (d) $(TMTSeF)_2PF_6$. Note also that the substitutions on the TTF backbone to obtain TMTTF, tTTF, DMCTTF, or BEDT-TTF have a small effect on the g eigenvalues, the largest effect being found for g_{max} (this is particularly true in the BEDT-TTF series).

organic materials lies on the fact that the three components of this tensor are always close to the free electron value. The molecular π orbitals of these radicals are usually built by the linear combination of p_z orbitals (mostly of carbon and chalcogen atoms) although there is a significant contribution of d orbitals when selenium is present.[13,14,15] In that case, the components of the *g* tensor can be obtained by a perturbation theory, following the A. J. Stone's theory[12,16]

$$g_{\alpha\alpha} = g_e - 2\sum_n \sum_{\mu,\nu} \frac{\langle\psi_0|\zeta_\mu l_{\alpha\mu}|\psi_n\rangle\langle\psi_n|l_{\alpha\nu}|\psi_0\rangle}{E_n - E_0} \quad (8)$$

where $\alpha = x$, y, or z, g_e is the free electron value, ψ_0 is the molecular orbital which is single occupied molecular orbital (SOMO), and ψ_n denotes one of the doubly occupied or unoccupied orbitals. E_0 and E_n are the energies of these orbitals, ζ_μ is the spin−orbit coupling for the atom μ and $l_{\alpha\mu}$ is the α component of the orbital angular momentum operator for the atom μ. Equation 8 shows that the *g* tensor is essentially in that case a characteristic of the radical ion. Eigendirections can be deduced from the molecular symmetry, whereas corresponding eigenvalues reveal the nature of the molecular orbitals. For example, for a planar molecule like TTF, eigendirections are respectively along the short and long axis of the molecule and perpendicular to the molecular plane.[17] In this latter case, the molecular orbitals being obtained as a linear combination of p_z atomic orbitals of C and S atoms, the corresponding eigenvalue remains very close to g_e (see Table 1). On the other hand, the molecular orbitals of the selenium analogue (TSF) incorporate Se 4d orbitals leading to three eigenvalues significantly different from g_e.

Finally, as rotation patterns are often taken on single crystals, we should note that rotating the applied magnetic field in a given plane, the theoretical *g* value variation is very simple. Let us call (x, y, z) the eigendirections of the g tensor. When the static magnetic field is applied along the unitary vector $u = (u_x, u_y, u_z)$, general algebra on second rank tensors gives

$$g_u = \sqrt{g_x^2 u_x^2 + g_y^2 u_y^2 + g_z^2 u_z^2} \quad (9a)$$

However, considering that eigenvalues of the *g* tensor remain very close to 2, an approximate expression can be used

$$g_u = g_x u_x^2 + g_y u_y^2 + g_z u_z^2 \quad (9b)$$

This result indicates that rotation patterns in any plane will give a $\cos^2(\theta)$ dependence. For example, for $u_x = \cos(\theta)$, $u_y = \sin(\theta)$, and $u_z = 0$, one obtains

$$g(\theta) = g_x \cos^2(\theta) + g_y \sin^2(\theta) = g_y + (g_x - g_y)\cos^2(\theta) \quad (9c)$$

2.1.3. Introducing the Spin Relaxation

To account for the finite line width of the resonance signal, it is necessary to consider relaxation effects. This means that eq 2 should be generalized. A first macroscopic approach was proposed in 1946 by Felix Bloch[18]

$$\frac{dM_z}{dt} = -(\mathbf{M} \times \gamma_e \mathbf{H})_z + \frac{M_{eq} - M_z}{T_1} \quad (10a)$$

and, for $\alpha = x$ or y

$$\frac{dM_\alpha}{dt} = -(\mathbf{M} \times \gamma_e \mathbf{H})_\alpha - \frac{M_\alpha}{T_2} \quad (10b)$$

Equations 10a and 10b are known as the Bloch equations. T_1 and T_2 are respectively the spin−lattice and the spin−spin relaxation times. The key assomption in the Bloch equations is that the magnetization decays exponentionally to reach the equilibrium. From these equations, the dynamic susceptibility and therefore the shape of the absorption EPR signal can be deduced. Far from the saturation, i.e., for weak applied microwave fields, the microwave absorption can be written[12]

$$p(\omega) = \frac{I_0}{(\omega - \omega_0)^2 + (1/T_2)^2} \quad (11)$$

i.e., a Lorenztian line with a $1/T_2$ line width, still centered at ω_0 (at the Larmor frequency). Note that the corresponding line width in field units becomes $1/\gamma_e T_2$. It should be noted that the Lorenztian frequency dependence can be deduced after a Fourier transform from the time dependence of the spin−spin correlation function which as expected decays exponentially.

A more detailed analysis requires a microscopic description of the spin relaxation process. The interaction of a given spin with its environment can be described as a time dependent local magnetic field. This fluctuating field is responsible for the electronic spin relaxation. One important aspect of the problem in metals is motional narrowing, i.e., the effect of the motion of the spin on the resulting line width.[19]

Another important parameter is the nature of the dominant spin relaxation process. This question is well documented in traditional metals where the spin−lattice coupling is dominant. The scattering Hamiltonian induces transitions between electronic states of different momentum with or without spin-flip. Both processes are simply related and this implies a simple law, called Elliot relation[20]

$$\frac{1}{T_2} = (\Delta g)^2 \tau^{-1} \tag{12}$$

where τ is the electron relaxation time also measured by the electrical resistivity and $\Delta g = g - g_e$. Therefore, when the Elliot relation is followed, the EPR line width is proportional to the electrical resistivity. At this point, three additional remarks should be made. First, although the above description of the resonance (eq 11) suggests to use frequency scans, it is experimentally easier to fix the frequency (for example 9.3 GHz for X band) and to realize scans of the magnetic field $\mathbf{H}_0$. Moreover, as the detection of the resonance signal uses a lock-in technique ($\mathbf{H}_0$ is modulated as shown in Figure 1b) the derivative of the absorption signal is obtained (Figure 1c). These technical points explain why the line width (ΔH) is most commonly given as the peak to peak value of the derivative signal, in magnetic field units. Finally, it should also be noted that skin effect in highly conducting materials modifies the EPR line-shape. In that case, a Dysonian line is observed (Figure 1d) with an asymmetry (A/B) related to the electrical conductivity of the material.[21,22]

2.1.4. EPR Linewidth of Low-Dimensional Systems

The situation in organic conductors may be different from that in 3D metals. Several examples given in the following will show that the Eliott relation is usually not satisfied for organic conductors. For example, the temperature dependence of the EPR line width and electrical resistivity may vary in opposite ways. The reason is the singular topology of the 1D Fermi surface which is reduced to two points, imposing that both forward and backward scattering do not give spin relaxation.[8] Then, some departure from strict one-dimensionality is necessary to obtain a finite EPR line width and the role of interchain electron tunneling is crucial. Several empirical generalizations of the Elliot relation have been suggested,[9,23,24] but the quantitative analysis of the EPR line width of organic conductors remains difficult. The effect of low dimensionality has been extensively studied for magnetic insulators. In nearly one-dimensional systems "inhibited-exchange narrowing" is predicted and observed.[25] In that case, the transverse magnetization decays no longer as an exponential but as $\exp(-(t/\tau)^{3/2})$. The line shape is then intermediate between a Gaussian and a Lorentzian and the anisotropy of ΔH does not follow the $\cos^2\theta$ dependence predicted by the standard theory. Instead, a $|3\cos^2\theta - 1|^{4/3}$ dependence is found. Similar arguments have been used for organic conductors. Motional narrowing results of the fluctuations of the dipolar field seen by a spin moving from site to site. This process is less efficient in quasi-one-dimensional systems and the EPR line width can be either dipolar or spin-phonon according to the magnitude of the interchain coupling. Therefore, non-Lorentzian line-shapes can also be observed in strongly anisotropic organic conductors.[26] Several experimental confirmations of this singular behavior have been reported.[27,28,29,30]

2.1.5. Composite EPR Signals

Several magnetic nonequivalent species may coexist in a single crystal. This is the case when several orientations of the same radical are present in the crystal structure but also when a donor and an acceptor (each of them bearing a spin) coexist. In these situations, the EPR signal results from all individual magnetic species. Two extreme cases should be considered depending on the magnitude of ν_{12}, the hopping rate between the two nonequivalent species:

- two separated signals should be observed in the "weak coupling limit", i.e., when $\nu_{12} \ll |\nu_1 - \nu_2|$, where ν_i is the Larmor frequency of the species i.[12,31] This situation can easily be observed for quasi-1D structures if the magnetic species are located on different chains and if the interchain hopping rate is weak. This is the case for TTF halides[23] or for several TCNQ salts, as described in the next sections.
- A single EPR line is observed in the "strong coupling limit", when $\nu_{12} \gg |\nu_1 - \nu_2|$, with a g factor and a linewitdh which are the result of a weighting between the characteristics of each magnetic species,[12,31] namely

$$g = \alpha g_1 + (1 - \alpha) g_2 \tag{13a}$$

and

$$\frac{1}{T_2} = \alpha \frac{1}{T_{2,1}} + (1 - \alpha) \frac{1}{T_{2,2}} \tag{13b}$$

where g_i and $T_{2,i}$ are the intrinsic characteristics of the species i, and $\alpha = \chi_1/(\chi_1 + \chi_2)$, where χ_i is the spin susceptibility of the species i. This kind of behavior will be described for TTF-TCNQ and related compounds in section 2.3.

Moreover, EPR experiments are sometimes performed on powder samples. In that case, even if there is a single molecular orientation for a single crystal, the powder spectrum is necessarily an average on all the possible field orientations. A complex signal is generally obtained as both the g factor and line width are dependent on the field orientation. Examples of powder spectra are given in Figure 2.

In the cases shown in Figure 2, single-crystal EPR measurements give Lorentzian signals and the structure of the powder signal should not be interpreted as resulting from the presence of several nonequivalent magnetic species in the material. This last remark emphasizes the importance of single-crystal EPR measurements providing simpler discussions of the experimental results.

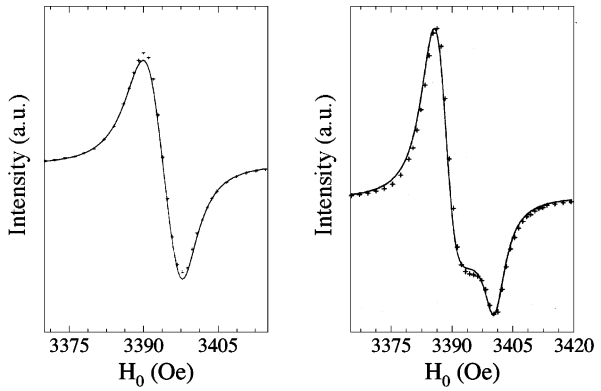

Figure 2. (left) Powder EPR spectrum of TTF-TCNQ at room temperature and (right) powder EPR spectrum of $(TMTTF)_2SCN$ at room temperature. Solid lines are calculated spectra obtained from single crystals data. It is worth noting that the structure of the resonance line is emphasized when the line width for a given orientation is of the same order or even smaller than ΔH_0, average of the variation of the resonance field during a rotation of the crystal (as it is the case for $(TMTTF)_2SCN$). (C. Coulon, *unpublished results*).

2.2. Early Studies of TCNQ Salts

A large number of organic salts incorporating TCNQ have been prepared.[2] For some of them, the TCNQ radical anions are organized into stacks, which can be mixed or segregated, regular or composed of diads, triads, etc. The general trend in these materials is to observe a semiconducting behavior. This characteristic can be explained considering the importance of on-site Coulomb interactions, at least of the same order of magnitude as the one-electron bandwidth. The resulting electron localization is even reinforced by the low dimensionality of these compounds.

2.2.1. Triplet Exciton in TCNQ Salts

Many TCNQ salts have a singlet (i.e., nonmagnetic) ground state. As a consequence, the magnetic susceptibility is activated and the EPR signal has been attributed to a thermally accessible triplet state.[32−34] After this pioneer work of Chesnut et al., a large number of results have been obtained in various TCNQ or related salts.[35−57] Rather than localized triplet states, the magnetic excitations should be described as triplet excitons delocalized over several TCNQ molecules. As a consequence, the triplet spin density sees a randomly changing nuclear spin environment and no hyperfine structure can be observed. In this case, a specific EPR signal composed of three lines is observed in an intermediate range of temperatures. The intensity of the two side-lines decreases at low temperature, whereas the whole fine structure collapses into a single narrow line at high temperature. This typical evolution of the EPR signal is illustrated in Figure 3.

To understand these spectra, let us introduce the effective spin Hamiltonian relevant for a triplet state, ignoring the hyperfine interaction

$$H = \mu_B \mathbf{S}\cdot\mathbf{g}\cdot\mathbf{H} + D(S_z^2 - \mathbf{S}^2/3) + E(S_x^2 - S_y^2) \quad (14a)$$

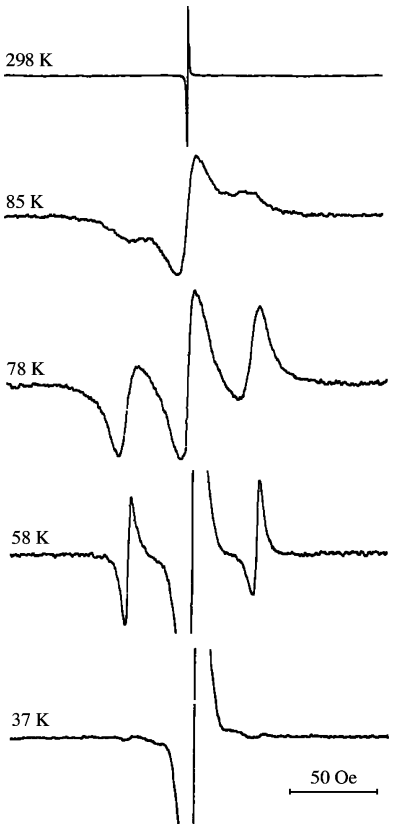

Figure 3. Temperature dependence of triplet exciton EPR spectra in a single crystal of $(TEA)(TCNQ)_2$ for an arbitrary orientation, showing the collapse of the fine structure. The sweep, but not the gain, is the same for all five spectra. Adapted from ref 48.

where D and E are the dipolar splitting parameters. The last two terms can be written in a tensorial form, introducing the dipolar splitting tensor $\mathbf{\Lambda}$

$$H = \mu_B \mathbf{S}\cdot\mathbf{g}\cdot\mathbf{H} + \mathbf{S}\cdot\mathbf{\Lambda}\cdot\mathbf{S} \quad (14b)$$

The presence of the dipolar splitting tensor implies that the degeneracy of the triplet levels is lifted, even in zero field. Figure 4 illustrates the effect of the dipolar term when the magnetic field is applied along the z direction.

The EPR spectrum is composed of two lines separated by a field interval proportional to D. More generally, the study of rotation patterns in the simple planes allows the diagonalization of the dipolar splitting tensor and the determination of D and E. A collection of experimental data for various TCNQ salts can be found in refs 35 and 58. Typical values range from 40 to 150 Oe for D and from 15 to 25 Oe for E when TCNQ molecules are organized into chains. Larger values are found when the triplet exciton is localized on a quasi-isolated dimer.[53] The comparison with calculations is not so simple as calculated values strongly depend on the molecular spin density. Moreover, the intensity of both side-lines follows an activated law which gives the singlet−triplet gap (Δ). If the spectrum is still detectable at low enough temperature, the intensity difference between these two lines gives the sign of D and E (Figure 4). Moreover, as the dipolar term mixes the

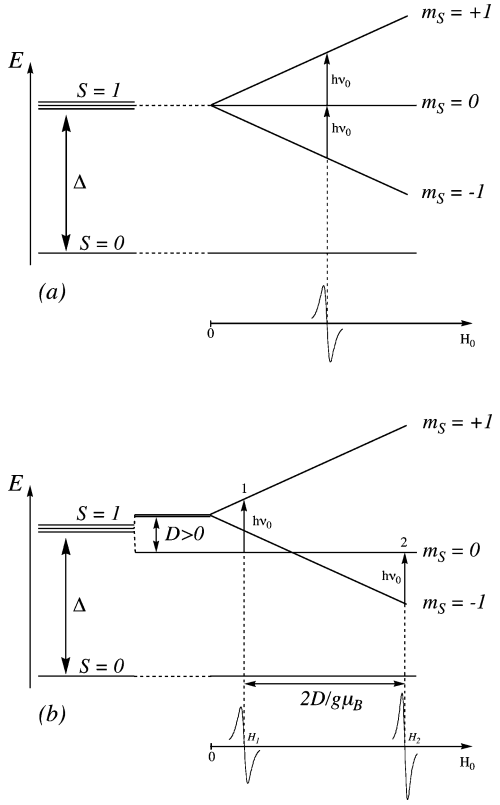

Figure 4. Effect of the dipolar term on the EPR spectrum: (a) when $D = 0$, a single resonance line is observed and (b) when $D > 0$ a set of two resonance lines is observed separated by $2D/g\mu_B$. A similar effect would be observed for $D < 0$, with the strongest line at low field. Note that for clarity the splitting due to the D parameter has been exaggerated in (b).

$m_S = +1$ and $m_S = -1$ sublevels, a weak signal, due to the previously "forbidden" $\Delta m_S = 2$ transition, is predicted and observed at approximately half of the resonance field.[33]

The above simple description explains the existence of two resonance lines but does not account for the central one shown in Figure 3. This so-called "impurity signal" has been found in many TCNQ salts[59] with the typical g value of the TCNQ anion. This central signal can be usually decomposed into two lines presenting different temperature behaviors.[35] One of them follows a Curie law, indicating isolated magnetic centers while the intensity of the other is thermally activated, with an activation energy smaller than Δ. To explain this difference, a contribution of solitons has been invoked.[60]

In several materials, the complex crystal structure implies independent orientations of the TCNQ ions. The result is the presence of several pairs of exciton lines and of complex rotation patterns. However, these lines are usually separated and EPR becomes a very powerful technique to obtain the different sets of dipolar splitting parameters.[43,58]

The temperature dependence of the EPR line width also provides information on the dynamics of triplet excitons. They were found to be diffusive and hopping activation energies can be deduced.[34,44] The dynamics of the excitons has also been studied under pressure.[61]

2.2.2. Peierls-Like Phase Transitions in TCNQ Salts

An important domain where EPR is very useful is the detection and study of phase transitions. In particular, considerable interest has arisen for the Spin-Peierls transition as observed in MEM-$(TCNQ)_2$ (where MEM stands for methyl-ethyl-morpholinium).[62] The mechanism of this instability is directly related to the low dimensionality of the spin network. The name "Spin-Peierls" has been given by reference to the so-called Peierls transition observed in quasi-1D metal as TTF-TCNQ (see next section). Starting from a quasi-1D model of exchange-coupled spins, introduction of the spin-phonon coupling allows an elastic distortion of the lattice, stabilizing a new magneto-elastic order at low temperature.[63] Starting from TCNQ dimers, this phase transition corresponds to a tetramerization in the TCNQ chains and opens a gap in the spin excitation spectrum. Therefore, the Spin-Peierls instability drives the system into a diamagnetic ground state. The temperature-dependent magnetic gap is revealed by the magnetic susceptibility and triplet excitons can be detected.[64,65] However, the system remains close to the uniform limit (i.e., to a uniform stacking of dimers) and most of the spins contribute to the central line, whereas the dipolar splitting is fairly small. A series of parent compounds of MEM-$(TCNQ)_2$ have been studied by changing slightly the nature of the donor molecule.[65] In particular, the phase transition observed in the dimethyl-morpholinium (DMM) salt has been interpreted as a Spin-Peierls instability but with a spatial modulation of the dimerisation order parameter.[66,67] High field EPR studies also suggest the modulation of the magnetic moment in the so-called M phase.[68] Another surprising result obtained in this series of salts is the "Schwerdtfeger effect".[69,70] This effect appears in TCNQ salts with nonparallel chains. These salts are in the weak coupling limit (see paragraph 2.1.5.) and two separated EPR signals are obtained, attributed to the two different TCNQ orientations in the crystal. Although the *total* spin susceptibility remains isotropic, *individual* spin susceptibilities change during rotation figures, in such a way that the low field line in always the most intense. As far as we know, no clear explanation of this phenomenon has been provided.

Other structural instabilities have been observed corresponding to diamagnetic to paramagnetic phase transitions. Their mechanism may not be strictly similar to the one of the Spin-Peierls instability found in MEM-$(TCNQ)_2$ even if the electronic low dimensionality may be also relevant. Many of these instabilities were however called Spin-Peierls or generalized Spin-Peierls transitions although they may be strongly first order or occurring at high temperature.[71−74] In fact, this situation is even more complicated considering that the characteristics of the Spin-Peierls transition can be different for TCNQ salts[75] and other organic conductors (see section 2.4.).[76]

To conclude this paragraph, let us take an example illustrating the relevance of EPR to study this type of electronic phase transitions. A series of ternary compounds have been synthesized with TCNQ, iodine and different ammonium cations.[77] The prototype salt

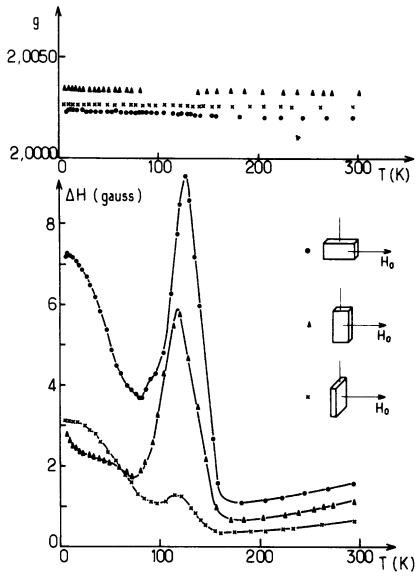

Figure 5. Temperature dependences of line width and *g* factor principal components for TMA-TCNQ-I. (Reprinted with permission from ref 83. Copyright 1985 EDP Science.)

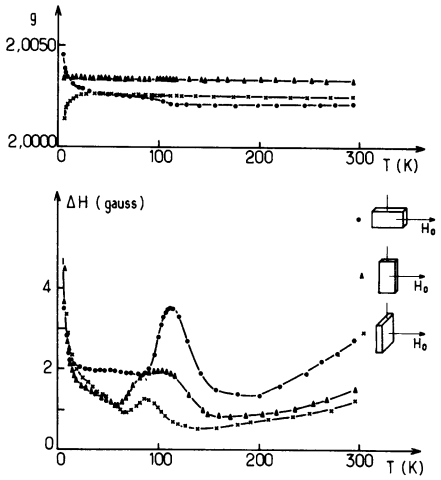

Figure 6. Temperature dependences of line width and *g* factor principal components for IPentDMA-TCNQ-I. (Reprinted with permission from ref 83. Copyright 1985 EDP Science.)

is TMA-TCNQ-I where TMA stands for the trimethylammonium cation.[78,79] This salt presents a phase transition at $T_c = 150$ K associated with a strong electronic localization and the appearance of gap in the spin susceptibility. At T_c, cristallographic data show the condensation of a superstructure.[80,81] This structural phase transition was systematically observed in the series, when changing the nature of the cation. In a band-structure description, the periodicity of the superstructure corresponds to the opening of a gap at the Fermi level. Consequently, this phase transition has been described as a "Peierls-like" instability although precursors effects seen by X-ray above T_c remains weak and quasi-isotropic.[82,83]

Figures 5 and 6 present the EPR data for two members of the series. Besides the observation of the magnetic gap on the spin susceptibility, it is obvious from these figures that EPR brings many more information. For example, a clear increase of the line width is observed when the electronic localization occurs at T_c. In fact, the temperature behavior of the line width is complex in the insulating phase, revealing the existence of two other phase transitions. The locking between the charge density waves developed on the TCNQ chains and the counterions potential has been evoked to explain low-temperature EPR and X-ray data.[81−83] An analogy can also be made between the temperature dependence of the line width of these salts and the one found for some TMTTF salts (SbF_6 or SCN salts for example) where a charge ordering is known to occur (see paragraph 2.4). Nevertheless, in the present series, no clear experimental evidence has been found to suggest such a scenario. Finally, it should be noted that the *g* factor for the IPentDMA (Isopentyl-dimethylammonium) salt becomes temperature dependent at the lowest investigated temperatures. As we will see in paragraph 2.4, this result is usually the sign of magnetic fluctuations. However, no long-range magnetic order has been found in this series of materials. Short-range antiferromagnetic order has also been revealed by magnetic measurements in the *N*-methyl-phenazinium (NMP)[84,] or quinolinium (Qn) salts.[85,86] In $Qn(TCNQ)_2$, disorder effects, most likely due to the cations, were evoked to explain the absence of long-range magnetic order. The low temperature dependence of the magnetic susceptibility follows a law in $T^{-\alpha}$ (with $\alpha \approx 0.8$) characteristic of a 1D random-exchange antiferromagnetic Heisenberg model.

2.3. TTF-TCNQ and Related Charge Transfer Salts

TTF-TCNQ and the family of charge transfer salts obtained by different substitution of the donor or of the acceptor molecule have been extensively studied.[87,88] EPR took a large place in this study in particular to quantify the respective role of the different stacks. In most of these materials, EPR experiments reveal a single resonance line indicative of the strong coupling between stacks as seen in paragraph 2.1.5. Experiments where two separated EPR lines can be detected remain rare and for TTF-TCNQ can be observed only at very low temperature.[89] It is worth noting that resolved EPR lines have also be reported in HMTTF-TCNQ[90] and HMTTF-$TCNQF_4$ (HMTTF stands for hexamethyl-TTF).[91] When a single EPR line is detected, eqs 13a and 13b have been used to separate the contribution of the donor and acceptor stacks.[92−99] Note that this *decomposition technique* implies that the line width is frequency independent as seen for TTF-TCNQ by Tomkiewicz et al.[93] Some frequency dependence of the EPR line width has however been reported later.[100] Figure 7 shows the susceptibility decomposition for TTF-TCNQ with the contribution of each kind of stacks and the total susceptibility which is consistent with the static result.[101] These data prove that a phase transition (described as a Peierls instability) first involves the TCNQ stacks at about 53 K while a gap is opened in the TTF susceptibility only at 38 K.[102] This finding is consistent with the occurrence of several successive phase transitions in this material[103] and with the determination of the local susceptibilities of each chains from the ^{13}C Knight shift.[104]

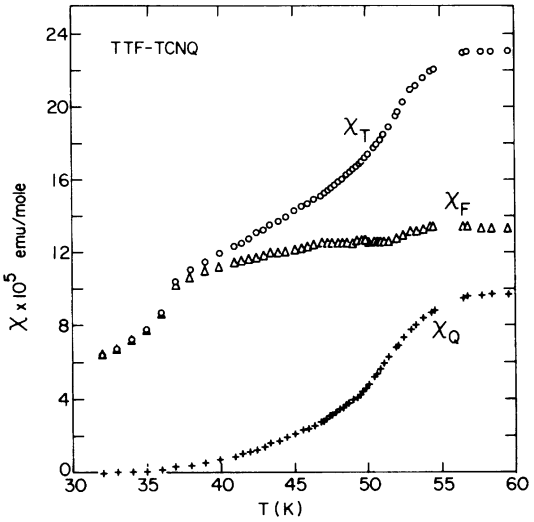

Figure 7. The total susceptibility χ_T and the susceptibilities of the donor and acceptor stacks respectively, χ_F and χ_Q as a function of the temperature for TTF-TCNQ. (Reprinted with permission from ref 102. Copyright 1980 D. Reidel.)

Another important result obtained by EPR in this series of materials is the analysis of the spin relaxation process. To show the relevance of the electron−phonon coupling, an isostructural family $(TSeF)_x(TTF)_{1-x}(TCNQ)$ has been studied (where TSeF is the selenium analogue of TTF).[105] In this series, the EPR line width varies from 5 to 500 Oe over the range $x = 0-1$. The spin-phonon relaxation mecanism is dominant and the line width should be proportional to $(\Delta g_D)^2$, where Δg_D is the deviation of the g factor of the donor stack from the free electron value (the much smaller value Δg_A for the TCNQ stacks has been neglected). In fact, the strong dependence with x is dramatically reduced by normalizing the line width by $(\Delta g_D)^2$. The remaining variation with x of the normalized line width has been interpreted as an anomalous dependence of the spin relaxation (i.e., of the spin-flip matrix). We will see in the next sections that a $(\Delta g)^2$ term quite generally enters in the expression of the EPR line width. In particular, selenium compounds have broader EPR lines than sulfur analogues. This is in agreement with eq 8 which implies that a larger Δg value is observed in the former materials because of the large spin−orbit coupling constant of selenium atoms.

Finally, it should be noted that many substitutions have been tried either on the TTF or on the TCNQ molecules to prepare new materials and to try to stabilize a conductor down to very low temperature or even an organic superconductor. Examples of EPR studies can be found for HMTTF-TCNQ,[98,106] TMTTF-TCNQ,[90,107] HMTTF-$TCNQF_4$,[91] TMTSeF-DMTCNQ,[96] and DEDMTTF-TCNQ (DEDMTTF stands for diethyl-dimethyl-TTF) which presents a line width angular dependence characteristic of 1D magnetic systems.[28] Note also that a comparison of EPR characteristics of several charge transfer and ion radical salts can be found in ref 108. Table 1 summarizes the principal values of the g tensor obtained with different anion and cation radicals. Some EPR

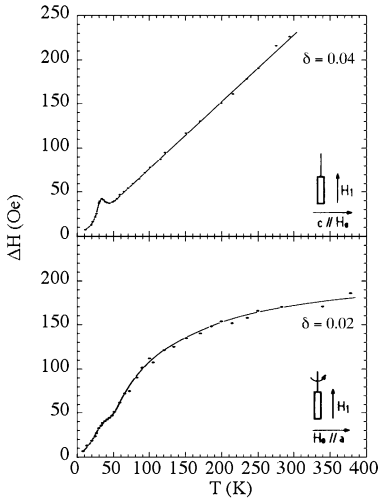

Figure 8. Line width of the ESR resonance line on two single crystals of $TTT_2(I_3)_{1+\delta}$ with two values of δ. Adapted from ref 118b.

studies under pressure have also been reported for these charge-transfer salts.[24,109,110]

Finally, it should be noted that other charge-transfer salts were synthesized in this period, using different donor molecules. Typical examples are TTT-TCNQ and TTT-$TCNQ_2$ (where TTT stands for tetrathiatetracene)[111,112] and the decomposition technique was also used to separate the susceptibility of each stack and discuss the observed Peierls instability.[113]

2.4. Cation Radical Salts Including Bechgaard and Fabre Salts

In the beginning of the 80s, the study of cation radical salts became more and more important. Several series of materials were synthesized, for example with TTF,[23,114−116] TTT,[117,118] TSeT[119,120] (where TSeT is the selenium analogue of TTT), or DIPSϕ_4 (tetraphenyldithiapiranylene).[121] Quite generally, incommensurate sublattices were observed, due to the complex stoichiometry of these salts. A consequence of the highly conducting state is the existence of ESR Dysonian lines in particular in the TTT salts.[118] As exemplified by the TTF salts, the components of the g tensor are characteristic of the ion radicals (see Table 1). On the other hand, the EPR line width and therefore the spin relaxation strongly depend on the nature of the counterions (see for example the comparison between $(TTF)_{12}(SCN)_7$ and $(TTF)_{12}(SeCN)_7$ in ref 116). Finally, it is interesting to note that a specific situation occurs for some TTT salts with peculiar stoichiometry, e.g., $(TTT)_2(I_3)_{1+\delta}$, where δ of the order of a few percents. Figure 8 illustrates the importance of δ on the EPR line width. This figure also shows that EPR is relevant to characterize the metal−insulator phase transition observed respectively at 43 and 29 K for these two samples.

These features seem to be closely related to the data obtained for TMA-TCNQ-I (Figure 5) or $(TMTTF)_2SCN$ and $(TMTTF)_2SbF_6$ (discussed in this section) suggesting that some charge localization may occur in $(TTT)_2(I_3)_{1+\delta}$. If the involved mechanism is

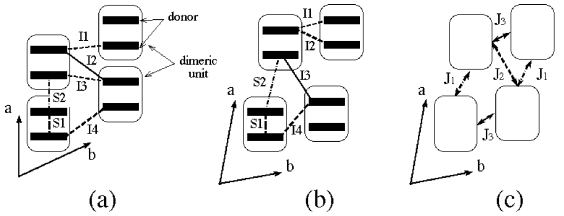

Figure 9. Schematic view of organic salt crystal structures. (a) Stacking observed in the TMTTF and TMTSeF series and referred as type I in the text. (b) Strongly dimerized structure referred as type II in the text. (c) Magnetic description of the structure shown in (b) in the strong coupling limit. Each dimer is described as an effective spin 1/2. These spins are coupled by exchange interactions J_i which can be estimated from the values of the transfer integrals shown in (b).

a Mott−Hubbard localization, this result would illustrate the importance of the stoichiometry on this instability, as predicted by the theory.[122]

Despites the high electrical conductivity obtained for some of the materials described above, these samples were rapidly supplanted by the cation radical salts incorporating TMTTF (tetramethyl-tetrathiafulvalene) or its selenium analogue, TMTSeF. These materials were at the origin of the major breakthrough in the field. By reference to the key role played by these two chemists, the TMTTF and TMTSeF salts are usually called Fabre salts and Bechgaard salts, respectively. After the pioneer work made by Wudl et al., who reported the first synthesis of TMTTF salts,[115,123] Fabre and co-workers described a more general study of the TMTTF series.[124] The first organic superconductors have been discovered with the synthesis of the selenium analogues.[125,126] Moreover, the preparation of high purity samples became possible for both sulfur and selenium salts with the electrochemical technique introduced in the field by Klaus Bechgaard. In this early period, several EPR studies were carried out, both on TMTSeF salts[127−132] and TMTTF salts,[82,133−135] but also on TMTTF/TMTSeF alloys.[136,137] A general signature of the EPR in these series of compounds is the decrease of the line width upon cooling the temperature whatever is the variation of the electrical conductivity.

More specific arguments can be given considering the crystal structure of these materials. In this review, we will not recall the structural data in details but rather focus on the stacking of cation radicals which is at the origin of the electronic properties. Figure 9 illustrates typical organizations of organic donor planes separated in the **c** direction by layers of counterions. The crystal structure of TMTTF or TMTSeF salts is schematized in Figure 9a showing the different transfer integrals. Because of the specific nature of their crystal structure composed of centro-symmetrical dimers, a torsional-oscillation-induced spin−orbit coupling has been evoked to account for the increase of the line width when $(TMTSeF)_2PF_6$ is doped with a small amount of $(TMTTF)_2PF_6$.[138,139] As already mentioned, the g factor of TMTSeF salts has been calculated and compared with experimental values to emphasize the role of d orbitals of selenium atoms.[14,15] ESR has also been used to study the effect of pressure[24] or irradiation[140,141] or to discriminate between the metastable state (obtained by fast cooling) and the stable state resulting of a slow cooling rate in $(TMTSeF)_2ClO_4$.[142] Moreover, ESR has been particularly useful to study the different phase transitions observed in this series of materials. In fact, TMTTF and TMTSeF salts present a wide variety of phase transitions, including anion ordering and electronic instabilities leading to Spin-Peierls, antiferromagnetic, or superconducting ground states. Note that the TMTSeF salts are generally highly conducting materials while a Mott localization is observed in most of the TMTTF salts at ambient pressure. These latter salts are therefore often taken as examples to illustrate the decoupling between charge and spin degrees of freedom which is expected in one dimension for correlated electrons.[122] ESR in magnetically ordered or superconducting states will be described in the next two parts; however, we must already mention that precursor effects can be characterized by EPR. Quite generally, short-range order becomes increasingly important approaching a second-order phase transition. In the case of a magnetic ordering, the magnetic correlations modify the environment of a given spin. The existence of a fluctuating local field leads to a specific temperature dependence of the g factor.[143] The spin-relaxation is also affected leading to a critical effect on the EPR line width. Close to the Néel temperature, T_N (antiferromagnetic ordering temperature), the g factor becomes strongly temperature dependent while the line width diverges such as $\Delta H \propto (T - T_N)^{-\mu}$. It has been shown theoretically that the critical exponent μ is equal to 1.5 in remarkable agreement with the experimental results.[144−146] We must mention a singular result, $\mu \approx 0.5$, found for $(TMTSeF)_2NO_3$.[147]

Various structural phase transitions have also been studied by EPR. First of them, anion orderings have been observed.[82,124,129,133,134,137] The influence of anion disorder in $(TMTSeF)_2BrO_4$,[148] the effect of alloying $(TMTSeF)_2ReO_4$ with ClO_4[149] and the electronic localization related to an incommensurate structural modulation in $(TMTSeF)_2SCN$[150] have also been reported. The study of the Spin-Peierls phase transition should also been mentioned. The superstructure and the X-ray diffuse scattering associated with this instability has been first reported in $(TMTTF)_2PF_6$.[151,152] This result emphasizes the importance of quasi-1D precursor effects which are also seen as a pseudo-gap on the spin susceptibility. This pseudo-gap predicted by the theory[153,154] has been observed for the AsF_6[155] and the PF_6[156] salts. The comparison with MEM-$(TCNQ)_2$ shows that the TMTTF salts exhibit a "true" Spin-Peierls transition triggered by one-dimensional fluctuations while an "unconventional" Spin-Peierls transition occurs in MEM-$(TCNQ)_2$ as described in paragraph 2.2.2.[76] Another important issue is the competition between the Spin-Peierls and the antiferromagnetic ground states.[157] EPR operating at low field (at a frequency of about 100 MHz) has been used to study the effect of pressure on the Spin-Peierls phase transition[154] and to conclude the existence of a universal phase dia-

gram where the Spin-Peierls ground state is first replaced by an antiferromagnetic ordering and finally by superconductivity as pressure increases (i.e. as electronic localization decreases). The whole sequence has been predicted theoretically[158] and reported for $(TMTTF)_2PF_6$.[159] Moreover, it should be mentioned that Spin-Peierls fluctuations sometimes exist above an antiferromagnetic ordering. This was suggested by EPR data on $(TMTTF)_2(SbF_6)_{1-x}(AsF_6)_x$ alloys[155,160,161] and $(TMTTF)_2Br$ which lies at the borderline between the localized and itinerant regimes.[162] The presence of long-wavelength lattice fluctuations above the AF ordering has been recently revealed by spin−lattice relaxation time measurements with pulsed EPR.[163] Moreover, the study of $(TMDTDSeF)_2PF_6$ (hybrid between TMTTF and TMTSeF molecules) has shown the proximity of the Spin-Peierls and AF ground states at ambient pressure for this material.[164] Finally, the charge ordering observed for $(TMTTF)_2ReO_4$ or in the MF_6 series (M = P, As, or Sb) should be mentioned. In the mid-80s, EPR measurements revealed an anomaly of the line width associated with an electronic localization seen by electrical conductivity and thermopower experiments.[149,155,165] These instabilities were labeled for a long time as "structureless transitions" as X-ray analysis failed to detect any change of the crystal structure. In 1988, Javadi et al. reported dielectrical measurements indicating the occurrence of a true phase transition associated with the divergence of the dielectric constant.[166] In 2000, new dielectric experiments exhibiting a clear divergence of the dielectric constant and NMR measurements have definitively proved the existence of this phase transition associated with a ferroelectric charge ordering.[167,168] Note that the phase transition found for $(TMTTF)_2SCN$ at 160 K presents some similarities with the 154 K transition of $(TMTTF)_2SbF_6$. Both correspond to a charge ordering although an antiferroelectric order is stabilized in $(TMTTF)_2SCN$. Figure 10 illustrates the ESR signature of this phase transition along the three principal directions of a $(TMTTF)_2SCN$ single crystal.[169] The charge localization is revealed by an increase of the line width, whereas the low temperature AF ordering is announced by typical precursor effects: a temperature dependent g factor and a diverging line width. As already mentioned, the 160 K anomaly of $(TMTTF)_2SCN$ is quite similar to the one observed in TMA-TCNQ-I or $(TTT)_2(I_3)_{1+\delta}$ salts.

In the past few years, new EPR studies have been devoted to the TMTTF and TMTSeF salts which essentially confirm the previous results with sometimes a better accuracy.[145,170−172] Fits of the spin susceptibility in the strong coupling limit (i.e., in the limit where electron−electron interactions overcome the electronic kinetic energy) have been proposed among the series and accurate angular dependence of the line width for $(TMTTF)_2Br$ have established the role of the dipole−dipole interaction. The divergence of the EPR line width with a critical exponent μ equal to 1.5 has also been confirmed.[171] A detailed analysis of the line width anomaly at the charge ordering for $(TMTTF)_2SbF_6$ have also been obtained and dipole−dipole interactions have been shown to be relevant below the anion ordering temperature of $(TMTTF)_2ReO_4$.[172]

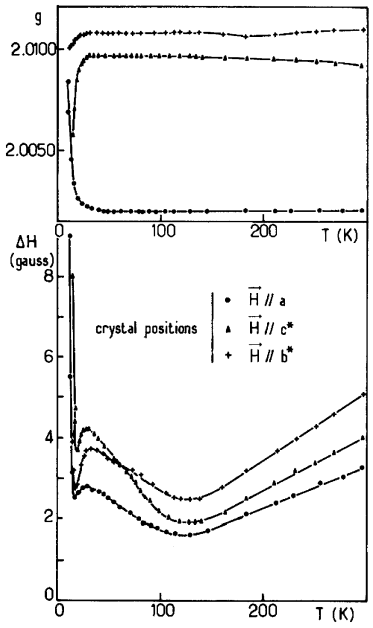

Figure 10. X-band EPR g factor and line width (ΔH) principal components on a single crystal of $(TMTTF)_2SCN$. (Reprinted with permission from ref 169. Copyright 1982, APS.)

Finally, we like to mention that EPR was performed on several salts incorporating TMTTF or TMTSeF and magnetic counterions.[173,174,175] In these cases also, the decomposition technique has been used to separate the contribution of the organic radical from the one of the counterion.[174] As this review is essentially devoted to organic systems, these results will not be discussed in more details.

2.5. Other Radical Cation Salts Including BEDT-TTF Salts

After the discovery of superconductivity in a conductor based on BEDT-TTF (bis-ethylenedithiotetrathiafulvalene),[176] a large number of new salts have been prepared, incorporating this molecule. Moreover, numerous related molecules, some of them being asymmetric, have also been synthesized. Several organic superconductors under pressure or even at ambient pressure and magnetically ordered phases have been described in the literature.[177] Although some charge-transfer salts were prepared,[178,179] most of these materials are cation radical salts. Compared to Bechgaard salts, a wide variety of counterions was also introduced, including polymeric anions.[180] All together, these salts lead to an important number of publications containing EPR experiments. As already mentioned, we will present latter in sections 3 and 4 the reports devoted to magnetic or superconducting ground states. In the present paragraph, only paramagnetic phases will be discussed. Even with this restriction, an exhaustive description of this very large amount of work would be difficult. Therefore, we have chosen a selection of results to illustrate the contribution of EPR.[181] Rather than a classification based on the nature of the radical cation, we will discuss the different materials according to their

magnetic properties. Some materials should be considered as quasi-1D systems and their magnetic properties can be compared to the one found for the Bechgaard and Fabre salts. On the other hand, 2D electronic properties have been found in several series of BEDT or BEDT derivative salts. In that case, another universal phase diagram has recently emerged based on the physical description of a two-dimensional correlated electron gas. This phase diagram emphasizes the competition between a metallic and an insulating paramagnetic phase at high temperature and between antiferromagnetism and superconductivity at low temperature.[182]

Some materials are rather close to the TMTTF or TMTSeF series, structurally speaking. Among them, tTTF (trimethylene-tetrathiafulvalene) salts usually present a larger electronic localization than the TMTTF salts and a low-temperature antiferromagnetic phase.[183,145] This ground state is also found at low temperatures in DMtTTF (dimethyl-trimethylene-TTF) salts which gave the first example of a material with strictly regular molecular stacks presenting some electronic localization.[184,185] Their selenium analogues, the DMtTSeF salts have also been prepared and present a metallic state.[186,187] The BCPTTF salts (where BCPTTF stands for benzocyclopentyl-TTF) with octahedral PF_6 and AsF_6 anions display low-temperature Spin-Peierls ground states.[188] This phase has the same characteristics as in the corresponding TMTTF salts; nevertheless, the BCPTTF salts, being less sensitive to irradiation, have been more deeply studied.[76,153] Figure 11, parts a and b, shows the spin susceptibility deduced from ESR. Both the pseudo-gap (below T_F) and the activated behavior below the Spin-Peierls transition temperature T_{SP} are visible. Figure 11c shows the fit obtained using the renormalization group combined with the functional integral method.

Like in the TMTTF and TMTSeF series, previously described organic salts have only weakly dimerized chains, also referred as type I. This type of organization shown in Figure 9a also exists in the DMCTTF (dimethyl-tetramethylene-TTF) or DMCTSeF series (where DMCTSeF is the selenium analogue of DMCTTF), although strongly dimerized chains (also referred as type II and shown in Figure 9b) have been identified in some structures.[189] Antiferromagnetic ordering at low temperature has been observed for both types of dimerization. With tetrahedral anions, the crystal structures may include either only type II or both of the different types of organic chains. The EPR signals are separated at low temperature, and the individual magnetic behavior of each chain has been studied.[190] We can note that the previous examples illustrate the fact that type I chains may lead to either antiferromagnetic or Spin-Peierls ground state while strongly dimerized (type II) chains favor an antiferromagnetic ordering.

Similar structural organizations are also found among the BEDT-TTF salts, although the situation is much more complex: more than 130 crystal structures of BEDT-TTF containing salts were already determined in 1992.[177] In most of them, the basic building block is a dimer of radical cations,

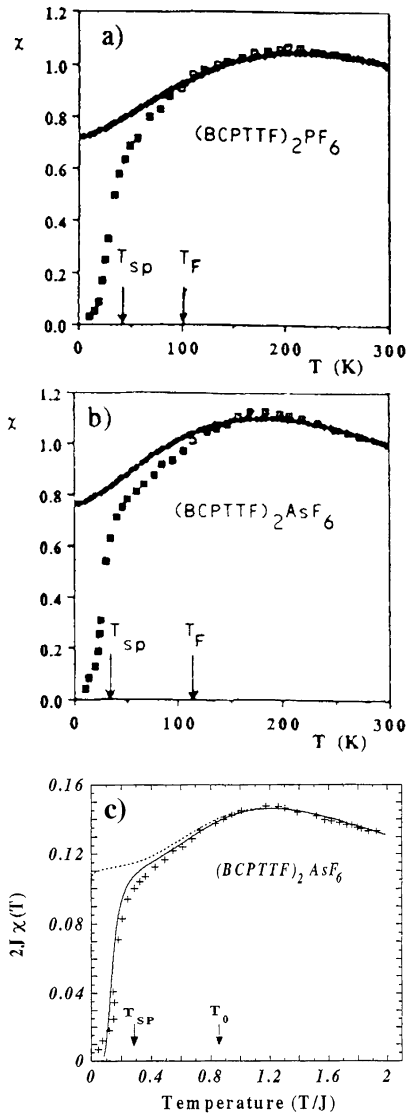

Figure 11. Temperature dependence of the EPR susceptibility of $(BCPTTF)_2PF_6$ (a) and $(BCPTTF)_2AsF_6$ (b) normalized at room temperature. The solid lines are the fit to the Bonner−Fisher law (i.e., to the quantum $S = 1/2$ Heisenberg chain model). Adapted from ref 76. (c) Spin susceptibility vs temperature. Comparison of theoretical results (continuous lines) with experimental data for $(BCPTTF)_2AsF_6$ (crosses), T_0 is equivalent to T_F in Figure 11a. The dashed line is the uniform magnetic susceptibility in absence of Spin-Peierls fluctuations. (Reprinted with permission from ref 153. Copyright 1997, Elsevier.)

although trimers have also been reported.[191] These dimers can be organized in weakly or strongly dimerized chains but can also form a 2D network. In a strong coupling description, the magnetic properties of these systems can be discussed considering each dimer as an effective site bearing a $S = 1/2$ spin as illustrated by Figure 9c. The anisotropy of the exchange interactions between these spins in the organic planes controls the effective electronic dimensionality of the material. According to the details of the crystal structure, the exchange interaction between two dimers, generally antiferromagnetic, may in some cases be ferromagnetic.[192,193] In the case of a triangular lattice, like in some κ-$(BEDT\text{-}TTF)_2X$ salts, a spin liquid state may be the result of the induced frustration.[194] In the weak coupling limit, the

nature of the Fermi surface becomes relevant to discuss the 1D or 2D character of the electron gas.

Examples of type II stacks (following the above definition) are found in β'-BEDT-TTF salts.[195−198] These semiconducting salts include small linear anions such as ICl_2 or $AuCl_2$. Their susceptibility goes through a maximum at a temperature of about 100 K. It was fitted using a 1D $S = {}^1/_2$ Heisenberg model,[199,200] or with a 2D $S = {}^1/_2$ Heisenberg model.[198] In the present case, the anisotropy of the magnetic interactions is rather in favor of a quasi-1D description. Due to smaller interchain couplings, a long range antiferromagnetic ordering is stabilized at a much lower temperature than the one of the susceptibility maximum (at respectively 22 and 28 K). Consistent with the low dimensionality of these salts, a narrow EPR line width (of about 10 Oe at room temperature) is observed. Figure 12, parts a and b, gives EPR data for β'-$(BEDT\text{-}TTF)_2ICl_2$ to illustrate precursor effects in the vicinity of the antiferromagnetic ordering.

As already mentioned, the EPR line width diverges at the antiferromagnetic ordering (Figure 12a) and the g factor becomes strongly temperature dependent (Figure 12b). At the same time, the EPR susceptibility goes to zero. However, this situation is qualitatively different from the Spin-Peierls instability. As shown in Figure 12c, the static magnetic susceptibility remains finite in the antiferromagnetic phase as long as the magnetic field is not applied along the easy axis (or if the magnitude of this field is above the Spin-flop field, as explained in the next section). In the antiferromagnetic case, there is no gap in the spin excitation spectrum. The EPR intensity measured at the paramagnetic g value goes to zero (Figure 12a) due to the building of an internal field below the Néel temperature. In that case, the resonance field is shifted from the EPR value and the rotation patterns are more complicated: it is the antiferromagnetic resonance (see section 3). Thus, as long as antiferromagnetic resonance has not been observed and with the only EPR susceptibility, the difference between a Spin-Peierls and an antiferromagnetic ordering is subtle and the analysis of the data mostly relies on the temperature dependence of the line width and of the g factor. In fact, some AF transitions in the BEDT-TTF series, like in β'-$(BEDT\text{-}TTF)_2SF_3CF_2SO_3$, have been first described as a Spin-Peierls instability[201] and later clearly identified as an antiferromagnetic ordering.[202]

Other examples described as Heisenberg systems (either 1D or 2D) can be found in the BEDT-TTF series,[203−209] with BEDSe-TTF[210] or with asymmetric molecules such as DIMET (dimethyl-ethylene-TTF),[192,211] BPDT-TTF (propylene-dithio-TTF),[212] or C_1TET-TTF (bis(methylthio)-ethylenedithio-TTF).[213] In the case of α'-$(BEDT\text{-}TTF)_2Ag(CN)_2$ or of $(BPDT\text{-}TTF)_2I_3$, a Spin-Peierls ground state, similar to the one observed in $MEM(TCNQ)_2$, has been identified.[204,212]

Besides these semiconducting or insulating materials, many BEDT-TTF salts present a metallic behavior and eventually become superconductors at low temperature. As already mentioned, the first example

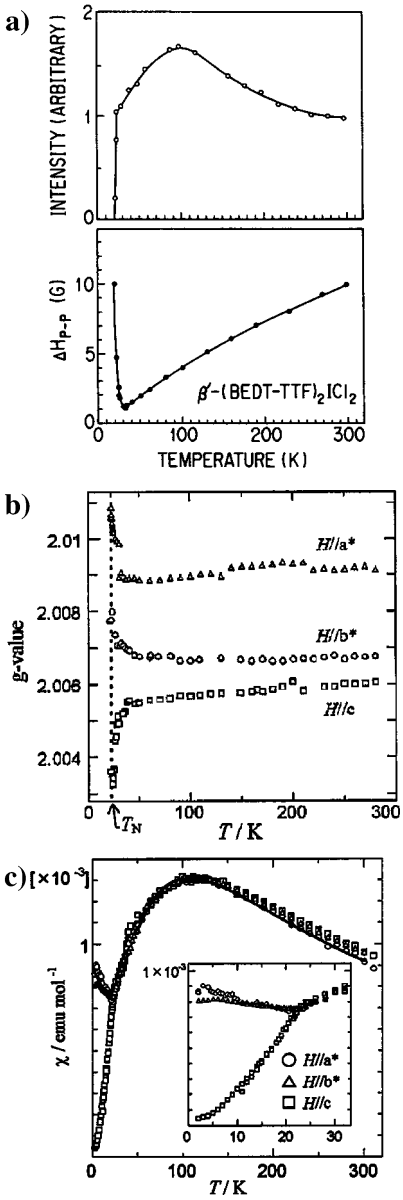

Figure 12. a. Temperature dependence of the EPR intensity and the peak-to-peak line width for β'-$(BEDT\text{-}TTF)_2ICl_2$. (Reprinted with permission from ref 197. Copyright 1987, Elsevier.) b. Temperature dependence of the g value in the three crystallographic directions. (Reprinted with permission from ref 198. Copyright 1997, Elsevier.) c. Temperature dependence of the spin susceptibility for β'-$(BEDT\text{-}TTF)_2ICl_2$ obtained from static measurements. Adapted from ref 198.

in the BEDT-TTF series was $(BEDT\text{-}TTF)_2ReO_4$ which becomes a superconductor for pressures above 4 kbar.[176] In fact, various phases with different EPR properties can be obtained with BEDT-TTF radicals and tetrahedral anions,[214−220] or octahedral anions.[221,222] An important step was realized with the use of linear anions to obtain ambient pressure superconductivity. Several phases were obtained with I_3^- and with other linear anions.[217,223−233] EPR experiments took a large place in the study of the thermal conversion between different phases.[229,234−238] Some of the obtained phases give a 2D magnetic behavior with Dysonian lines when the microwave electric field is applied parallel to the organic plane and a weakly (Pauli like) temperature-dependent

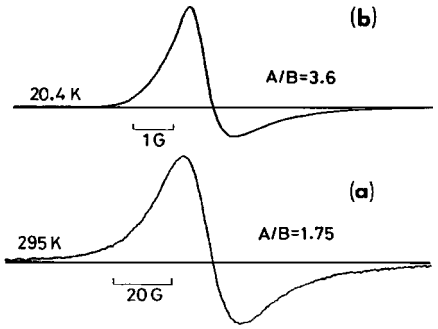

Figure 13. EPR spectra in β-(BEDT-TTF)$_2$IBr$_2$ observed with (a) $E_{\parallel}(001)$ at 295 K and (b) $E_{\perp}(001)$ at 20.4 K where E is the microwave electric field. (Reprinted with permission from ref 228. Copyright 1987, APS.)

spin susceptibility. Typical EPR signals are given in Figure 13. In this case, the evolution of the line-shape with the temperature gives an estimation of the spin-diffusion time which can be compared to electrical conductivity measurements.[225,228]

Another important class of BEDT-TTF salts has been synthesized with polymeric anions.[180] Among them, the so-called κ-phases gave several superconductors, either at ambient or above a moderate pressure.[239] From the electronic point of view, their structures can be considered as two-dimensional and the large electrical conductivity in the molecular plane leads to Dysonian EPR lines. EPR studies were made for different series, as κ-(BEDT-TTF)$_2$Ag(CN)$_2$(H$_2$O),[240,241] κ-(BEDT-TTF)$_2$Cu(NCS)$_2$,[230,242−244] the κ-(BEDT-TTF)$_2$Cu[N(CN)$_2$]X,[245−252] κ-(BEDT-TTF)$_4$Hg$_{3-\delta}$X$_8$,[253−255] and κ-(BEDT-TTF)$_2$Cu$_2$(CN)$_{3-\delta}$X$_\delta$ salts (where X is an halogen atom).[246,248] As already mentioned, a generic phase diagram has been proposed for the κ-phases, taking the example of κ-(BEDT-TTF)$_2$Cu[N(CN)$_2$]Cl, explained in the frame of the 2D Hubbard model.[182] Indeed, EPR data of these different materials present some recurrent features. For example, an increase of the EPR line width when cooling is quite general and indicates that the Eliott relation is also not verified in this class of organic materials. When a superconducting phase is reached at low temperature, there is no general trend for the observed EPR result. For example, the line width strongly increases in κ-(BEDT-TTF)$_2$Cu(NCS)$_2$ suggesting some kind of precursor effect, whereas it decreases for κ-(BEDT-TTF)$_2$Cu[N(CN)$_2$]Br. When a magnetic ordering is reached, as in κ-(BEDT-TTF)$_2$Cu[N(CN)$_2$]Cl at ambient pressure, typical precursor effects are observed.[246] In this compound, the magnetic phase has been described as a weak ferromagnet (see section 3).

Many other materials including BEDT-TTF radicals have been studied, and it would be very hard to refer to all of them. These series illustrate the complexity reached by the field. Among them, let us just mention the α-(BEDT-TTF)$_2$MHg(SCN)$_4$ salts, with M = NH$_4$, K, or Rb where a competition between superconductivity and antiferromagnetism has also been discussed.[256−261] The situation is even more complex if one realizes that many new molecules were also synthesized, including asymmetric ones. A well-known example is the DMET (dimethyl-ethylenedithioTSeF) series where superconducting and antiferromagnetic κ-phases were also obtained.[262−264] At least in the case of the AuBr$_2$ salt, the temperature dependence of the EPR line width follows the electrical resistivity, indicating that the Eliott relation can be applied. This result may be the consequence of a larger electronic dimensionality of this compound which remains an exception among organic conductors. Indeed, an unusual broad line (of about 1000 Oe near 100 K) is observed for this compound, in agreement with a three-dimensional character.[263]

2.6. Other Selected EPR Results

As described in the previous sections, most of the materials studied after the discovery of the organic superconductivity were cation radical salts with a molecular donor derived from the TTF backbone. However, interesting results have also been obtained with other molecules such as the two examples chosen in this paragraph.

Cation radical salts have been obtained with arenes,[265−273] like pyrene,[274,275] perylene,[276−283] fluoroanthene,[284−290] or naphthalene.[291] These molecules being only composed of light elements, i.e., carbone and hydrogen, the effect of the spin−orbit coupling is minimized and extremely narrow EPR line width have been obtained. For example, a line width as narrow as 2.5 mOe have been reported for the (naphthalene)$_2$AsF$_6$ salt.[291] In the cases of perylene or fluoroanthene salts, Peierls phase transitions have been observed upon cooling, inducing a large modification of the spin relaxation. Moreover, because of the extremely narrow lines in the metallic phase, pulsed EPR was successfully applied to deduce the longitudinal and transverse relaxation times.[290−300] In particular, a decay of the correlation function as $\exp(-(t/\tau)^{3/2})$, characteristic of one-dimensional systems was observed.[301] Accurate low field magnetometers were built with these materials taking advantage of the very small line width.[302,303] Unfortunately, this application has been limited by the instability of these materials at room temperature. Their kinetic of decomposition has also been studied by EPR.[304,305]

Another interesting series has been obtained starting from radical anions close to TCNQ, namely dicyanoquinonediimine (DCNQI). Substituents can be introduced on the DCNQI molecule to prepare (2-R$_1$-5-R$_2$-DCNQI)$_2$M compounds with various cations.[306] One should distinguish the Cu salts as a mixed valency on copper ions has been established. As a consequence, the EPR signal is not purely organic. This compound exhibits a unique rich phase diagram with reentrance of the metallic state.[307] Large g shifts are found and the EPR line is usually too broad to be observed at room temperature.[306] Several EPR studies have however been made, in particular because the Cu^{2+} states become detectable in the insulating state.[308−314] A low temperature, antiferromagnetic ordering was identified by EPR in some of these salts,[315,316] in particular in (DMe-DCNQI)$_2$Cu (i.e., R$_1$ = R$_2$ = CH$_3$), whereas static measurements show the existence of a weak ferromagnetism.[317] The origin of the canting in this magnetic phase was attributed to the existence of two nonequivalent Cu sites. With other metal ions such

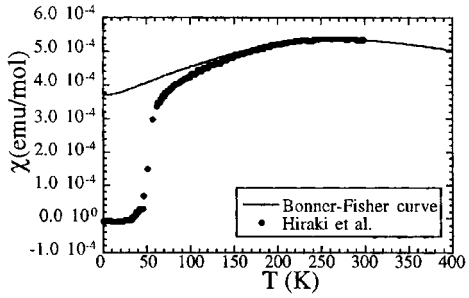

Figure 14. Temperature dependence of the spin susceptibility of $(DMe\text{-}DCNQI)_2Li$. The solid line is the Bonner–Fisher curve (i.e., for the quantum $S = 1/2$ Heisenberg chain). (Reprinted with permission from ref 321. Copyright 2001, Elsevier.)

as Li^+ or Ag^+, narrow EPR lines easily detectable even with the pulse technique have been obtained coming from DCNQI radicals.[318,319] $(DMe\text{-}DCNQI)_2Li$ and $(DMe\text{-}DCNQI)_2Ag$ present a Spin-Peierls phase transition.[320–322] Figure 14 gives the magnetic susceptibility of the Li salt.

Remarkably, like in TMTTF or BCPTTF salts (see section 2.4), a pseudo-gap seems to be observed below 130 K, suggesting 1D precursor effects above the transition temperature at 65 K. In another study under pressure, Curie spins were detected at low temperature and identified to spin solitons.[323] Recent W- and Q-band studies of the anomalous line broadening above the Spin Peierls phase transition quantified the spin exchange between neighboring columns.[324] On the other hand, $(DI\text{-}DCNQI)_2Ag$ (i.e., $R_1 = R_2 =$ iodine) presents an antiferromagnetic ordering at about 5.5 K.[322,325–327] All of the $(2\text{-}R_1\text{-}5\text{-}R_2\text{-}DCNQI)_2M$ compounds have the same crystal symmetry and present uniform DCNQI stacks. In contrast with Bechgaard or Fabre salts, they should therefore be considered as real quarter filled band systems.[328] Despite their regular stacks, these salts present some electronic (Mott) localization and may become electrical insulators well above any magnetic or Spin-Peierls phase transition.[329] This remark emphasizes the role of 1/4 Umklapp terms on the 1D Mott localization which is presently actively discussed in the Fabre series.[161] Another strongly localized quarter filled system, closer to the Bechgaard salts, has recently been published: $(EDTTTF{-}CONMe_2)_2AsF_6$, where the donor is a tertiary amide-functionalized ethylene-dithio-tetrathiafulvalene.[330] This salt presents an antiferromagnetic ground state and brings new information to discuss the competition between the Spin-Peierls and antiferromagnetic instabilities in organic conductors. A detailed comparison of the data obtained with the DMtTTF (paragraph 2.5), DCNQI and $EDTTTF{-}CONMe_2$ series would certainly be useful to discuss the Mott localization in quarter-filled systems.

2.7. EPR of Fullerene Salts

Since the discovery of fullerenes, many attempts have been made to introduce these molecules in new materials. This is particularly the case for C_{60} which can be nowadays prepared in large quantity. A wide variety of C_{60} compounds including superconductors have been synthesized. Although C_{60} is not strictly speaking an organic molecule, as it does not contain hydrogen atoms, the C_{60} salts should be considered as molecular solids. When the unpaired electrons are located only on the C_{60} molecule (i.e., when the counterion is diamagnetic), the magnetic properties are closely related to the ones of organic conductors, as the involved molecular orbitals are also combinations of p_z carbon orbitals. For example, the measured g factors remain very close to the free electron value.

A large number of publications have been devoted to the EPR properties of C_{60} salts and our ambition in this section is not to give an exhaustive review of this work. As in previous paragraphs, we will rather select striking examples to illustrate the relevance of EPR spectroscopy. The reader may find complementary information in several recent reviews.[10,331–333] If with the organic conductors single crystals of the desired materials were usually obtained and studied, fullerene salts have been most of the time obtained in the form of polycrystalline samples. Therefore, their EPR characteristics have been measured on such samples and only at some rare occasions on single crystals.[334] As previously mentioned, this is a severe limitation for ESR studies, in particular in magnetically ordered phases. We have chosen to select two examples of paramagnetic materials presenting either magnetically ordered or superconducting phases at low temperature to introduce their discussion in sections 3 and 4. A ferromagnetic ground state was reported in two cases, namely $(TDAE)C_{60}$ (where TDAE stands for tetrakis-(dimethylamino)-ethylene)[335] and for cobaltocene salts.[336,337] In the former case, a more complete study has been made thanks to the synthesis of single crystals. We will take $(TDAE)C_{60}$ as a first example. Antiferromagnetic and superconducting ground states were reported in M_xC_{60} salts, where M is an alkali metal, essentially with $x = 1$ and 3 and, we will discuss these materials as a second example.

2.7.1. Studies on the Paramagnetic Phase of $(TDAE)C_{60}$

EPR on $(TDAE)C_{60}$ was first described on polycrystalline samples.[338–345] Although it was soon recognized that a magnetic ordering takes place at 16 K, the nature of this magnetic ground state and the role of TDAE in the magnetic exchange were not immediately identified. In fact, the discussion was obscured by the presence of two competing phases, called α and α′, the α phase only being ferromagnetic at low temperature. The situation became less confused with the preparation of single crystals.[346–351] As we will see in the next section a single crystal study in the ferromagnetic phase was the key experiment to characterize this magnetic phase. Keeping in mind the paramagnetic phase, it should be noted that EPR was very useful to discriminate between the α and α′ phases.[352,353] EPR under pressure was also used to identify a [2+2] cycloadditive polymer phase under pressure.[354–357]

2.7.2. Studies on the Paramagnetic Phases of Alkali C_{60} Salts

M_xC_{60} salts have been obtained by doping a C_{60} sample with an alkali metal. EPR was used to follow

Table 2. Selection of Average *g* Values, ⟨*g*⟩, (Often Obtained from Powder Spectra) for Different Reduction or Oxidation States of C_{60}

	⟨*g*⟩	ref
C_{60}^{-a}	1.997−2.000	332, 333, 383, 390, 465
C_{60}^{2-b}	2.0010	332, 382
C_{60}^{3-}	1.999−2.002	332, 377
C_{60}^{+} or $C_{120}O^{-c}$	2.0012−2.0025	332, 365, 366, 367, 390

[a] Slightly different values, from 2.002[342,343] to 2.008[345,350] have been reported for TDAE-C_{60}, with a weak line attributed to C_{60}^{-} present as an "impurity" observed at $g = 1.994$.[345] However, a single-crystal ESR experiment on TDAE-C_{60} has given: $g_a = 2.0001$, $g_b = 1.999$, $g_c = 2.0003$,[349] which implies $\langle g \rangle = 2.000$, consistent with values obtained from other C_{60}^{-} salts. [b] Some authors claim that C_{60}^{2-} is silent and that the signal comes from impurities.[367] [c] ESR signal observed in contaminated neutral C_{60} samples.

this intercalation, mostly in K and Rb cases.[358−363] The Avrami model was usually applied to fit the kinetic data although it is not possible, within the data accuracy, to exclude other models. For example, an intercalation model based on a negligible effect of the interfacial energy between doped and undoped domains is also consistent with the experimental results.[364]

In the different M_xC_{60} phases, it is important to recall that EPR experiments were in a large majority made on powder samples. Moreover, because of the existence of several phases, the EPR spectra may be the superposition of several contributions.[365] In particular, the presence of sharp signals, also called "spikes",[366] was recently discussed and assigned to $C_{120}O$ impurities rather than to C_{60}^{+}.[367] Despite this problem, the average *g* factor for the different radical anions C_{60}^{n-} has been determined and are summarized in Table 2. As for the organic conductors, the EPR line width is characteristic of a material rather than a reduction state of C_{60}. A typical illustration is given by the A_3C_{60} series for which several EPR studies have been made;[358,365,368−374] the line width of Rb_3C_{60} is for example much larger than for K_3C_{60}. As for organic conductors, the effect of spin−orbit coupling has been discussed to explain the line width.[375] These materials present a superconducting phase discussed in section 4. Other materials have been prepared incorporating C_{60}^{3-}. First, one may mention the ammoniated alkali fulleride salts of general formula $(NH_3)K_{3-x}Rb_xC_{60}$.[376−378] The effect of intercalation of neutral ammonia molecules is the suppression of the superconducting phase and the appearance of a low-temperature magnetic phase, described as an antiferromagnetic ordering. A second series has a general formula Na_2AC_{60}, where A is an alkali metal.[373,379−381] In some of these materials, a polymeric phase is formed and superconductivity is suppressed. In this case, an antiferromagnetic ordering was suggested from EPR data. A metal−insulator phase transition has also been observed in the same temperature range for Na_2C_{60}.[382] In that case, a low-temperature nonmagnetic ground state has been suggested with a possible implication of a Jahn−Teller distortion of the C_{60} molecule.

Another interesting series of materials has a general formula AC_{60}, with A = K, Rb, or Cs. A specific characteristic of these salts is the existence

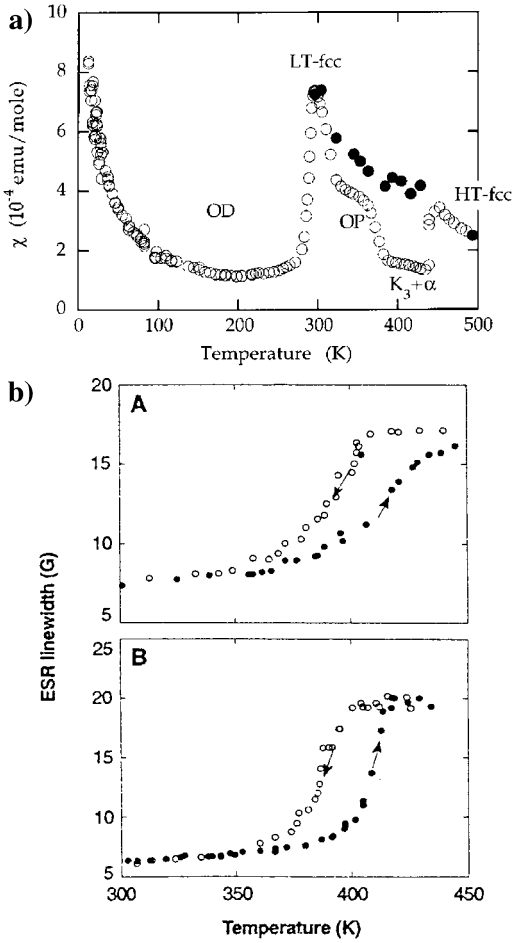

Figure 15. a. Open circles: ESR susceptibility of KC_{60} measured in a continuous run experiment with increasing temperature starting from the pseudo-orthorhombic dimer phase (OD). The labels indicate the various phases encountered and OP is the orthorhombic polymer phase. Closed circles: Susceptibility of the low temperature-fcc phase measured by quenching the high temperature-fcc phase. (Reprinted with permission from ref 386. Copyright 1997, Springer-Verlag.) b. The hysteretic change of the EPR line width indicating the polymerization-depolymerization transition (A) in microcrystalline KC_{60} powder synthesized by standard methods and (B) for few coevaporated single crystals. (Reprinted with permission from ref 388. Copyright 1994, Science.)

of a cubic (fcc)-orthorhombic phase transition at a temperature slightly above room temperature. The structure of the low-temperature phase is characterized by a [2+2] cycloadditive polymerization of the C_{60}^{-} into chains. The samples being prepared at a higher temperature, this polymerization occurs during the last step of the synthesis, and the details of the thermal treatment during this final step are important. For example, a quench from the cubic phase prevents the polymerization from occurring and gives several metastable phases. EPR has been used to identify the different phases and to follow the kinetics.[383−386] Figures 15 give examples of these EPR data and shows how both the spin susceptibility and the EPR line width are relevant to discriminate between the different phases.

Slowly cooled samples present the thermodynamically stable polymerized phase and their physical properties depend on the alkali metal.[387] With potas-

sium, an intermediate phase is observed between the cubic and the orthorhombic phases. Moreover, the polymer phase of KC_{60} was first described as a metallic phase down to the liquid helium temperature.[388−390] In the case of the rubidium or cesium salts, a phase transition has been observed around 50 K,[371,391−393] which was described as corresponding to the onset of an antiferromagnetic ordering. However, the situation may be more complex. This point will be further discussed in paragraph 3.3. In the case of KC_{60}, a recent study combining X-ray and EPR on single crystals has revealed a structural phase transition around 60 K.[394] This result which differs from the conclusions of the previous studies[388−390] emphasizes the importance of the sample preparation.

3. Electron Spin Resonance (ESR) in Magnetically Ordered Phases

3.1. Basic Ideas

When a magnetic phase transition has occurred, the sample is no longer in the paramagnetic phase. This means that the spins cannot be anymore considered as independent species and spin interactions play an important role. To describe the dynamic of these spins, the simplest description introduces an internal field superposed to the applied external magnetic field.[395] This so-called "mean field approximation" is a good approximation for temperatures not too close to the transition temperature where the magnetic ordering appears. In this critical region, more sophisticated theories such as the dynamic scaling theory may be necessary to interpret the experimental data.[396]

3.1.1. Ferromagnetic Resonance

The simplest example of resonance in a magnetically ordered phase is the ferromagnetic case with no magnetic anisotropy.[397] At the mean field approximation, the dynamics of the magnetization is given by a generalization of eq 2. This new equation describes the dynamics of a collective variable, the total magnetization, rather than the evolution of a single spin

$$\frac{d\mathbf{M}}{dt} = -\gamma_e \mathbf{M} \times (\mathbf{H}_0 + \lambda\mathbf{M} - \mathbf{N}\mathbf{M} + \mathbf{H}_{MW}) \quad (15)$$

where $\lambda\mathbf{M}$ is the exchange field (playing no role, as it is parallel to $\mathbf{M}$) and $\mathbf{N}$ is the demagnetization factor (a matrix in the general case) which depends on the sample shape. In the simplest case of a spherical sample, $\mathbf{N}$ is isotropic but for a nonspherical shape, three different coefficients, N_α, should be introduced in eq 15.

As shown in paragraph 2.1, the resonance frequency can be found as an eigenvalue of the linearized equation deduced from eq 15 when $\mathbf{H}_{MW}$ goes to zero. In the present case, this gives

$$\begin{pmatrix} i\omega/\gamma_e & H_0 + (N_y - N_z)M_{eq} & 0 \\ -H_0 + (N_z - N_x)M_{eq} & i\omega/\gamma_e & 0 \\ 0 & 0 & i\omega/\gamma_e \end{pmatrix} \times \begin{pmatrix} m_x \\ m_y \\ m_z \end{pmatrix} = 0 \quad (16)$$

where M_{eq} is the equilibrium value of the magnetization. From eq 16, the resonance frequency is readily obtained

$$\omega = \gamma_e \sqrt{(H_0 + (N_y - N_z)M_{eq})(H_0 + (N_x - N_z)M_{eq})} \quad (17)$$

This equation shows that the resonance frequency is dependent on the sample shape through the demagnetization factor. Thus, to study ferromagnetic resonance, the shape of the sample should be controlled. The same remark applies for the resonance in any magnetic phase exhibiting a spontaneous magnetization.

Let us now discuss the effect of the magnetic anisotropy. To avoid any complicated discussion, we will assume that the shape of the sample is spherical. In that case, the demagnetization factor is isotropic and the $\mathbf{NM}$ term plays no role in the dynamic equation. This equation can be then reduced to

$$\frac{d\mathbf{M}}{dt} = -\gamma_e \mathbf{M} \times (\mathbf{H}_0 + \mathbf{H}_a) \quad (18)$$

where $\mathbf{H}_a$ is the anisotropy field. This equation will be solved after a linearization, starting from the equilibrium state, i.e., writing $\mathbf{M} = \mathbf{M}_{eq} + \delta\mathbf{M}$. This implies that the description of this equilibrium state is the first step. In the general case, the anisotropy energy E_a is given by

$$E_a = \frac{1}{2}K_1\beta^2 + \frac{1}{2}K_2\gamma^2 \quad (19)$$

where (α, β, γ) are the direction cosines of the magnetization $\mathbf{M}$.[398] With this notation, (x, y, z) are respectively the easy, intermediate and hard axes, assuming $K_1 < K_2$ with K_1 and K_2 being the easy-intermediate and easy-hard anisotropy energies. The corresponding anisotropy field is deduced from $\delta E_a = -\mathbf{H}_a\delta\mathbf{M}$ and reads

$$\mathbf{H}_a = (0, \ -K_1\beta/M_0 \ \ -K_2\gamma/M_0) \quad (20)$$

where M_0 is the magnetization modulus.

The equilibrium state is given by $\mathbf{M}_{eq} \times (\mathbf{H}_0 + \mathbf{H}_{a,eq}) = 0$. An analytical solution can be obtained when the magnetic field is applied along the principal magnetic directions:

- When $\mathbf{H}_0$ is along the Easy axis (x), $\alpha_{eq} = 1$, i.e., the magnetization is always aligned along x.
- When $\mathbf{H}_0$ is along the Intermediate axis (y), $\gamma_{eq} = 0$ and $\beta_{eq} = H_0/H_1$ for $H_0 < H_1$; $\beta_{eq} = 1$ for $H_0 > H_1$, with $H_1 = K_1/M_0$. This means that the magnetization rotates in the Easy−Intermediate plane, from x ($\beta_{eq} = 0$) to y ($\beta_{eq} = 1$) as the magnetic field increases, to be aligned with the applied field for $H_0 > H_1$.

• When $\mathbf{H}_0$ is along the Hard axis (z), $\beta_{eq} = 0$ and $\gamma_{eq} = H_0/H_2$ for $H_0 < H_2$; $\gamma_{eq} = 1$ for $H_0 > H_2$. The magnetization now rotates in the Easy−Hard plane, to be aligned with the applied field for $H_0 > H_2 = K_2/M_0$.

This alignment of the magnetization at a critical value of the applied field is still observed for any orientation of $\mathbf{H}_0$ in the Intermediate−Hard plane. It corresponds to a second-order phase transition also revealed by the ferromagnetic resonance, as we will see below.

Ferromagnetic resonance describes the dynamics of the magnetization. The eigenfrequencies can be deduced from the linearization of eq 18 which gives

$$\frac{\mathrm{d}\delta\mathbf{M}}{\mathrm{d}t} = -\gamma_e \delta\mathbf{M} \times (\mathbf{H}_0 + \mathbf{H}_{a,eq}) - \gamma_e \mathbf{M}_{eq} \times \delta\mathbf{H}_a \quad (21)$$

With, $\delta\mathbf{M} = \mathbf{m}e^{i\omega t}$ and when $\mathbf{H}_0$ along the Easy axis (x), we obtain

$$\begin{pmatrix} i\omega/\gamma_e & 0 & 0 \\ 0 & i\omega/\gamma_e & H_0 + H_2 \\ 0 & -H_0 - H_1 & i\omega/\gamma_e \end{pmatrix} \begin{pmatrix} m_x \\ m_y \\ m_z \end{pmatrix} = 0 \quad (22)$$

and therefore (keeping the positive eigenvalue)

$$\omega/\gamma_e = \sqrt{(H_0 + H_1)(H_0 + H_2)} \quad (23)$$

In the same way, when $\mathbf{H}_0$ is along the Intermediate axis (y)

$$\begin{pmatrix} i\omega/\gamma_e & 0 & -H_0 + \beta_{eq}(H_1 - H_2) \\ 0 & i\omega/\gamma_e & \alpha_{eq}H_2 \\ H_0 - \beta_{eq}H_1 & -\alpha_{eq}H_1 & i\omega/\gamma_e \end{pmatrix} \times \begin{pmatrix} m_x \\ m_y \\ m_z \end{pmatrix} = 0 \quad (24)$$

The expression of the positive eigenvalue depends on the equilibrium solution and therefore changes at the critical field H_1. The resonance frequency is given by

$$\omega/\gamma_e = \sqrt{H_1H_2 - {H_0}^2H_2/H_1} \text{ for } H_0 < H_1 \quad (25a)$$

$$\omega/\gamma_e = \sqrt{(H_0 - H_1)(H_0 + H_2 - H_1)} \text{ for } H_0 > H_1 \quad (25b)$$

Note that the frequency goes to zero at the critical point (when $H_0 = H_1$).

Finally, an analytical solution can also be obtained when the magnetic field is applied along the Hard axis (z)

$$\omega/\gamma_e = \sqrt{H_1H_2 - {H_0}^2H_1/H_2} \text{ for } H_0 < H_2 \quad (26a)$$

$$\omega/\gamma_e = \sqrt{(H_0 - H_2)(H_0 - H_2 + H_1)} \text{ for } H_0 > H_2 \quad (26b)$$

The frequency also vanishes at the critical point $H_0 = H_2$.

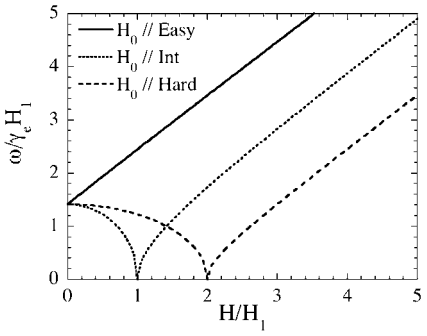

Figure 16. Field dependence of the ferromagnetic resonance frequency for a given H_2/H_1 ratio (here $H_2/H_1 = 2$).

Figure 16 summarizes the field dependence of the ferromagnetic resonance frequency given by eq 23, 25, and 26. The calculation may be generalized introducing the demagnetization factor for a nonspherical sample. The conclusions remain qualitatively the same.

The important point is that there is only one mode (as there is only one macroscopic variable, $\mathbf{M}$, involved in the dynamics) for any orientation of the magnetic field. However two modes can be found experimentally if a scan of the magnetic field is realized for a fixed value of the applied frequency (for example is $\omega/\gamma_e < (H_1H_2)^{1/2}$ when the magnetic field is applied in the Intermediate−Hard plane). Numerically, rotation patterns can be generated and compared to the experiment, in particular when the magnetic field is rotated in simple magnetic planes. The most characteristic results will be obtained if the experimental frequency is chosen to satisfy $\omega/\gamma_e \approx (H_1H_2)^{1/2}$. On the other hand, a classical quasi-sinusoidal rotation pattern will be obtained if $\omega/\gamma_e \gg (H_1H_2)^{1/2}$ similar to the one obtained in the paramagnetic state.

3.1.2. Antiferromagnetic Resonance

The main difference with the ferromagnetic case is the existence of at least two magnetic sublattices A and B.[399,400] In that case, the most general form of the anisotropy energy becomes

$$E_a = \frac{1}{2}K_1({\beta_A}^2 + {\beta_B}^2) + \frac{1}{2}K_2({\gamma_A}^2 + {\gamma_B}^2) \quad (27)$$

where β_i and γ_i are the direction cosines between $\mathbf{M}_i$, magnetization of the sublattice i, and the principal magnetic axes, respectively y (Intermediate axis) and z (hard axis). K_1 and K_2 are the easy-intermediate and easy-hard anisotropy energies. In practice, the exchange is much larger than the anisotropy energy in organic conductors. Therefore $\mathbf{M}_A$ and $\mathbf{M}_B$ remain almost antiparallel when the applied magnetic field is small compared with the exchange field and the anisotropy energy can be reduced to a simpler form

$$E_a = K_1\beta'^2 + K_2\gamma'^2 \quad (28)$$

where β' and γ' are the direction cosines between $\mathbf{M}' = \mathbf{M}_A - \mathbf{M}_B$ and the principal magnetic axes, y and z, respectively.

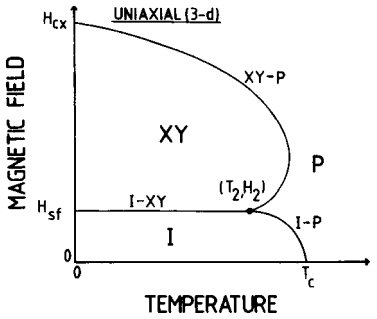

Figure 17. Phase diagram of the 3-d Heisenberg antiferromagnet with weak uniaxial anisotropy and for applied fields along the easy axis ($H = H_x$). The different phases are: P (paramagnetic), I (Ising Ordered), XY (spin-flopped ordered). The bicritical (Heisenberg) point is denoted by (T_2, H_2). The spin-flop occurs for $H_x = H_{SF}$. (Reprinted with permission from ref 401. Copyright 1986, Elsevier.)

The phase diagram when the static magnetic field in applied along the easy axis is depicted in Figure 17.

Two ordered phases are observed:[401]

- Below a characteristic field called the spin-flop field H_{SF}, $\mathbf{M}'$ is along the easy axis x.
- Above the spin-flop field, $\mathbf{M}'$ is along the intermediate axis y.

Between these two phases, a first-order phase transition takes place where the orientation of $\mathbf{M}'$ jumps from one orientation to the other. The magnitude of the spin-flop field can be obtained writing that the Zeeman energy exactly compensates the anisotropy, i.e.

$$K_1 = \frac{1}{2}(\chi_\perp - \chi_{||}){H_{SF}}^2 \tag{29}$$

where $\chi_\perp$ and $\chi_{||}$ are the magnetic susceptibilities, when the magnetic field is applied perpendicular and parallel to $\mathbf{M}'$ respectively. The above equation shows that the spin-flop transition results from the competition between the Zeeman and anisotropy energies. Such a competition specifically occurs when the magnetic field is applied along the Easy axis (x). The spin-flop phenomenon does not occur when the magnetic field is applied along the intermediate or the hard axes. A first-order phase transition is however still present close to x, in the easy-hard plane.

As for the ferromagnetic case, the antiferromagnetic resonance (AFMR) describes the dynamics of the sublattices magnetizations.[399,400,402,403] In the two sublattices case, the dynamic equations are

$$\frac{d\mathbf{M}_A}{dt} = -\gamma_e \mathbf{M}_A \times (\mathbf{H}_0 + \mathbf{H}_{e,A} + \mathbf{H}_{a,A} + \mathbf{H}_{MW}) \tag{30a}$$

$$\frac{d\mathbf{M}_B}{dt} = -\gamma_e \mathbf{M}_B \times (\mathbf{H}_0 + \mathbf{H}_{e,B} + \mathbf{H}_{a,B} + \mathbf{H}_{MW}) \tag{30b}$$

where $\mathbf{H}_{e,i}$ and $\mathbf{H}_{a,i}$ are respectively the exchange and the anisotropy field for the sublattice i. The demagnetization field is always negligible as the total magnetization remains very small in the described limit. As before, the eigenfrequencies are obtained taking the limit $H_{MW} = 0$ and by a linearization of eq 30 around the equilibrium state. As two coupled dynamic equations have to be considered, two resonance frequencies will be obtained, i.e., two AFMR modes for any value of the applied magnetic field. The results can be expressed introducing three essential parameters

$$\Omega_- = \gamma_e\sqrt{\frac{2K_1}{\chi_\perp}}, \quad \Omega_+ = \gamma_e\sqrt{\frac{2K_2}{\chi_\perp}}, \quad \text{and } r = 1 - \frac{\chi_{||}}{\chi_\perp} \tag{31}$$

These three parameters are temperature dependent and vanish at the Néel phase transition. The two characteristic frequencies, Ω_- and Ω_+, are the zero-field frequencies and Ω_- is related to H_{SF} and r through

$$\Omega_- = \gamma_e H_{SF}\sqrt{r} \tag{32}$$

When the anisotropy energy is due to dipolar interactions, both K_1 and K_2 vary with the temperature like the square of the order parameter (the staggered magnetization $\mathbf{M}'$). In this case, Ω_- and Ω_+ are proportional to the order parameter. The parameter r has a more complicated temperature dependence, mostly coming from the dependence of $\chi_{||}$ with T.

The eigenmodes correspond to a precession of the two sublattices magnetizations. Moreover, the corresponding planes of precession are not usually perpendicular to the applied static magnetic field.[403] As a consequence, the optimum experimental configuration to observe the AFMR is not generally the standard geometry used for EPR (i.e., microwave and static fields applied in perpendicular directions). In some extreme situations, the optimum orientation of the microwave field is even parallel to the static field. Keeping the standard configuration (for example used in commercial spectrometers), the intensity of the AFMR modes is hence strongly dependent on the sample orientation. This intensity is not proportional to the magnetic susceptibility (as in the paramagnetic phase) but also depends of the observed mode polarization.

The above expressions (eq 31) were initially deduced to describe magnetic insulators, i.e., the condensation of an antiferromagnetic ordering from localized spins. A straightforward generalization can be made to describe itinerant antiferromagnetism and the condensation of a spin density wave ground state. In this case, the wave vector describing the magnetic ordering is usually incommensurate with the underlying lattice. The essential difference is the introduction of an ajustable magnetic moment per site, μ,which can be much smaller than the Bohr magneton[404,405]

$$\Omega_- = \gamma_e\frac{\mu}{\mu_B}\sqrt{\frac{2K_1}{\chi_\perp}}, \quad \Omega_+ = \gamma_e\frac{\mu}{\mu_B}\sqrt{\frac{2K_2}{\chi_\perp}} \tag{33}$$

In any case (commensurate or incommensurate superstructure), the characteristics of the anisotropy energies can be deduced when the magnetic superstructure is known (see section 3.2).

Figure 18 gives the field dependence of the two resonance frequencies for the three principal mag-

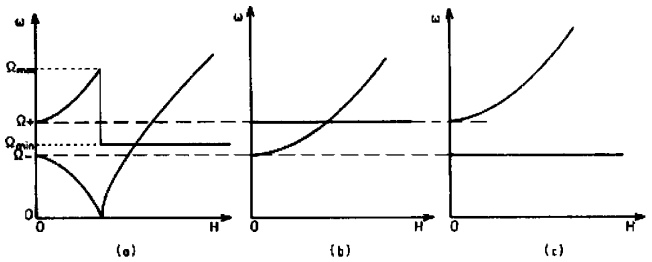

Figure 18. Field dependence of the AFMR frequencies (a) when the magnetic field is along the Easy axis, (b) when the magnetic field is along the Intermediate axis, and (c) when the magnetic field is along the Hard axis. The two characteristic frequency Ω_- and Ω_+ are defined in the text. Moreover $\Omega_{min} = [\Omega_+^2 - \Omega_-^2]^{1/2}$ and $\Omega_{max} = [3\Omega_-^2 + \Omega_+^2]^{1/2}$. (Reprinted with permission from ref 421. Copyright 1986, APS.)

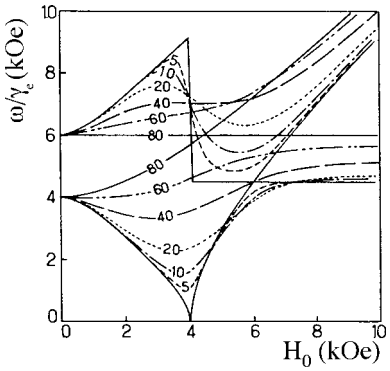

Figure 19. Calculated behavior of the AFMR modes as a function of the field for various angles in the Easy-Intermediate plane for $\Omega_-/\gamma_e = 4$ kOe, $\Omega_+/\gamma_e = 6$ kOe, and $r = 1$ (the angle is given from the easy axis). Adapted from ref 199.

netic orientations, at zero temperature. When the temperature increases, the value of Ω_- and Ω_+ decreases while the Spin-Flop field, H_{SF}, remains approximatively temperature independent. Figure 19 shows the effect of the field rotation in a simple magnetic plane, in the $T = 0$ limit (a more complete set of data can be found in ref 199). A qualitatively similar result is found at finite temperature.

As for the ferromagnetic resonance, the simplest procedure would certainly be a scan of the frequency for a given magnetic field. This would give two modes, whatever is the value or the orientation of the field. However, as for ESR in the paramagnetic state, it is often much more convenient to fix the applied frequency and to scan the magnetic field. Moreover, rotation patterns in simple magnetic planes give characteristic figures strongly dependent on the ratio between the experimental frequency and the characteristic frequencies of the sample. In the limit where $\omega_0 \gg \Omega_-$, quasi-sinisoidal rotation patterns are obtained, while AFMR is only observed close to the easy axis for $\omega_0 \ll \Omega_-$. Finally, the most convenient case to realize the experiment is $\omega_0 \approx \Omega_-$. Fortunately, this condition is satisfied operating in X band, for most organic conductors which may therefore be considered as model systems to study antiferromagnetic resonance. Examples of rotation patterns in simple magnetic planes are given in Figure 20.

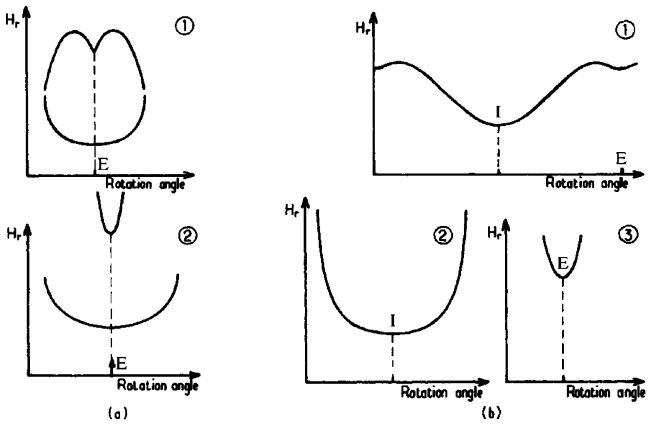

Figure 20. Theoretical rotation patterns (a) corresponding to $\omega_0 < \Omega_{min}$ and $\omega_0 < \Omega_-$, (1) rotating the field around the Hard axis and (2) rotating the field around the Intermediate axis; no mode is observed rotating around the Easy axis. (b) Patterns corresponding to $\Omega_- < \omega_0 < \Omega_+$ and $\omega_0 < \Omega_{min}$, (1) rotating the field around the Hard axis, (2) rotating the field around the Easy axis and (3) rotating the field around the Intermediate axis. (Reprinted with permission from ref 421. Copyright 1986, APS.)

Finally, it may be noted some analogy between the field dependence of the ferromagnetic resonance frequency and the one of lower branchs of the antiferromagnetic resonance, when the field is respectively applied perpendicular or parallel to the easy axis (see Figures 16 and 18a). In both cases, the frequency goes to zero at a critical field, indicating a phase transition. However, an important difference exists between these two cases: the ferromagnetic case leads to a second order phase transition, whereas the first order character of the transition is emphasized by the discontinuity of the higher branch in the antiferromagnetic case. Moreover the characteristic field only depends on the anisotropy energy in the ferromagnetic case (ignoring the demagnetization field), whereas the spin-flop field also depends on the exchange field. In other words, the phase diagram and the coupling of the magnetization with the applied field are not the same in the two cases.

3.1.3. Electronic Resonance in the Weak Ferromagnetic Case

Weak ferromagnetism is found when the magnetizations $\mathbf{M}_A$ and $\mathbf{M}_B$ are not exactly opposite vectors even in absence of an applied field. Initially introduced to explain the magnetic properties of hematite (α-Fe_2O_3), the theory of weak ferromagnetism has been initiated by Dzyaloshinskii who introduced the phenomenological expression of the antisymmetric exchange interaction[406]

$$F_D = \mathbf{D}\cdot\mathbf{M}_A \times \mathbf{M}_B \qquad (34)$$

A theoretical derivation of this term was then given by Moriya.[407] The effect of this new term in the free energy is to introduce a canting angle of the order of D/J between the two sublattices magnetizations (J is the antiferromagnetic exchange between the two sublattices). In other words, a new characteristic field $\mathbf{H}_D = \mathbf{D}M_0$ has to be introduced. The direction of the vector $\mathbf{D}$ should be consistent with the crystal sym-

metry but several cases are generally possible and the discussion becomes more complex.[408−410] Experimentally, **D** is generally very small and the situation remains close to the antiferromagnetic case. As before, the nature of the equilibrium state should be discussed before the determination of the resonance frequency.

As an example, we have chosen to describe the situation previously giving a Spin-Flop instability, i.e., the case where the magnetic field is applied along the Easy axis. We also choose the simple case of **D** parallel to the Hard axis which ensures the net magnetic moment to remain in the Easy−Intermediate plane for any value of the applied magnetic field. The minimization of the total free energy gives the angle, ψ, between the staggered magnetization $\mathbf{M}' = \mathbf{M}_A - \mathbf{M}_B$ and the easy axis[410]

$$\sin \psi = \frac{H_D H_0}{H_{SF}^2 - H_0^2} \tag{35}$$

where H_0 is amplitude of the applied field. H_{SF} is the Spin-Flop field for which ψ jumps discontinuously from 0 to $\pi/2$ in the antiferromagnetic case (for $H_D = 0$). A phase transition with an alignment of $\mathbf{M}'$ along the Intermediate axis is still observed (when $\sin(\psi) = 1$) but the spin reorientation now occurs continuously, as in the ferromagnetic case. The study of the dynamics still gives two branches (there are still two sublattices), and for small values of **D**, the shape of their field dependence is reminiscent of the one observed for the antiferromagnetic case.[411]

Finally, it should be mentioned that another case would be the ferrimagnetic resonance. As we will not describe ferrimagnetic materials in the following paragraph, we will not develop the ferrimagnetic case in this review.

3.2. Electronic Resonance in Magnetically Ordered Phases of Organic Conductors

The antiferromagnetic ground state remains the most commonly magnetically ordered phase observed in organic conductors. In the 70s, a few antiferromagnetic resonance studies of organic free radicals were already published,[412−414] before this technique was intensively applied to organic conductors. The magnetic nature (spin density wave) of the low-temperature phase of some Bechgaard salts was first discovered from the comparison of the static and ESR spin susceptibilities[415,404] quickly followed by the observation of antiferromagnetic resonance in $(TMTSeF)_2AsF_6$[416] and $(TMTSeF)_2ClO_4$.[417,418] In this pionner work, high frequencies were used (11, 17, or even 35 GHz for the AsF_6 salt) to observe rather weak AFMR signals due to the crystal size and of the broad line width of the resonance signal. However, characteristic rotation patterns were already obtained which unambiguously prove the antiferromagnetic nature of the ground state. Soon after these studies, AFMR was studied in sulfur analogues of the Bechgaard salts, $(TMTTF)_2Br$,[419] $(TMTTF)_2SbF_6$, and SCN.[420,421] AFMR appeared to be an excellent tool to prove unambiguously the ground-state nature of these organic conductors and to study its characteristics.[422,423] In a short period of time, many other materials were studied by this technique.[146,160,185,192,193,200,424] A quantitative agreement exists between the theory and the experiment. The experimental AFMR rotation patterns can be fitted to deduce the characteristic parameters introduced in section 3.1 (Ω_-, Ω_+, and r), and the position of the magnetic axes (Easy, Intermediate, and Hard axes). Examples of these rotation patterns and their related fits are given in Figures 21 and 22. Figure 23, taken from a more recent study of some TMTSeF and TMTTF salts,[425] illustrates the effect of the temperature on the AFMR.

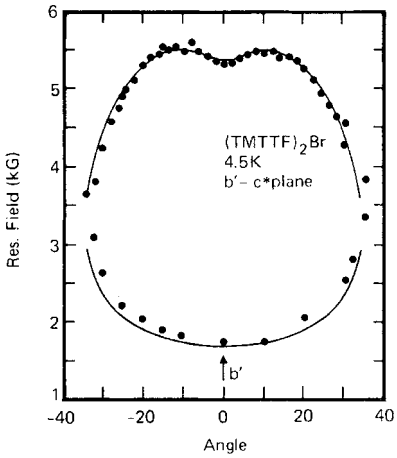

Figure 21. Resonance field in the (**b′**, **c***) plane in $(TMTTF)_2Br$. The solid lines are computed using equations given by Nagamiya[399,400] with values $\Omega_-/\gamma_e = 4.25$ kOe and $\Omega_+/\gamma_e = 6.6$ kOe. (Reprinted with permission from ref 419. Copyright 1982, APS.)

The analysis of the AFMR parameters deduced from the fits first requires the description of the magnetic super-structure. In the TMTSeF salts, the magnetic ordering has been described as an instability of the Fermi surface at a given nesting wave-vector.[405,426] The resulting spin-density wave has an incommensurate wave vector and an amplitude of about $0.1\mu_B$.[427] The influence of the nesting wave-vector has been discussed considering that both dipole−dipole interactions and the spin−orbit coupling contribute to the anisotropy energy.[405] The rather large ratio Ω_+/Ω_- (of the order of 2.9) and the hard axis close to **c*** are in agreement with the nesting wave-vector deduced from NMR experiments.[427]

As already mentioned, TMTTF salts and other sulfur compounds can be classified into two groups, labeled as types I and II respectively (Figure 9), according to the amplitude of the chains dimerization. TMTTF salts belong to the first group, whereas other materials such as $(DIMET)_2SbF_6$[192] or $(BEDT\text{-}TTF)_2ICl_2$[200] should be classified in the second group. Samples of type II, which present a weak electrical conductivity and strongly dimerized chains, can be described in the strong localized limit where each organic dimer bear a localized spin. The situation is more controversial for samples belonging to the first group. In this case, it is generally believed that the strong coupling limit of an $S = 1/2$ Heisenberg

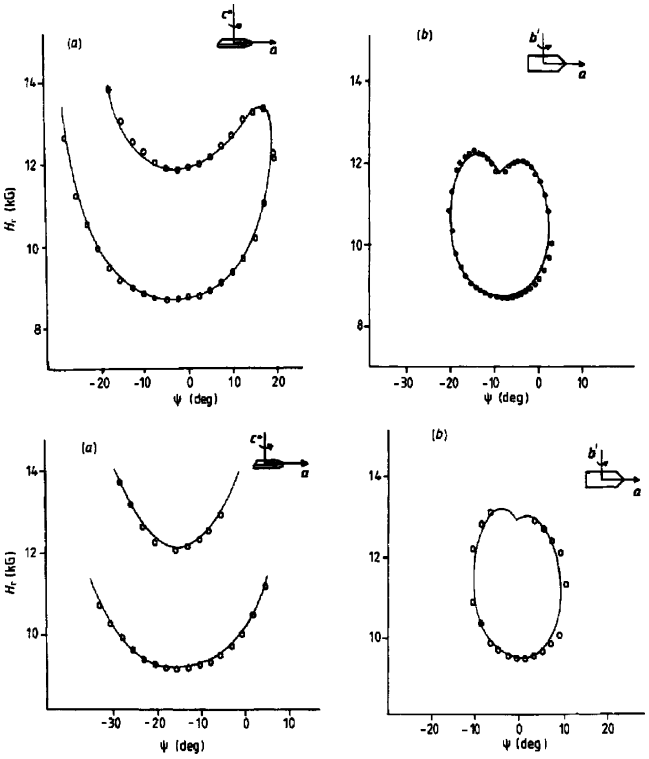

Figure 22. (top) Antiferromagnetic rotation pattern for the (BEDT-TTF)$_2$ICl$_2$ salt at 4.5 K, (a) rotating the sample around an axis close to **c*** (the misorientation was estimated to be about 8°) (b) around **b**′. The full curves give the fits obtained using the Nagamiya theory[399,400] with Ω_+/γ_e = 13 kOe, Ω_-/γ_e = 11 kOe, and r = 1. The polar angles of the rotation axes relative to the magnetic frame are (a) θ = 85.5°, ϕ = 95°; (b) θ = 15°, ϕ = −60° (Reprinted with permission from ref 200. Copyright 1986, IOP.) (bottom) The antiferromagnetic rotation patterns for the (BEDT-TTF)$_2$AuCl$_2$ salt at 4.5 K, (a) rotating the sample around **c***; (b) around **b**′. The full curves give the fits obtained using the AFMR theory[399,400] with Ω_+/γ_e = 13.7 kOe, Ω_-/γ_e = 11.6 kOe, r = 1. The polar angles of the rotation axes relative to the magnetic frame are (a) θ = 80°, ϕ = 90°; (b) θ = 15°, ϕ = −50° (Reprinted with permission from ref 200. Copyright 1986, IOP.)

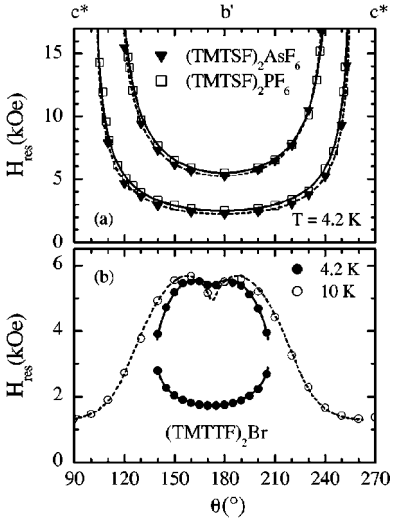

Figure 23. Angular dependence of the AFMR field H_{res} observed in the (**b**′, **c***) plane of the materials investigated. The lines were calculated using the equations derived by Nagamiya et al.[399,400] (a) At T = 4.2 K, the fit gives for (TMTSF)$_2$AsF$_6$ (dashed lines): Ω_- = 11.5 GHz and Ω_+ = 34.1 GHz and for (TMTSF)$_2$PF$_6$ (solid lines): Ω_- = 12.2 GHz and Ω_+ = 36.5 GHz. (b) For (TMTTF)$_2$Br, the data at T = 4.2 K (closed circles) can be fitted (solid lines) to Ω_- = 11.8 GHz, Ω_+ = 19.4 GHz, and r = 0.88 and at T = 10 K (open circles) with Ω_- = 8.8 GHz, Ω_+ = 14.7 GHz, and r = 0.44 (dashed line). (Reprinted with permission from ref 425. Copyright 2000, APS.)

chain is not completely valid and the so-called IEX (interchain exchange coupling) mechanism was evoked to explain the stabilization of the antiferromagnetic phase.[428] Although this description incorporates electronic correlations, it predicts the same optimum antiferromagnetic wave-vector as the band structure calculation analysis (the previously called best nesting wave-vector). Therefore, this optimum wave-vector is in general incommensurate with the underlying lattice. Experimentally, single crystals NMR studies lead to a commensurate magnetic superstructure in (TMTTF)$_2$SCN[429] and even in (TMTTF)$_2$Br (the less localized salt in the TMTTF series) at ambient pressure.[430,431] The same wave-vector, with a **b*** component q_b = $^1/_4$, is deduced in these two compounds. At first sight, this experimental result seems to favor a strongly localized description of these TMTTF salts. However, the amplitude of the spin polarization (of the order of 0.14μ_B per molecule) remains significantly smaller than 0.5μ_B (the expected value for S = $^1/_2$ spins fully localized on organic dimers, neglecting quantum fluctuations). Moreover, it is worth noting that, for (TMTTF)$_2$Br, the magnetic wave-vector becomes incommensurate under a moderate pressure. Nevertheless, this value stays very close to the previous commensurate one, and the amplitude of the spin density wave is still close to 0.14μ_B per molecule.[432] This last result emphasizes that the ambient pressure ground state of TMTTF salts is closer to the delocalized limit than the strong coupling one. In coherence with these arguments, AFMR parameters in the TMTTF series have been analyzed using the same theoretical description as for the TMTSeF salts.[145,405] The essential difference is that the spin−orbit coupling is negligible compared to dipolar interactions in sulfur compounds. The anisotropy energy is therefore solely determined by dipolar terms. For similar values of the antiferromagnetic wave-vector, the loss of the spin−orbit term in the anisotropy energy leads to different antiferromagnetic parameters. Smaller value of the ratio Ω_+/Ω_- (of ca. 1.7) and an orientation of the Hard axis close the stacking axis **a** are predicted. Both results are observed experimentally for TMTTF salts but also for other sulfur compounds presenting weakly dimerized chains.[422,423]

In the case of type II salts, the strong localization implies that the magnetic superstructure can be deduced from the minimization of the exchange energy, starting from one spin localized on each dimer.[192] In that case, the position of the magnetic axes is mainly influenced by the sign of the exchange interaction between side-by-side dimers (see Figure 9c). This interaction is ferromagnetic for (DIMET)$_2$SbF$_6$[192] and (BEDT-TTF)$_2$ICl$_2$ (or AuCl$_2$)[200] and the Hard axis is close to the stacking axis. The situation is different in the DMCTTF (dimethyl-tetramethylene-tetrathiafulvalene) series[424,193] where the side-

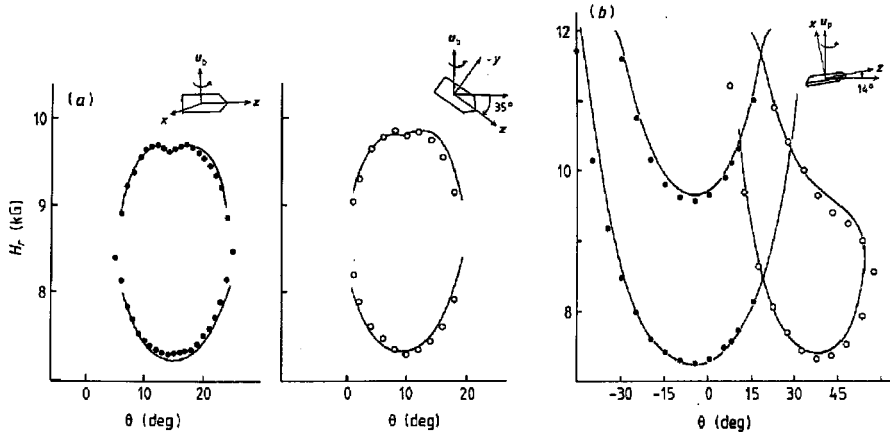

Figure 24. AFMR rotation patterns for α-(DMCTTF)$_2$ClO$_4$. The orientations of the rotation axes are given in inset (the shape of the crystal is schematic). The continuous curves give the fits with the Nagamiya theory[399,400] The same characteristic frequencies are obtained for both layers, but with different orientations of the magnetic axes. (Reprinted with permission from ref 193. Copyright 1989, IOP.)

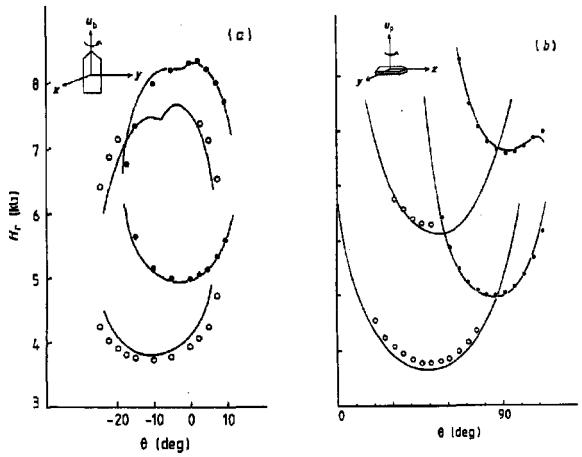

Figure 25. AFMR rotation patterns for β-(DMCTTF)$_2$ClO$_4$. The orientations of the rotation axes are given in inset (the shape of the crystal is schematic). The continuous curves give the fits with the Nagamiya theory.[399,400] Different characteristic frequencies and magnetic axes are found for the two layers. (Reprinted with permission from ref 193. Copyright 1989 IOP.)

by-side interaction between dimers is expected to be antiferromagnetic and where the Hard axis is almost perpendicular to the molecular planes. In both cases, there is a very good agreement between the experiment and the eigendirections deduced from the diagonalization of the dipolar energy.

AFMR can also be useful in more complex systems. As mentioned in section 2, some compounds present several orientations of the radical ions in their crystal structure. This is the case of some DMCTTF salts where two different types of organic layers are present.[190,193] Figures 24 and 25 give the AFMR rotation patterns in simple crystallographic planes for each phase of the ClO$_4$ salt. It is easy to realize that each type of layer gives its own rotation pattern. In the α phase (monoclinic phase), the different organic layers are symmetry-related through a 2-fold screw axis parallel to the monoclinic axis. Thus, the AFMR parameters Ω_+, Ω_-, and r are the same for the two layers and the orientation of the magnetic axes are also symmetry-related. On the other hand, the two types of layers are independent in the triclinic structure of the β phase and two series of independent AFMR parameters are found.

With the discovery of magnetic ground states in some BEDT-TTF salts and the evidence for weak ferromagnetism in κ-(BEDT-TTF)$_2$Cu[N(CN)$_2$]Cl,[433,434] several ESR studies were performed to probe this ground state.[249,435,436] Fitting of the experimental rotation patterns has been attempted in frame of the AFMR theory.[437−439] Moreover, low field modulated microwave absorption has been observed around the transition temperature on polycrystalline sample.[440] This nonresonant absorption which is commonly found in superconductors (see section 4) has also detected in the weak ferromagnetic phase of a verdazyl radical and attributed to the motion of ferromagnetic domain walls.[441]

Recent resonance studies have been reported on α-(BEDT-TTF)2MHg(XCN)$_4$ salts,[442,443] β'-(BEDT-TTF)$_2$SF$_5$CF$_2$SO$_3$,[202] and on β'-(BEDT-TTF)$_2$-ICl$_2$ which has been revisited.[444] The antiferromagnetic ground state has also been studied by ESR technique in molecular perovskites,[445,446] and (DI-DCNQI)$_2$Ag.[322,325−327] Finally, it is worth noting that antiferromagnetic resonance has been described in molecular systems where the spin cannot be considered as purely organic. This is the case for (DCNQI)$_2$-Cu salts[447] or when the counterion of a TTF derivative radical is magnetic like [FeCl$_4$]$^-$ or [FeBr$_4$]$^-$.[448−450] Materials prepared with organometallic systems also enter into this category.[451−453] In this latter case also, the antiferromagnetic theory has been successfully used to fit the experimental rotation patterns.

3.3. Electronic Resonance in Magnetically Ordered Phases of Fullerene Salts.

As it was mentioned in section 2.7, several kinds of magnetic ordering were found with C$_{60}$ salts. The first remarkable compound is (TDAE)C$_{60}$ which presents a ferromagnetic ground state at low temperature. Most of the papers related to this compound deal with the change of the ESR line characteristics at the phase transition: shift of the resonance field, increase of the line width and intensity.[344−350] Low-

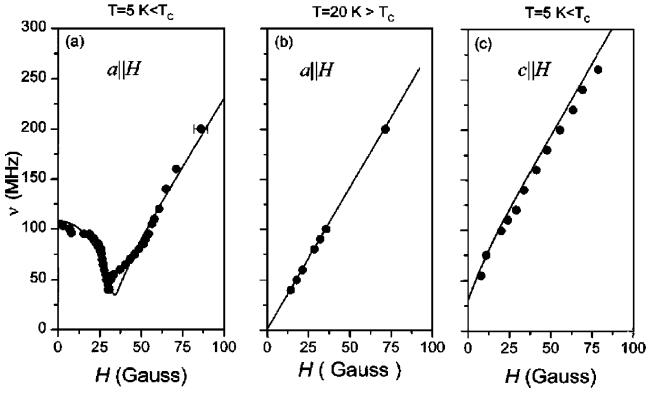

Figure 26. (TDAE)C_{60}: Observed ferromagnetic resonance frequency versus resonance field relations for (a) **a** || **H**, $T = 5$ K < T_C, (b) **a** || **H**, $T = 20$ K > T_C, and (c) **c** || **H**, $T = 5$ K < T_C. (Reprinted with permission from ref 456. Copyright 1998, APS.)

frequency data (45 MHz) were compared to X-band results to establish the existence of an internal field below the transition temperature[454] and low field absorption was also observed.[455] Finally, a more complete study at low frequency (30 MHz − 1.2 GHz) definitively established the ferromagnetic order as a single resonance branch has been observed.[456] These results were fitted including an anisotropy and a demagnetization field. They are reproduced in Figure 26. This analysis was confirmed by high field ESR, where the ESR line becomes structured, suggesting the occurrence of standing waves in the crystals.[457,458]

The occurrence of an antiferromagnetic ground state has also been suggested for several C_{60} salts (see paragraph 2.7). These materials have been studied by ESR. Unfortunately, only powder data are presently available, and the conclusions of some these studies remain controversial. In ammoniated alkali fulleride salts, the general trend in the community is to accept the existence of a long-range antiferromagnetic order. [377,378,459] Nevertheless, NMR results do not show an enhancement in the spin−lattice relaxation rate, T_1^{-1}, as expected for an antiferromagnetic ordering.[376] The situation is even more controversial in Na_2AC_{60} salts.[379−381] Evidence for "spatial disorder and inhomogeneity effects" was noted.[379] Some authors concluded by that no long-range magnetically ordered state was in fact developed.[380] Finally, an antiferromagnetic ground state was reported for RbC_{60} and CsC_{60}.[393,460] In these cases, magnetic fluctuations have been seen by NMR,[461] although this technique has also revealed a strong heterogeneity of the samples.[462,463] The ESR data can also be analyzed in a different way.[392,464] Bennati et al. reports different scenarios including spin glass or spin clusters. From the antiferromagnetic analysis, a Spin-Flop field of a few kOe[464,460] was deduced in contradiction with static susceptibility data.[465,466] A multifrequency study was often made to probe the magnetic character of the low-temperature phase and a $1/H_0$ dependence of the line width was taken as a proof for a long-range magnetic ordering.[459,460] However, short range order[465] or a spin-glass behavior[464] is also consistent with this result. In any case, it seems that disorder plays an important role in the C_{60} salts and could explain for example the spread of the estimated transition temperatures.[467] Characteristic AFMR rotation patterns on single crystals are still missing to definitively establish the nature of the magnetic ground state.

4. Electron Spin Resonance in the Superconducting Phase

4.1. Basic Ideas

Observing the ESR signal of conduction electron in a superconducting phase is not an easy task. It is considered as very difficult in type I superconductors,[468] whereas it becomes more accessible in superconductors of type II.[469,470] Indeed in type I superconductors, the magnetic field is expulsed from the bulk except in a thin layer of the surface. For type II superconductors, a better field penetration and therefore a stronger intensity of the ESR signal are expected in the vortex state or for thin films. In this case, there are several possible mecanisms to explain the spin relaxation, one of them being the interaction with nonmagnetic impurities.[470] When this latter process is dominant, the theory predicts a decrease of the spin relaxation rate and therefore a decrease of the ESR line width. Moreover, the ESR intensity at $T = 0$ K is then proportional to H/H_{c2} (H_{c2} is the upper critical field).[374] On the other hand, scattering by magnetic impurities would lead to an increase of the line width just below T_c.[469] In practice, there are very few and rather controversial experimental results. In most superconductors, the spin-relaxation is very fast and the ESR line is too broad to be observed. Moreover, the so-called "vortex noice" may prevent the observation of the resonance with a conventional 9.3 Ghz spectrometer.[374] A few experimental results concerning molecular systems are described in paragraph 4.2.

Another characteristic of the superconducting state is the existence of a nonresonant low-field microwave absorption which has been studied in details in superconducting copper oxides.[471,472] This absorption can be called depending of the authors: low field signal (LFS), magnetically modulated microwave absorption (MMMA), or microwave magneto-absorp-

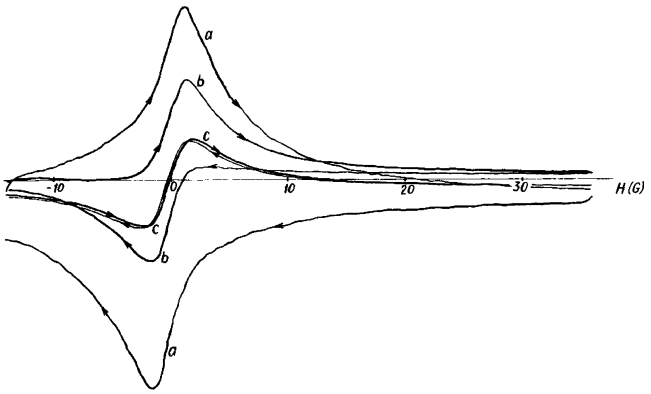

Figure 27. Absorption signal from $La_{1.85}Sr_{0.15}CuO_4$ for different modulation amplitudes ($T = 15$ K). (a) Modulation amplitude, $A_M = 0.01$ Oe and receiver gain, $G_R = 2500$. (b) $A_M = 0.1$ Oe and $G_R = 250$. (c) $A_M = 1$ Oe and $G_R = 25$. Microwave power for all spectra is 20 dB (Reprinted with permission from ref 474. Copyright 1997, APS.)

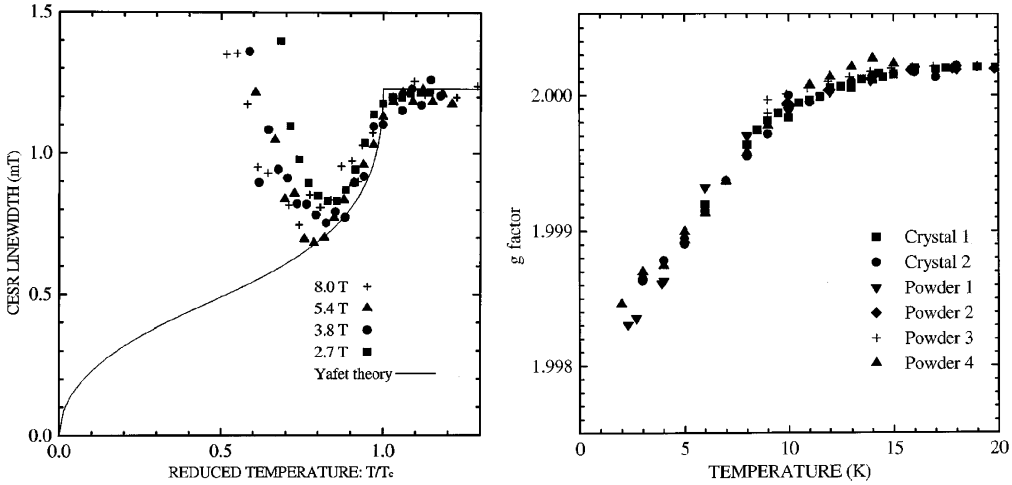

Figure 28. (left) CESR line width vs reduced temperature of K_3C_{60} at various magnetic fields in the superconducting state. The sharp decrease of the relaxation rate below T_C is field independent. Below 0.7 T_C the broadening is inhomogeneous. The solid line is the theoretical prediction of Yafet for scattering of normal excitations on nonmagnetic impurities. (right) Variation of the g factor below T_C of several powder and crystal K_3C_{60} samples measured at 225 Ghz. (Reprinted with permission from ref 374. Copyright 2000, APS.)

tion (MMA). It can be observed with a conventional ESR spectrometer through a standard field scan at a given temperature or with a temperature scan at a given static magnetic field. Both methods are very sensitive. The percolation of the superconducting phase in the bulk material is not necessary and small volume fractions of the superconducting phase (as low as 0.01%) can be detected. Therefore, this technique is a very powerful tool to characterize new superconducting phases and their transition temperature. Low field absorption is also found in other systems such as conducting polymers or weak ferromagnetism (see paragraphs 3.2 and 3.3). This absorption is usually assigned to superconductivity when some hysteresis and a dependence on the microwave field amplitude are found.[472] Figure 27 illustrates these two characteristics in the case of a high T_c oxide. Other experimental details, like a previous exposure to a magnetic field also affect the obtained low field absorption.[473,474]

Several mechanisms have been proposed to explain this microwave absorption which appears to be a complex process. One approach is based on the dissipation of the microwave power due to viscous fluxon motion.[471] Alternative models rely on resistivity losses[475] or on a nonequilibrium contribution of the ac susceptibility.[476]

Low field microwave absorption of superconducting single crystals has also been studied. In some cases, series of lines uniformly spaced in field are found.[473] They were explained considering the mixing of flux states stabilized by the microwave field.[477]

4.2. ESR in the Superconducting State of Molecular Conductors

As mentioned in paragraph 4.1, the observation of conduction electron spin resonance (CESR) in the superconducting state has been reported in only a few examples. Some of them concern organic or fullerene salts. Delrieu et al. observed CESR in the superconducting state of $(TMTSeF)_2ClO_4$ with a homemade low-frequency spectrometer[478] and found

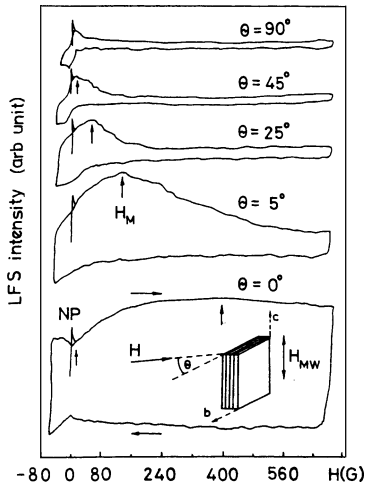

Figure 29. Angle dependence of hysteretic low field absorption spectra in κ-$(BEDT\text{-}TTF)_2Cu(NCS)_2$ for $\mathbf{H}_{MW} \parallel \mathbf{c}$ axis: minimal low field absorption at $\mathbf{H} \perp \mathbf{bc}$, maximal low field absorption at $\mathbf{H} \parallel \mathbf{bc}$, (zero-field cooling, $P_{MW} = 1.98$ mW, $H_{mod} = 0.5$ Oe, Receiver gain = 50, $T = 5$ K, θ is the angle between the applied field and the conducting **bc** planes). (Reprinted with permission from ref 483. Copyright 1991, Elsevier.)

a progressive broadening of the line. CESR has also been reported by Nemes et al. in the superconductor K_3C_{60} at several frequencies (9−225 GHz; Figure 28).[374] Concerning the line width, the theoretical prediction of Yafet is followed until an unexpected broadening is found below 0.7 T_c. At the same time, the decrease of the apparent g factor when cooling is attributed to the reduction of the local field due to screening effects.

The nonresonant low field absorption is more documented, either for organic and C_{60} salts. As far as organic superconductors are concerned, low field nonresonant microwave absorption was used to characterize the superconducting phase,[246,247,479,480] taking profit of the sensitivity of the method to also probe thin films.[481] For κ-$(BEDT\text{-}TTF)_2Cu(NCS)_2$, the experiment was made on single crystals.[440,482] The angle dependence of the hysteretic absorption was shown

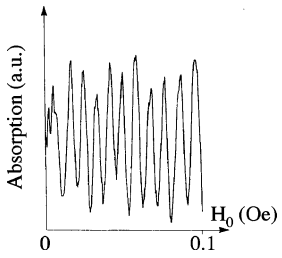

Figure 30. Low field microwave absorption as a function of the external magnetic field $\mathbf{H}_0$ for κ-(BEDT-TTF)$_2$Cu(NCS)$_2$. Temperature is 1.8 K, modulation amplitude 10 Oe and $P_{MW} = 0.008$ mW. Adapted from ref 482.

(see Figure 29),[483] whereas a pattern of resolved periodic lines was found for very good quality crystals, as shown in Figure 30.[440,482]

Low field microwave absorption was also used to characterize superconductivity in C_{60} salts, essentially on powder samples.[484−492] The kinetics of formation of a superconducting phase,[360,361,493−496] the air stability of K_3C_{60}[497] or the isotopic effect in M_xC_{60} salts[498] was also studied by this technique. Because of its sensibility, thin films or Langmuir Blodgett multilayers were also characterized.[499,500] Figure 31 shows a typical result found for A_3C_{60} salts.[486a] The onset of the low field microwave absorption at the superconducting phase transition (at 18 and 38 K for the K and Rb salts, respectively) together with hysteresis effects are clear.

Finally, it should be noted that an organic radical (giving by itself a narrow ESR signal) can be placed at the surface of a superconducting material, to probe this material. This technique was applied to ceramics of high-T_c superconductors[501] absorbing DPPH (diphenyl-picrylhydrazil) at the surface of the sample. A dramatic increase of the DPPH line width is observed at the superconducting phase transition of the ceramic, which was interpreted as an inhomogeneous broadening. In that case, the temperature dependence of the DPPH line width can be fitted to give the penetration depth in the superconducting material. The same technique was recently applied fixing a microprobe of BDPA (bisdiphenylene-β-phenylallyl) at the surface of a single crystal of κ-(BEDT-TTF)$_2$Cu(NCS)$_2$.[502] Inhomogeneous broadening was also observed which depends on the field excursion.

5. Concluding Remarks

During the last 30 years, the research on molecular conductors led to many important discoveries and to a very large number of publications. In this review, selected results have been chosen to illustrate the relevance of the ESR technique in this field. Molecular conductors display a wide variety of electronic ground states including paramagnetic, ferromagnetic, antiferromagnetic, Spin-Peierls, Peierls and superconducting ground states. In all of these cases, electron spin resonance detected in these different phases, was a major probe. Even the most common commercial version, operating in X-band (9.3 GHz), gives detailed information on very small samples such as single crystals. As seen in this review, molecular conductors can often be considered as model systems for ESR. This is true in the paramagnetic phase where narrow lines are usually observed but also when a magnetic ordering is present. Ferromagnetic or antiferromagnetic resonance give a very detailed picture in these systems, including very distinctive rotation patterns which cannot be obtained so easily in inorganic materials.

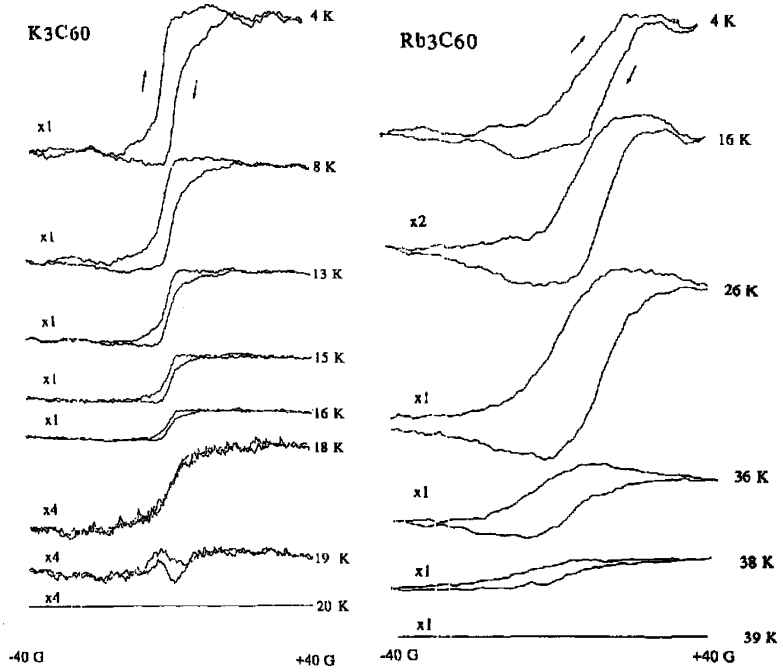

Figure 31. (left) low field microwave absorption response versus temperature for K_3C_{60} showing forward and backward magnetic field sweeps as shown by the arrows. Experimental conditions are 2 mW microwave power and 5 Oe modulation amplitude. (right) low field microwave absorption response versus temperature for Rb_3C_{60} showing forward and backward magnetic field sweeps as shown by the arrows. Experimental conditions are 2 mW microwave power and 10 Oe modulation amplitude. (Reprinted with permission from ref 486a. Copyright 1992, ACS.)

Moreover, thanks to technical developments, it becomes now easier to operate at different frequencies even at low temperature. In this review, we have reported several experimental results at either lower or higher frequencies than 9.3 GHz. For the narrowest lines, the pulse technique can also be applied which gives more information on the spin relaxation. Finally, experiments under pressure have also become available. With all these improvements, ESR is now a very competitive method, which comes in addition to other magnetic measurements and even brings exclusive information through the resonance field and the line width.

6. Acknowledgments

It is a pleasure to acknowledge fruitful discussions with P. Delhaès during the preparation of this review. The work made in Bordeaux on organic conductors is the result of an active collaboration with many colleagues. The contribution of J. Amiell, P. Batail, K. Boubekeur, C. Bourbonnais, D. Chasseau, F. Creuzet, L. Ducasse, J. M. Fabre, S. Flandrois, M. Fourmigué, B. Gallois, J. Gaultier, K. Heuzé, R. Laversanne, P. Launois, R. Moret, S. S. P. Parkin, A. Pénicaud, J. P. Pouget, S. Ravy, J. C. Scott, J. Torrance, and P. Vaca is warmly acknowledged. We also thank the Centre National de la Recherche Scientifique, the University of Bordeaux 1, and the Conseil Régional d'Aquitaine for their financial support.

7. References

(1) For a review, see: Krogmann, K. *Angew. Chem., Int. Ed. Engl.* **1969**, *8*, 35. Although these materials were important to reveal some singular behavior of quasi-1D materials, we will not describe their ESR properties in the following review as they contain inorganic spin carriers.
(2) Endres, H. *Extended Linear Chain Coumpounds*; Miller, J. S., Ed.; Plenum Press: New York, 1983; Vol. 3, p 263.
(3) Ferraris, J.; Cowan, D. O.; Walatka, V.; Perlstein, J. H., Jr. *J. Am. Chem. Soc.* **1973**, *95*, 948.
(4) Coleman, L. B.; Cohen, M. J.; Sandman, D. J.; Yamagishi, F. G.; Garito, A. F.; Heeger, A. J. *Solid State Commun.* **1973**, *12*, 1125.
(5) Jérome, D.; Mazaud, A.; Ribault, M.; Bechgaard, K. *J. Phys. Lett.* **1980**, *41*, L95.
(6) Bechgaard, K.; Carneiro, K.; Olsen, M.; Rasmussen, F. B.; Jacobsen, C. S. *Phys. Rev. Lett.* **1981**, *46*, 852.
(7) Krief, A. *Tetrahedron* **1986**, *42*, 1209; Schukat, G.; Fanghänel, E. *Sulfur Rep.* **1996**, *18*, 1.
(8) Yaffet, Y. *Solid State Physics*; Ehrenreich, H., Seitz, F., Turnbull, D., Eds.; Academic Press: New York, 1963; Vol. 14, p 1.
(9) Weger, M. *J. Phys. Colloq. C6* **1978**, *39*, 1456.
(10) Forró, L.; Mihály, L. *Rep. Prog. Phys.* **2001**, *64*, 649.
(11) Griswold, T. W.; Kip, A. F.; Kittel, C. *Phys. Rev.* **1952**, *88*, 951.
(12) See for example: Atherton, N. M. *Electron Spin Resonance*; Wiley and Sons: New York, 1973.
(13) Kinoshita, N.; Ukachi, T.; Tokumoto, M.; Anzai, H.; Ishiguro, T.; Saito, G.; Yamabe, T.; Teramae, H. *J. Phys. Colloq. C3* **1983**, *44*, 1029.
(14) Kinoshita, N.; Tokumoto, M.; Anzai, H.; Ishiguro, T.; Saito, G.; Yamabe, T.; Teramae, H. *J. Phys. Soc. Jpn.* **1984**, *53*, 1504.
(15) Terahara, A.; Ohya-Nishiguchi, H.; Hirota, N.; Awaji, H.; Kawase, T.; Yoneda, S.; Sugimoto, T.; Yoshida, Z. *Bull. Chem. Soc. Jpn.* **1984**, *57*, 1760.
(16) Stone, A. J. *Proc. R. Soc. London* **1963**, *A271*, 424.
(17) At this point, these axes are the "local" eigendirections for a single molecule. This is also the eigendirections for the whole solid if all of the molecules have the same orientation. We will discuss at the end of this paragraph the case where several molecular orientations are present in the crystal structure.
(18) Bloch, F. *Phys. Rev.* **1946**, *70*, 460.
(19) Pines, D.; Slichter, C. P. *Phys. Rev.* **1955**, *100*, 1014.
(20) Beuneu, F.; Monod, P. *Phys. Rev. B* **1978**, *18*, 2422.
(21) Fehér, G.; Kip, A. F. *Phys. Rev.* **1955**, *98*, 337. Dyson, F. J. *Phys. Rev.* **1955**, *98*, 349.
(22) Pifer, J. H.; Magno, R. *Phys. Rev. B* **1971**, *3*, 663.
(23) Tomkiewicz, Y.; Taranko, A. R. *Phys. Rev. B* **1978**, *18*, 733.
(24) Forró, L.; Cooper, J. R.; Sekretarczyk, G.; Krupski, M.; Kamarás, K. *J. Phys.* **1987**, *48*, 413.
(25) (a) Hennessy, M. J.; McElwee, C. D.; Richards, P. M. *Phys. Rev. B* **1973**, *7*, 930. (b) Dietz, R. E.; Merritt, F. R.; Dingle, R.; Hone, D.; Silbernagel, B. G.; Richards, P. M. *Phys. Rev. Lett.* **1971**, *26*, 1186.
(26) Tomkiewicz, Y. *Phys. Rev. B* **1979**, *19*, 4038.
(27) Huang, T. Z.; Taylor, R. P.; Soos, Z. G. *Phys. Rev. Lett.* **1972**, *28*, 1054.
(28) Keryer, G.; Delhaès, P.; Amiell, J.; Flandrois, S.; Tissier, B. *Phys. Status Solidi B* **1980** *100*, 251.
(29) Michel, P.; Moradpour, A.; Ribault, M.; Petit, P.; André, J.-J. *J. Chem. Soc., Chem. Commun.* **1989**, 1173.
(30) Takagi, S.; Tanaka, M.; Deguchi, H.; Mito, M.; Takeda, K. *Mol. Cryst. Liq. Cryst.* **1999**, *334*, 247.
(31) Carrington, A.; McLachlan, A. D. *Introduction to Magnetic Resonance*; Harper and Row: New York, 1966; p 204.
(32) Chesnut, D. B.; Phillips, W. D. *J. Chem. Phys.* **1961**, *35*, 1002.
(33) Chesnut, D. B.; Arthur, P. J., Jr. *J. Chem. Phys.* **1962**, *36*, 2669.
(34) Jones, M. T.; Chesnut, D. B. *J. Chem. Phys.* **1963**, *38*, 1311.
(35) Bailey, J. C.; Chesnut, D. B. *J. Chem. Phys.* **1969**, *51*, 5118.
(36) Kepler, R. G. *J. Chem. Phys.* **1963**, *39*, 3528.
(37) Thomas, D. D.; Keller, H.; McConnell, H. M. *J. Chem Phys.* **1963**, *39*, 2321.
(38) Faucher, J. P.; Robert, H. *C. R. Acad. Sci. Ser. B* **1970**, *270*, 174.
(39) Blanc, J. P.; Cheminat, B.; Robert, H. *C. R. Acad. Sci. Ser. B* **1971**, *273*, 147.
(40) Hove, M. J.; Hoffmann, B. M.; Ibers, J. A. *J. Chem. Phys.* **1972**, *56*, 3940.
(41) Hibma, T.; Dupuis, P.; Kommandeur, J. *Chem. Phys. Lett.* **1972**, *15*, 17.
(42) Hibma, T.; Sawatzky, G. A.; Kommandeur, J. *Chem. Phys. Lett.* **1973**, *23*, 21.
(43) Hibma, T.; Kommandeur, J. *Solid State Commun.* **1975**, *17*, 259.
(44) Hibma, T.; Kommandeur, J. *Phys. Rev. B* **1975**, *12*, 2608.
(45) Hibma, T.; Sawatzky, G. A.; Kommandeur, J. *Phys. Rev. B* **1977**, *15*, 3959.
(46) Nordio, P. L.; Soos, Z. G.; McConnell, H. M. *Annu. Rev. Phys. Chem.* **1966**, *17*, 237.
(47) Silverstein, A. J.; Soos, Z. G. *Chem. Phys. Lett.* **1976**, *39*, 525.
(48) Flandrois, S.; Amiell, J.; Carmona, F.; Delhaès, P. *Solid State Commun.* **1975**, *17*, 287.
(49) Flandrois, S.; Boissonade, J. *Chem. Phys. Lett.* **1978**, *58*, 596.
(50) Flandrois, S.; Choukroun, M. L.; Delhaès, P.; Giuntini, J. C.; Jullien, D.; Zanchetta, J. V. *Mol. Cryst. Liq. Cryst.* **1979**, *52*, 339.
(51) Harms, R. H.; Keller, H. J.; Nöthe, D.; Werner, M.; Gundel, D.; Sixl, H.; Soos, Z. G.; Metzger, R. M. *Mol. Cryst. Liq. Cryst.* **1981**, *65*, 179.
(52) Metzger, R. M.; Heimer, N. E.; Gundel, D.; Sixl, H.; Harms, R. H.; Keller, H. J.; Nöthe, D.; Wehe, D. *J. Chem. Phys.* **1982**, *77*, 6203.
(53) Grossel, M. C.; Evans, F. A.; Hriljac, J. A.; Morton, J. R.; LePage, Y.; Preston, K. F.; Sutcliffe, L. H.; Williams, A. J. *J. Chem. Soc. Chem. Commun.* **1990**, 439.
(54) Grossel, M. C.; Evans, F. A.; Hriljac, J. A.; Prout, K.; Weston, S. C. *J. Chem. Soc. Chem. Commun.* **1990**, 1494.
(55) Hynes, R. C.; Morton, J. R.; Preston, K. F.; Williams, A. J.; Evans, F.; Grossel, M. C.; Sutcliffe, L. H.; Weston, S. C. *J. Chem. Soc., Faraday Trans.* **1991**, *87*, 2229.
(56) Hynes, R. C.; Krusic, P. J.; Preston, K. F.; Springs, J. J.; Williams, A. J.; Miller, J. S. *J. Am. Chem. Soc.* **1995**, *117*, 2547.
(57) Meneghetti, M.; Teffeletti, A. *Synth. Met.* **1999**, *103*, 2318.
(58) Hibma, T. Ph.D. Thesis, Groningen, Holland, 1974.
(59) Kommandeur, J. *The Physics and Chemistry of Low Dimensional Solids*; Alcacer, L., Ed.; NATO Adv. Series C; D. Reidel Publishing: Dordrecht, The Netherlands, 1980; Vol. 56, p 197.
(60) Suzuki, N. *Phys. Lett. A* **1982**, *89*, 208.
(61) Graja, A.; Sekretarczyk, G.; Krupski, M. *J. Phys.* **1985**, *46*, 1743.
(62) Huizinga, S.; Kommandeur, J.; Sawatzky, G. A.; Thole, B. T.; Kopinga, K.; De Jonge, W. J. M.; Roos, J. *Phys. Rev. B* **1979**, *19*, 4723.
(63) For a review, see: Bray, J. W.; Interrante, L. V.; Jacobs, I. S.; Bonner *Extended Linear Chain Coumpounds*; Miller, J. S., Ed.; Plenum Press: New York, 1983; Vol. 3, p 353.
(64) Oostra, S.; De Lange, P.; Visser, R. J. J. *J. Phys. Colloq. C3* **1983**, *44*, 1383.
(65) Oostra, S. PhD Thesis, Groningen, Holland, 1985; Schwerdtfeger, C. F.; Oostra, S.; Sawatzky, A. *Phys. Rev. B* **1982**, *26*, 1462.
(66) Korving, W. H.; Hijmans, T. W.; Brom, H. B.; Oostra, S.; Sawatzky, G. A.; Kommandeur, J. *J. Phys. Colloq. C3* **1983**, *44*, 1425.
(67) Hijmans, T. W.; Brom, H. B. *J. Phys. C: Solid State Phys.* **1986**, *19*, 5629. Hijmans, T. W.; Brom, H. B.; De Jongh, L. J. *Synth. Met.* **1987**, *19*, 373.
(68) Nojiri, H.; Hamamoto, T.; Fujita, O.; Akimitsu, J.; Takagi, S.; Motokawa, M. *J. Magn. Magn. Mater.* **1998**, *177*−*181*, 687. Note that high-field ESR studies have also been made in inorganic

Spin-Peierls materials such as $CuGeO_3$: Brill, T. M.; Boucher, J. P.; Voiron, J.; Dhalenne, G.; Revcolevschi, A.; Renard, J. P. *Phys. Rev. Lett.* **1994**, *73*, 1545.
(69) Schwerdtfeger, C. F.; Wagner, H. J.; Sawatzky, G. A. *Solid State Commun.* **1980**, *35*, 7.
(70) Schwerdtfeger, C. F.; Oostra, S.; Sawatzky, G. A. *Phys. Rev. B* **1982**, *25*, 1786.
(71) Sekikawa, T.; Okamoto, H.; Mitani, T.; Inabe, T.; Maruyama, T.; Kobayashi, T. *Phys. Rev. B* **1997**, *55*, 4182.
(72) Radhakrishnan, T. P.; Van Engen, D.; Soos, Z. G. *Mol. Cryst. Liq. Cryst.* **1987**, *150b*, 473.
(73) Lépine, Y.; Caillé, A.; Larochelle, V. *Phys. Rev. B* **1978**, *18*, 3585.
(74) Takaoka, Y.; Motizuki, K. *J. Phys. Soc. Jpn* **1979**, *47*, 1752.
(75) Matsuda, Y.; Sakakibara, T.; Goto, T.; Ito, Y. *J. Phys. Soc. Jpn* **1986**, *55*, 3225.
(76) Liu, Q.; Ravy, S.; Pouget, J. P.; Coulon, C.; Bourbonnais, C. *Synth. Met.* **1993**, *56*, 1840.
(77) Coulon, C.; Flandrois, S.; Delhaès, P.; Hauw, C.; Dupuis, P. *Phys. Rev. B* **1981**, *23*, 2850.
(78) Abkowitz, M. A.; Epstein, A. J.; Griffiths, C. H.; Miller, J. S.; Slade, M. L. *J. Am. Chem. Soc.* **1977**, *99*, 5304.
(79) Dupuis, P.; Flandrois, S.; Delhaès, P.; Coulon, C. *J. Chem. Soc. Chem. Commun.* **1978**, *8*, 328.
(80) Filhol, A.; Gallois, B.; Laugier, J.; Dupuis, P.; Coulon, C. *Mol. Cryst. Liq. Cryst.* **1982**, *84*, 17.
(81) Gallois, B.; Gaultier, J.; Pouget, J. P.; Coulon, C.; Filhol, A. *J. Phys. Colloq. C3* **1983**, *44* 1307.
(82) Coulon, C. Ph.D. Thesis, Bordeaux, France, 1982.
(83) Coulon, C.; Delhaès, P.; Flandrois, S.; Amiell, J.; Bonjour, E.; Dupuis, P. *J. Phys.* **1985**, *46*, 783.
(84) Epstein, A. J.; Etemad, S.; Garito, A. F.; Heeger, A. J. *Phys. Rev. B* **1972**, *5*, 952.
(85) Bozler, H. M.; Gould, C. M.; Clark, W. G. *Phys. Rev. Lett.* **1980**, *45*, 1303.
(86) Sanny, J.; Grüner, G.; Clark, W. G. *Solid State Commun.* **1980**, *35*, 657.
(87) Bechgaard, K.; Andersen, J. R. *The Physics and Chemistry of Low Dimensional Solids*; Alcacer, L., Ed.; Nato Adv. Study Institutes Series C; D. Reidel Publishing: Dordrecht, The Netherlands, 1979; Vol. 56, p 247.
(88) Fabre, J. M.; Gousmia, A. K.; Giral, L.; Galtier, M. *New J. Chem.* **1988**, *12*, 119.
(89) Walsh, W. M., Jr.; Rupp, L. W., Jr; Schafer, D. E.; Thomas, G. A. *Bull. Am. Phys. Soc.* **1976**, *19*, 296.
(90) Tomkiewicz, Y.; Taranko, A. R.; Schumaker, R. *Phys. Rev. B* **1977**, *16*, 1380.
(91) Tomkiewicz, Y.; Torrance, J. B.; Bechgaard, K.; Mayerle, J. J. *Bull. Am. Phys. Soc.* **1979**, *24*, 232.
(92) Tomkiewicz, Y.; Scott, B. A.; Tao, L. J.; Title, R. S. *Phys. Rev. Lett.* **1974**, *32*, 1363.
(93) Tomkiewicz, Y.; Taranko, A. R.; Torrance, J. B. *Phys. Rev. Lett.* **1976**, *36*, 751.
(94) Tomkiewicz, Y.; Taranko, A. R.; Engler, E. M. *Phys. Rev. Lett.* **1976**, *37*, 1705.
(95) Tomkiewicz, Y.; Taranko, A. R.; Torrance, J. B. *Phys. Rev. B* **1977**, *15*, 1017.
(96) Tomkiewicz, Y.; Andersen, J. R.; Taranko, A. R. *Phys. Rev. B* **1978**, *17*, 1579.
(97) Tomkiewicz, Y.; Welber, B.; Seiden, P. E.; Schumaker, R. *Solid State Commun.* **1977**, *23*, 471.
(98) Torrance, J. B.; Tomkiewicz, Y.; Bozio, R.; Pecile, C.; Wolfe, C. R.; Bechgaard, K. *Phys. Rev. B* **1982**, *26*, 2267.
(99) Tomkiewicz, Y.; Taranko, A. R.; Green, D. C. *Solid State Commun.* **1976**, *20*, 767.
(100) Mizoguchi, K.; Watanabe, H.; Sakamoto, H.; Kume, K.; Kubota, M.; Saito, G. *Synth. Met.* **1997**, *86*, 2041.
(101) Gulley, J. E.; Weiher, J. F. *Phys. Rev. Lett.* **1975**, *34*, 1061.
(102) Tomkiewicz, Y. *The Physics and Chemistry of Low Dimensional Solids*; Alcacer, L., Ed.; Nato Adv. Study Institutes Series C; D. Reidel Publishing: Dordrecht, The Netherlands, 1980; Vol. 56, p 187.
(103) Kagoshima, S.; Anzai, H.; Kaumura, K.; Ishiguro, T. *J. Phys. Soc. Jpn* **1975**, *39*, 1143.
(104) Rybaczewski, E. F.; Smith, L. S.; Garito, A. F.; Heeger, A. J.; Silberganel, B. G. *Phys. Rev. B* **1976**, *14*, 2746.
(105) Tomkiewicz, Y.; Engler, E. M.; Schultz, T. D. *Phys. Rev. Lett.* **1975**, *35*, 456.
(106) Delhaès, P.; Flandrois, S.; Amiell, J.; Keryer, G.; Toreilles, E.; Fabre, J. M.; Giral, L.; Jacobsen, C. S.; Bechgaard, K. *J. Phys. Lett.* **1977**, *38*, L-233.
(107) Ehrenfreund, E.; Khanna, S. K.; Garito, A. F.; Heeger, A. J. *Solid State Commun.* **1977**, *22*, 139.
(108) Walsh, W. M.; Rupp, L. W., Jr.; Wudl, F.; Kaplan, M. L.; Schafer, D. E.; Thomas, G. A.; Gemmer, R. *Solid. State Commun.* **1980**, *33*, 413.
(109) Sakamoto, H.; Mizoguchi, K.; Hasegawa, T. *Synth. Met.* **2003**, *133*, 627.
(110) Berthier, C.; Cooper, J. R.; Jérome, D.; Soda, G.; Weyl, C.; Fabre, J. M.; Giral, L. *Mol. Cryst. Liq. Cryst.* **1976**, *32*, 267.
(111) Jeszka, J. K.; Tracz, A.; Kryszewski, M.; Ulanski, J. *Synth. Met.* **1988**, *27*, B115.
(112) Jeszka, J. K. *Synth. Met.* **1993**, *59*, 151.
(113) Takahashi, M.; Sugano, T.; Kinoshita, M. *Bull. Chem. Soc. Jpn.* **1984**, *57*, 26.
(114) La Placa, S. J.; Corfield, P. W. R.; Thomas, R.; Scott, B. A. *Solid State Commun.* **1975**, *17*, 635.
(115) Wudl, F.; Schafer, D. E.; Walsh, W. M., Jr.; Rupp, L. W.; DiSalvo, F. J.; Waszczack, J. V.; Kaplan, M. L.; Thomas, G. A. *J. Chem. Phys.* **1977**, *66*, 377.
(116) Somoano, R. B.; Gupta, A.; Hadek, V.; Novotny, M.; Jones, M.; Datta, T.; Deck, R.; Hermann, A. M. *J. Chem. Phys.* **1975**, *63*, 4970; *Phys. Rev. B* **1977**, *15*, 595.
(117) Somoano, R. B.; Yen, S. P. S.; Hadek, V.; Khanna, S. K.; Novotny, M.; Datta, T.; Hermann, A. M.; Woollam, J. A. *Phys. Rev. B* **1978**, *17*, 2853.
(118) (a) Delhaès, P.; Manceau, J. P.; Coulon, C.; Flandrois, S.; Hilti, B.; Mayer, C. W. Quasi-One-Dimensional Conductors. *Lecture Notes in Physics*; Springer, Berlin, 1979; Vol. 96, p 324. (b) Coulon, C. "Thèse 3rd cycle", Bordeaux, France, 1979.
(119) Delhaès, P.; Coulon, C.; Flandrois, S.; Hilti, B.; Mayer, C. W.; Rihs, G.; Rivory, J. *J. Chem. Phys.* **1980**, *73*, 1452.
(120) Weyl, C.; Brossard, L.; Tomic, S.; Mailly, D.; Jérome, D. *Mol. Cryst. Liq. Cryst.* **1985**, *120*, 263.
(121) Amiell, J.; Delhaès, P.; Flandrois, S.; Strzelecka, H. *Solid State Commun.* **1981**, *39*, 55.
(122) Giamarchi, T. *Phys. Rev. B* **1991**, *44*, 2905.
(123) Wudl, F. *Chemistry and Physics of one-dimensional metals*; NATO Adv. Institutes, Series B; Plenum Press: New York, 1976; Vol. 25, p 233.
(124) Delhaès, P.; Coulon, C.; Amiell, J.; Flandrois, S.; Toreilles, E.; Fabre, J. M.; Giral, L. *Mol. Cryst. Liq. Cryst.* **1979**, *50*, 43.
(125) Jérome, D.; Mazaud, A.; Ribault, M.; Bechgaard, K. *J. Phys. Lett.* **1980**, *41*, L-95.
(126) Bechgaard, K.; Carneiro, K.; Olsen, M.; Rasmussen, F. B.; Jacobsen, C. S. *Phys. Rev. Lett.* **1981**, *46*, 852.
(127) Pedersen, H. J.; Scott, J. C.; Bechgaard, K. *Solid State Commun.* **1980**, *35*, 207.
(128) Scott, J. C.; Pedersen, H. J.; Bechgaard, K. *Chem. Scripta* **1981**, *17*, 55.
(129) Pedersen, H. J.; Scott, J. C.; Bechgaard, K. *Phys. Rev. B* **1981**, *24*, 5014.
(130) Bechgaard, K.; Carneiro, K.; Rasmussen, F. B.; Olsen, M.; Rindorf, G.; Jacobsen, C. S.; Pedersen, H. J.; Scott, J. C. *J. Am. Chem. Soc.* **1981**, *103*, 2440.
(131) Azevedo, L. J.; Schirber, J. E.; Greene, R. L.; Engler, E. M. *Mol. Cryst. Liq. Cryst.* **1982**, *79*, 123.
(132) Maaroufi, A.; Coulon, C.; Flandrois, S.; Delhaès, P.; Mortensen, K.; Bechgaard, K. *Solid State Commun.* **1983**, *48*, 555.
(133) Coulon, C.; Delhaès, P.; Flandrois, S.; Lagnier, R.; Bonjour, E.; Fabre, J. M. *J. Phys.* **1982**, *43*, 1059.
(134) Onoda, M.; Nagasawa, H.; Kobayashi, K. *J. Phys. Soc. Jpn.* **1985**, *54*, 1240.
(135) Laversanne, R.; Coulon, C.; Gallois, Pouget, J. P.; Moret, R. *J. Phys. Lett.* **1984**, *45*, L-393.
(136) Mortensen, K.; Tomkiewicz, Y.; Schultz, T. D.; Engler, E. M.; Patel, V. V.; Taranko, A. R. *Solid State Commun.* **1981**, *40*, 915.
(137) Coulon, C.; Delhaès, P.; Amiell, J.; Manceau, J. P.; Fabre, J. M.; Giral, L. *J. Phys.* **1982**, *43*, 1721.
(138) Adrian, F. J. *Phys. Rev. B* **1986**, *33*, 1537.
(139) Adrian, F. J. *J. Phys. C: Solid State Phys.* **1987**, *20*, 5135.
(140) Forró, L.; Beuneu, F. *Solid State Commun.* **1982**, *44*, 623.
(141) Sanquer, M.; Bouffard, S. *Mol. Cryst. Liq. Cryst.* **1985**, *119*, 147.
(142) Tomic, S.; Jérome, D.; Monod, P.; Bechgaard, K. *J. Phys. Lett.* **1982**, *43*, L-839.
(143) Tazuke, Y.; Nagate, K. *J. Phys. Soc. Jpn.* **1975**, *32*, 337.
(144) Baillargeon, P.; Bourbonnais, C.; Tomic, S.; Vaca, P.; Coulon, C. *Synth. Met.* **1988**, *27*, B83.
(145) Dumm, M.; Loidl, A.; Alavi, B.; Starkey, K. P.; Montgomery, L. K.; Dressel, M. *Phys. Rev. B* **2000**, *62*, 6512.
(146) Vaca, P.; Coulon, C.; Ravy, S.; Pouget, J. P.; Fabre, J. M. *J. Phys. I* **1991**, *1*, 125.
(147) Tomic, S.; Jérome, D.; Cooper, J. R.; Bechgaard, K. *Synth. Met.* **1988**, *27*, B645. Tomic, S.; Cooper, J. R.; Kang, W.; Jérome, D.; Maki, K. *J. Phys. I France* **1991**, *1*, 1603.
(148) Tomic, S.; Pouget, J. P.; Jérome, D.; Bechgaard, K.; Williams, J. M. *J. Phys.* **1983**, *44*, 375.
(149) Coulon, C.; Parkin, S. S. P.; Laversanne, R. *Phys. Rev. B* **1985**, *31*, 3583; *Mol. Cryst. Liq. Cryst.* **1985**, *119*, 325.
(150) Parkin, S. S. P.; Coulon, C.; Moret, R.; Pouget, J. P. *Phys. Rev. B* **1987**, *36*, 2246.
(151) Pouget, J. P. *Chem. Scripta* **1981**, *17*, 85.
(152) Pouget, J. P.; Moret, R.; Comès, R.; Bechgaard, K.; Fabre, J. M.; Giral, L. *Mol. Cryst. Liq. Cryst.* **1982**, *79*, 129.
(153) Dumoulin, B.; Bourbonnais, C.; Ravy, S.; Pouget, J. P.; Coulon, C. *Phys. Rev. Lett.* **1996**, *76*, 1360; *Synth. Met.* **1997**, *85*, 1773.
(154) Caron, L. G.; Creuzet, F.; Butaud, P.; Bourbonnais, C.; Jérome, D.; Bechgaard, K. *Synth. Met.* **1988**, *27*, B123.

(155) Laversanne, R.; Amiell, J.; Coulon, C.; Garrigou-Lagrange, C.; Delhaès, P. *Mol. Cryst. Liq. Cryst.* **1985**, *119*, 317.
(156) Creuzet, F.; Bourbonnais, C.; Caron, L. G.; Jérome, D.; Bechgaard, K. *Synth. Met.* **1987**, *19*, 289.
(157) Coulon, C. *J. Phys. Colloq. C3* **1983**, *44*, 885.
(158) Bourbonnais, C.; Jérome, D. *Science* **1998**, *281*, 1155.
(159) Wilhelm, H.; Jaccard, D.; Duprat, R.; Bourbonnais, C.; Jérome, D.; Moser, J.; Carcel, C.; Fabre, J. M. *Eur. Phys. J. B* **2001**, *21*, 175.
(160) Laversanne, R.; Amiell, J.; Coulon, C. *Mol. Cryst. Liq. Cryst.* **1986**, *137*, 169.
(161) Coulon, C. *J. Phys. IV France* **2004**, *114*, 15.
(162) Wzietek, P.; Bourbonnais, C.; Creuzet, F.; Jérome, D.; Bechgaard, K. *Europhys. Lett.* **1990**, *12*, 453.
(163) Zorko, A.; Arcon, D.; Biljakovic, K.; Carcel, C.; Fabre, J. M.; Dolinsek, J. *Phys. Rev. B* **2001**, *64*, 172404−1.
(164) Auban, P.; Jérome, D.; Lerstrup, K.; Johannsen, I.; Jorgensen, M.; Bechgaard, K. *J. Phys. France* **1989**, *50*, 2727.
(165) Laversanne, R.; Coulon, C.; Gallois, B.; Pouget, J. P.; Moret, R. *J. Phys. Lett.* **1985**, *45*, L393.
(166) Javadi, H. H. S.; Laversanne, R.; Epstein, A. J. *Phys. Rev. B* **1988**, *37*, 4280.
(167) Chow, D. S.; Zamborsky, F.; Alavi, B.; Tantillo, D. J.; Baur, A.; Merlic, C. A.; Brown, S. E. *Phys. Rev. Lett.* **2000**, *85*, 1698.
(168) Nad, F.; Monceau, P.; Carcel, C.; Fabre, J. M. *Phys. Rev. B* **2000**, *62*, 1753.
(169) (a) Coulon, C.; Maaroufi, A.; Amiell, J.; Dupart, E.; Flandrois, S.; Delhaès, P.; Moret, R.; Pouget, J. P.; Morand, J. P. *Phys. Rev. B* **1982**, *26*, 6322. (b) Maaroufi, A. Ph.D. Thesis, Bordeaux, France, 1986.
(170) Dumm, M.; Dressel, M.; Loidl, A.; Fravel, B. W.; Montgomery, L. K. *Physica B* **1999**, *259*−*261*, 1005. Dumm, M.; Dressel, M.; Loidl, A.; Fravel, Starkey, K. P.; Montgomery, L. K. *Synth. Met.* **1999**, *103*, 2068. Dressel, M.; Hesse, P.; Kirchner, S.; Unteriener, G.; Dumm, M.; Hemberger, J.; Loidl, A.; Montgomery, L. K. *Synth. Met.* **2001**, *120*, 719.
(171) Dumm, M.; Loidl, A.; Fravel, B. W.; Starkey, K. P.; Montgomery, L. K.; Dressel, M. *Phys. Rev. B* **2000**, *61*, 511.
(172) Nakamura, T. *Synth. Met.* **2003**, *137*, 1181; *J. Phys. Soc. Jpn.* **2003**, *72*, 213; *Physica B* **2003**, *329*−*333*, 1148.
(173) Batail, P.; Ouahab, L.; Torrance, J. B.; Pylman, M. L.; Parkin, S. S. P. *Solid State Commun.* **1985**, *55*, 597.
(174) Pénicaud, A.; Batail, P.; Tomic, S.; Jérome, D.; Coulon, C. *Synth. Met.* **1988**, *27*, B103. Pénicaud, A.; Batail, P.; Davidson, P.; Levelut, A. M.; Coulon, C.; Perrin, C. *Chem. Mater.* **1990**, *2*, 117. Pénicaud, A.; Batail, P.; Coulon, C.; Canadell, E.; Perrin, C. *Chem. Mater.* **1990**, *2*, 123.
(175) Yamaguchi, T. *Physica B* **2000**, *284*−*288*, 1585.
(176) Parkin, S. S. P.; Engler, E. M.; Schumaker, R. R.; Lagier, R.; Lee, V. Y.; Scott, J. C.; Greene, R. L. *Phys. Rev. Lett.* **1983**, *50*, 270. Parkin, S. S. P.; Engler, E. M.; Schumaker, R. R.; Lagier, R.; Lee, V. Y.; Voiron, J.; Carneiro, K.; Scott, J. C.; Greene, R. L. *J. Phys. Colloq. C3* **1983**, *44*, 791.
(177) For a review, see for example: Williams, J. M.; Ferraro, J. R.; Thorn, R. J.; Carlson, K. D.; Geiser, U.; Wang, H. H.; Kini, A. M.; Whangbo, M.-H. *Organic Superconductors (including fullerenes)*; Prentice Hall: New Jersey, 1992.
(178) Hasegawa, T.; Akutagawa, T.; Nakamura, T. *Synth. Met.* **2003**, *133*−*134*, 623. Sakamoto, H.; Mizoguchi, K.; Hesegawa, T. *Synth. Met.* **2003**, *133*−*134*, 627.
(179) Yamamoto, H. M.; Hagiwara, M.; Kato, R. *Synth. Met.* **2003**, *133*−*134*, 449. Yamamoto, H. M.; Tajima, N.; Hagiwara, M.; Kato, R.; Yamaura, J.-I. *Synth. Met.* **2003**, *135*−*136*, 623.
(180) Graja, A.; Dyachenko, O. A. *Macromol. Symp.* **1996**, *104*, 223.
(181) For an extensive review of the results before 1992, see for example chapter 5 in reference 177.
(182) McKenzie, R. H. *Comments Cond. Matt. Phys.* **1998**, *18*, 309. Limelette, P.; Wzietek, P.; Florens, S.; Georges, A.; Costi, T. A.; Pasquier, C.; Jérome, D.; Mézière, C.; Batail, P. *Phys. Rev. Lett.* **2003**, *91*, 016401−1.
(183) Chasseau, D.; Gaultier, J.; Miane, J. L.; Coulon, C.; Delhaès, P.; Flandrois, S.; Fabre, J. M.; Giral, L. *J. Phys. Colloq. C3* **1983**, *44*, 1223.
(184) Fabre, J. M.; Giral, L.; Dupart, E.; Coulon, C.; Delhaès, P. *J. Chem. Soc., Chem Commun.* **1983**, 426. Delhaès, P.; Dupart, E.; Amiell, J.; Coulon, C.; Fabre, J. M.; Giral, L.; Chasseau, D.; Gallois, B. *J. Phys. Colloq. C3* **1983**, *44*, 1239.
(185) Coulon, C.; Laversanne, R.; Amiell, J.; Dupart, E.; Manhal, E.; Fabre, J. M. *Synth. Met.* **1987**, *19*, 367.
(186) Kikuchi, K.; Yakushi, K.; Kuroda, H.; Kobayashi, K.; Honda, M.; Katayama, C.; Tanaka, J. *Chem. Lett.* **1984**, 1885; Kikuchi, K.; Yakushi, K.; Kuroda, H.; Ikemoto, I.; Kobayashi, K. *Mol. Cryst. Liq. Cryst.* **1985**, *125*, 345.
(187) Delhaès, P.; Dupart, E.; Manceau, J. P.; Coulon, C.; Chasseau, D.; Gaultier, J.; Fabre, J. M.; Giral, L. *Mol. Cryst. Liq. Cryst.* **1985**, *119*, 269.
(188) Ducasse, L.; Coulon, C.; Chasseau, D.; Yagbasan, R.; Fabre, J. M.; Gouasmia, A. K. *Synth. Met.* **1988**, *27*, B543.
(189) Coulon, C.; Vaca, P.; Granier, T.; Gallois, B. *Synth. Met.* **1988**, *27*, B449.
(190) Vaca, P.; Granier, T.; Gallois, B.; Coulon, C.; Gouasmia, A. K.; Fabre, J. M. *J. Phys. C: Solid Stat. Phys.* **1988**, *211*, 5719.
(191) Yoneyama, N.; Miyazaki, A.; Enoki, T.; Saito, G. *Bull. Chem. Soc. Jpn.* **1999**, *72*, 639.
(192) Laversanne, R.; Coulon, C.; Amiell, J.; Morand, J. P. *Synth. Met.* **1987**, *19*, 425; *Europhys. Lett.* **1986**, *2*, 401.
(193) Vaca, P.; Coulon, C.; Ducasse, L.; Granier, T.; Gallois, B.; Fabre, J. M.; Gouasmia, A. K. *J. Phys.: Condens. Matter* **1989**, *1*, 4971.
(194) Shimizu, Y.; Miyagawa, K.; Kanoda, K.; Maesato, M.; Saito, G. *Phys. Rev. Lett.* **2003**, *91*, 107001−1.
(195) Emge, J. T.; Wang, H. H.; Leung, P. C. W.; Rust, P. R.; Cook, J. D.; Jackson, P. L.; Carlson, K. D.; Williams, J. M.; Whangbo, M.-H.; Venturini, E. L.; Schirber, J. E.; Azevedo, L. J.; Ferraro, J. R. *J. Am. Chem. Soc.* **1986**, *108*, 695. Note that is this paper type I means *strongly dimerized*.
(196) Emge, J. T.; Wang, H. H.; Bowman, M. K.; Pipan, C. M.; Carlson, K. D.; Beno, M. A.; Hall, L. N.; Anderson, B. A.; Williams, J. M.; Whangbo, M.-H. *J. Am. Chem. Soc.* **1987**, *109*, 2016.
(197) Kinoshita, N.; Tokumoto, M.; Anzai, H.; Saito, G. *Synth. Met.* **1987**, *19*, 203.
(198) Yoneyama, N.; Miyazaki, A.; Enoki, T.; Saito, G. *Synth. Met.* **1997**, *86*, 2029.
(199) Laversanne, R. Ph.D. Thesis, Bordeaux, France, 1987.
(200) Coulon, C.; Laversanne, R.; Amiell, J.; Delhaès, P. *J. Phys. C: Solid State Phys.* **1986**, *19*, L753.
(201) Ward, B. H.; Rutel, I. B.; Brooks, J. S.; Schlueter, J. A.; Winter, R. W.; Gard, G. L. *J. Phys. Chem.* **2001**, *105*, 1750.
(202) Rutel, I. B.; Zvyagin, S. A.; Brooks, J. S.; Krzystek, J.; Kuhns, P.; Reyes, A. P.; Jobiliong, E.; Ward, B. H.; Schlueter, J. A.; Winter, R. W.; Gard, G. L. *Phys. Rev. B* **2003**, *67*, 214417.
(203) Chasseau, D.; Watkin, D.; Rosseinsky, M. J.; Kurmoo, M.; Talham, D. R.; Day, P. *Synth. Met.* **1988**, *24*, 117.
(204) Obertilli, S. D.; Friend, R. H.; Talham, D. R.; Kurmoo, M.; Day, P. *J. Phys. Condens. Matter* **1989**, *1*, 5671.
(205) Watson, W. H.; Kini, A. M.; Beno, M. A.; Montgomery, L. K.; Wang, H. H.; Carlson, K. D.; Gates, B. D.; Tytko, S. F.; Derose, J.; Cariss, C.; Rohl, C. A.; Williams, J. H. *Synth. Met.* **1989**, *33*, 1.
(206) Zaman, Md. B.; Toyoda, J.; Morita, Y.; Nakamura, S.; Yamochi, H.; Saito, G.; Nishimura, K.; Yoneyama, N.; Enoki, T.; Nakasuji, K. *J. Mater. Chem.* **2001**, *11*, 2211.
(207) Ward, B. H.; Schlueter, A.; Geiser, U.; Wang, H. H.; Morales, E.; Parakka, J. P.; Thomas, S. Y.; Williams, J. M. *Chem. Mater.* **2000**, *12*, 343.
(208) Pénicaud, A.; Lenoir, C.; Batail, P.; Coulon, C.; Perrin, A. *Synth. Met.* **1989**, *32*, 25.
(209) Kurmoo, M.; Day, P.; Guionneau, P.; Bravic, G.; Chasseau, D.; Ducasse, L.; Allan, M. L.; Marsden, I. D.; Friend, R. H. *Inorg. Chem.* **1996**, *35*, 4719.
(210) Wang, H. H.; Montgomery, L. K.; Geiser, U.; Porter, L. C.; Carlson, K. D.; Ferraro, J. R.; Williams, J. M.; Cariss, C. S.; Rubinstein, R. L.; Whitworth, J. R.; Evain, M.; Novoa, J. J.; Whangbo, M.-H. *Chem. Mater* **1989**, *1*, 140.
(211) Laversanne, R.; Coulon, C.; Amiell, J.; Dupart, E.; Delhaès, P.; Morand, J. P.; Manigand, C. *Solid. Stat. Commun.* **1986**, *58*, 765.
(212) Kushch, N. D.; Merzhanov, V. A.; Romanyukha, A. A. *Sov. Phys. JETP* **1989**, *69*, 205.
(213) Yamaura, J.-I.; Miyazaki, A.; Enoki, T.; Saito, G. *Phys. Rev. B* **1997**, *55*, 3649.
(214) Carneiro, K.; Scott, J. C.; Engler, E. M. *Solid State Commun.* **1984**, *50*, 477.
(215) Saito, G.; Enoki, T.; Kobayashi, M.; Imaeda, K.; Sato, N.; Inokuchi, H. *Mol. Cryst. Liq. Cryst.* **1985**, *119*, 393. Kobayashi, M.; Enoki, T.; Imaeda, K.; Inokuchi, H.; Saito, G. *Physica B* **1986**, *143B*, 550. Enoki, T.; Imaeda, K.; Kobayashi, M.; Inokuchi, H.; Saito, G. *Phys. Rev. B* **1986**, *33*, 1553.
(216) Parkin, S. S. P.; Miljak, M.; Cooper, J. R. *Phys. Rev. B* **1986**, *34*, 1485.
(217) Azevedo, L. J.; Venturini, E. L.; Kwak, J. F.; Schirber, J. E.; Williams, J. E.; Wang, H. H.; Reed, P. E. *Mol. Cryst. Liq. Cryst.* **1985**, *125*, 169.
(218) Wang, H. H.; Allen, T. J.; Schlueter, J. A.; Hallenbeck, S. L.; Stupka, D. L.; Chen, M. Y.; Despotes, A. M.; Kao, H.-C. I.; Carlson, K. D.; Geiser, U.; Williams, J. M. *Phosphorus, Sulfur Silicon Relat. Elem.* **1988**, *38*, 329.
(219) Mallah, T.; Hollis, C.; Bott, S.; Day, P.; Kurmoo, M. *Synth. Met.* **1988**, *27*, A381.
(220) Enoki, T.; Tsujikawa, K.; Suzuki, K.; Uchida, A.; Ohashi, Y.; Yamakado, H.; Yakushi, K.; Saito, G. *Phys. Rev. B* **1994**, *50*, 16287.
(221) Laversanne, R.; Amiell, J.; Delhaès, P.; Chasseau, D.; Hauw, C. *Solid State Commun.* **1984**, *52*, 177; *Mol. Cryst. Liq. Cryst.* **1985**, *119*, 405.
(222) Sekretarczyk, G.; Krupski, M.; Graja, A.; Delhaès, P.; Laversanne, R. *Physica B* **1986**, *143B*, 547.
(223) Venturini, E. L.; Azevedo, L. J.; Schirber, J. E.; Williams, J. M.; Wang, H. H. *Phys. Rev. B* **1985**, *32*, 2819.

(224) Emge, T. J.; Wang, H. H.; Beno, M. A.; Leung, P. C. W.; Firestone, M. A.; Jenkins, H. C.; Cook, J. D.; Carlson, K. D.; Williams, J. M.; Venturini, E. L.; Azevedo, L. J.; Schirber, J. E. *Inorg. Chem.* **1985**, *24*, 1736.
(225) Sugano, T.; Saito, G.; Kinoshita, M. *Phys. Rev. B* **1986**, *34*, 117.
(226) Rothaemel, B.; Forró, L.; Cooper, J. R.; Schilling, J. S.; Weger, M.; Bele, P.; Brunner, H.; Schweitzer, D.; Keller, H. J. *Phys. Rev. B* **1986**, *34*, 704.
(227) Forró, L.; Sekretarczyk, G.; Krupski, M.; Schweitzer, D.; Keller, H. *Phys. Rev. B* **1987**, *35*, 2501.
(228) Sugano, T.; Saito, G.; Kinoshita, M. *Phys. Rev. B* **1987**, *35*, 6554.
(229) Schweitzer, D.; Bele, P.; Brunner, H.; Gogu, E.; Haeberlen, U.; Hennig, I.; Klutz, I.; Swietlik, R.; Keller, H. J. *Z. Phys. B−Condensed Matter* **1987**, *67*, 489.
(230) Klotz, S.; Schilling, J. S.; Gärtner, S.; Schweitzer, D. *Solid State Commun.* **1988**, *67*, 981.
(231) Wang, H. H.; Ferraro, J. R.; Carlson, K. D.; Montgomery, L. K.; Geiser, U.; Williams, J. M.; Witworth, J. R.; Schlueter, J. A.; Hill, S.; Whangbo, M.-H.; Evain, M.; Novoa, J. J. *Inorg. Chem.* **1989**, *28*, 2267.
(232) Venturini, E. L.; Schirber, J. E.; Wang, H. H.; Williams, J. M. *Synth. Met.* **1988**, *27*, A243.
(233) Talham, D. R.; Kurmoo, M.; Day, P.; Obertilli, D. S.; Parker, I. D.; Friend, R. H. *J. Phys. C: Solid State Phys.* **1986**, *19*, L383.
(234) Montgomery, L. K.; Geiser, U.; Wang, H. H.; Beno, M. A.; Schultz, A. J.; Kini, A. M.; Carlson, K. D.; Williams, J. M.; Whitworth, J. R.; Gates, B. D.; Cariss, C. S.; Pipan, C. M.; Donega, K. M.; Wenz, C.; Kwok, W. K.; Crabtree, G. W. *Synth. Met.* **1988**, *27*, A195.
(235) Montgomery, L. K.; Wang, H. H.; Schlueter, J. A.; Geiser, U.; Carlson, K. D.; Williams, J. M.; Rubinstein, R. L.; Brennan, T. D.; Stupka, D. L.; Whitworth, J. R.; Jung, D.; Whangbo, M.-H. *Mol. Cryst. Liq. Cryst.* **1990**, *181*, 197.
(236) Hurdequint, H.; Creuzet, F.; Jérome, D. *Synth. Met.* **1988**, *27*, A183.
(237) Zhilyaeva, E. I.; Konovalikhin, S. V.; Dyachenko, O. A.; Lyubovskaya, R. N.; Makova, M. K.; Atovmyan, L. O.; Sekretarczyk, G. *Synth. Met.* **1993**, *55*, 2465.
(238) Laukhina, E.; Vidal-Gancedo, J.; Khasanov, S.; Tkacheva, V.; Zorina, L.; Shibaeva, R.; Singleton, J.; Wojciechowski, R.; Ulanski, J.; Lauklin, V.; Veciana, J.; Rovira, C. *Adv. Mater* **2000**, *12*, 1205. Laukhina, E.; Vidal-Gancedo, J.; Lauklin, V.; Veciana, J.; Chuev, I.; Tkacheva, V.; Wurst, K.; Rovira, C. *J. Am. Chem. Soc.* **2003**, *125*, 3948.
(239) Williams, J. M.; Schultz, A. J.; Geiser, U.; Carlson, K. D.; Kini, A. M.; Wang, H. H.; Kwok, W.-K.; Whangbo, M.-H.; Schirber, J. E. *Science* **1991**, *252*, 1501.
(240) Kurmoo, M.; Talham, D. R.; Pritchard, K. L.; Day, P.; Stringer, A. M.; Howard, J. A. K. *Synth. Met.* **1988**, *27*, A177.
(241) Mori, H.; Hirabayashi, I.; Tanaka, S.; Mori, T.; Inokuchi, H. *Solid State Commun.* **1990**, *76*, 35.
(242) Urayama, H.; Yamochi, H.; Saito, G.; Sugano, T.; Kinoshita, M.; Inabe, T.; Mori, T.; Maruyama, Y.; Inokuchi, H. *Chem. Lett.* **1988**, 1057. Urayama, H.; Yamochi, H.; Saito, G.; Sato, S.; Sugano, T.; Kinoshita, M.; Kawamoto, A.; Tanaka, J.; Inabe, T.; Mori, T.; Maruyama, Y.; Inokuchi, H.; Oshima, K. *Synth. Met.* **1988**, *27*, A393.
(243) Wang, H. H.; Montgomery, L. K.; Kini, A. M.; Carlson, K. D.; Beno, M. A.; Geiser, U.; Cariss, C. S.; Williams, J. M.; Venturini, E. L. *Physica C* **1988**, *156*, 173.
(244) Delhaès, P.; Amiell, J.; Ducasse, L.; Hilti, B.; Mayer, C. W.; Zambounis, J. *Physica B* **1992**, *182*, 99.
(245) Williams, J. M.; Kini, A. M.; Wang, H. H.; Carlson, K. D.; Geiser, U.; Montgomery, L. K.; Pyrka, G. J.; Watkins, D. M.; Kommers, J. M.; Boryschuk, S. J.; Strieby Crouch, A. V.; Kwok, W. K.; Schirber, J. E.; Overmyer, D. L.; Jung, D.; Whangbo, M.-H. *Inorg. Chem.* **1990**, *29*, 3262.
(246) Wang, H. H.; Carlson, K. D.; Geiser, U.; Kini, A. M.; Schultz, A. J.; Williams, J. M.; Welp, U.; Darula, K. E.; Hitsman, V. M.; Lathrop, M. W.; Megna, L. A.; Mobley, P. R.; Yaconi, G. A.; Schirber, J. E.; Overmyer, D. L. *Mater. Res. Soc. Symp. Proc.* **1992**, *247*, 471.
(247) (a) Kataev, V.; Winkel, G.; Knauf, N.; Gruetz, A.; Khomskii, D.; Wohlleben, D.; Crump, W.; Hahn, J.; Tebbe, K. F. *Physica B* **1992**, *179*, 24. (b) Kataev, V.; Winkel, G.; Khomskii, D.; Wohlleben, D.; Crump, W.; Tebbe, K. F.; Hahn, J. *Solid Stat. Commun.* **1992**, *83*, 435.
(248) Nakamura, T.; Nobutoki, T.; Takahashi, T.; Mori, H.; Mori, T.; Saito, G. *Synth. Met.* **1995**, *70*, 959.
(249) Ishiguro, T.; Ito, H.; Yamauchi, Y.; Ohmichi, E.; Kubota, M.; Yamochi, H.; Saito, G.; Kartsovnik, M. V.; Tanatar, M. A.; Sushko, Yu. V.; Logvenov, G. Yu. *Synth. Met.* **1997**, *85*, 1471.
(250) Minagawa, W.; Nakamura, T.; Takahashi, T. *Synth. Met.* **1997**, *85*, 1565.
(251) Tanakar, M. A.; Ishiguro, T.; Kondo, T.; Saito, G. *Phys. Rev. B* **2000**, *61*, 3278.
(252) Wang, H. H.; Beno, M. A.; Carlson, K. D.; Geiser, U.; Kini, A. M.; Montgomery, L. K.; Thompson, J. E.; Williams, J. M. In *Organic Superconductivity*; Kresin, V., Little, W. L., Eds.; Plenum Press: New York, 1990; p 51.
(253) Sekretarczyk, G.; Graja, A.; Goldenberg, L. M. *Synth. Met.* **1988**, *24*, 161. Firlej, L.; Graja, A.; Wolak, J.; Lyubovskaya, R. N.; Goldenberg, L. M. *Phys. Stat. Sol. B* **1989**, *154*, 333.
(254) Sekretarczyk, G.; Graja, A.; Pichet, J.; Lyubovskaya, R. N.; Lyubovskii, R. B. *J. Phys.* **1988**, *49*, 653. Sekretarczyk, G.; Graja, A.; Lyubovskaya, R. N. *Mater. Sci.* **1988**, *14*, 59.
(255) Wang, H. H.; Vogt, B. A.; Geiser, U.; Beno, M. A.; Carlson, K. D.; Kleinjan, S.; Thorup, N.; Williams, J. M. *Mol. Cryst. Liq. Cryst.* **1990**, *181*, 135.
(256) Oshima, M.; Mori, H.; Saito, G.; Oshima, K. *Chem. Lett.* **1989**, 1159.
(257) Wang, H. H.; Carlson, K. D.; Geiser, U.; Kwok, W. K.; Vashon, M. D.; Thompson, J. E.; Larsen, N. F.; McCabe, G. D.; Hulscher, R. S.; Williams, J. M. *Physica C* **1990**, *166*, 57.
(258) Kinoshita, N.; Tokumoto, M.; Anzai, H. *J. Phys. Soc. Jpn.* **1990**, *59*, 3410; Kinoshita, N.; Tokumoto, M.; Tanaka, Y.; Anzai, H. *Physica C* **1991**, *185−189*, 2677.
(259) Kinoshita, N.; Tokumoto, M.; Anzai, H. *J. Phys. Soc. Jpn.* **1991**, *60*, 2131.
(260) Tsuchiya, R.; Nakamura, T.; Takahashi, T.; Sasaki, T.; Toyota, N. *Synth. Met.* **1995**, *70*, 965.
(261) Nakamura, T.; Minagawa, W.; Takahashi, T. *Synth. Met.* **1997**, *86*, 2027.
(262) Kanoda, K.; Takahashi, T.; Kikuchi, K.; Saito, K.; Ikemoto, I.; Kobayashi, K. *Synth. Met.* **1988**, *27*, B385. Kanoda, K.; Takahashi, T.; Tokiwa, T.; Kikuchi, K.; Saito, K.; Ikemoto, I.; Kobayashi, K. *Phys. Rev. B* **1988**, *38*, 39.
(263) Kanoda, K.; Takahashi, T.; Kikuchi, K.; Saito, K.; Honda, Y.; Ikemoto, I.; Kobayashi, K.; Murata, K.; Anzai, H. *Solid State Commun.* **1989**, *69*, 415.
(264) Kanoda, K.; Takahashi, T.; Kikuchi, K.; Saito, K.; Ikemoto, I.; Kobayashi, K. *Phys. Rev. B* **1989**, *39*, 3996. Ikemoto, I.; Kikuchi, K.; Saito, K.; Kanoda, K.; Takahashi, T.; Murata, K.; Kobayashi, K. *Mol. Cryst. Liq. Cryst.* **1990**, *181*, 185.
(265) Fritz, H. P.; Gebauer, H.; Friedrich, P.; Ecker, P.; Artes, R.; Schubert, U. *Z. Naturforsch.* **1978**, *B33*, 498.
(266) Kröhnke, C.; Enkelmann, V.; Wegner, G. *Angew. Chem., Int. Ed. Engl.* **1980**, *19*, 912.
(267) Keller, H. J.; Nöthe, D.; Pritzkow, H.; Wehe, D.; Werner, M.; Koch, P.; Schweitzer, D. *Mol. Cryst. Liq. Cryst.* **1980**, *62*, 181.
(268) Kleinberg, R. L.; Ebert, L. B. *Solid Stat. Commun.* **1981**, *37*, 437.
(269) Dormann, E.; Stöcklein, W.; Sachs, G.; Bail, B.; Schwoerer, M. *J. Phys. Colloq. C3* **1983**, *44*, 1413; Dormann, E. *Phys. Blatter* **1983**, *39*, 220.
(270) Denninger, G.; Stöcklein, W.; Dormann, E.; Schwoerer, M. *Chem. Phys. Lett.* **1984**, *107*, 222.
(271) Sachs, G.; Dormann, E.; Schwoerer, M. *Solid Stat. Commun.* **1985**, *53*, 73.
(272) Maresch, G. G.; Grupp, A.; Mehring, M.; Von Schütz, J. U. *J. Phys.* **1985**, *46*, 461.
(273) Kispert, L. D.; Joseph, J.; McGraw, J.; Robinson, T.; Drobner, R. *Synth. Met.* **1987**, *19*, 67.
(274) Schätzle, A.; Von Schütz, J. U.; Wolf, H. C. *Mater. Sci.* **1984**, *10*, 235.
(275) Schätzle, A.; Von Schütz, J. U.; Wolf, H. C.; Schäfer, H.; Helberg, H. W. *Mol. Cryst. Liq. Cryst.* **1985**, *120*, 229.
(276) Koch, P.; Schweitzer, D.; Harms, R. H.; Keller, H. J.; Schäfer, H.; Helberg, H. W.; Wilckens, R.; Geserich, H. P.; Ruppel, W. *Mol. Cryst. Liq. Cryst.* **1982**, *86*, 1827.
(277) Lapouyade, R.; Morand, J. P.; Chasseau, D.; Hauw, C.; Delhaès, P. *J. Phys. Colloq. C3* **1983**, *44*, 1235.
(278) Henriques, R. T.; Alcacer, L.; Almeida, M.; Tomic, S. *Mol. Cryst. Liq. Cryst.* **1985**, *120*, 237.
(279) Morgado, J.; Alcacer, L.; Henriques, R. T.; Almeida, M. *Synth. Met.* **1995**, *71*, 1945.
(280) Wolter, A.; Burggraf, M.; Dragan, H.; Fasol, U.; Dormann, E.; Helberg, H. W.; Mueller, D. *Synth. Met.* **1995**, *71*, 1957.
(281) Fasol, U.; Dormann, E. *Phys. Lett. A* **1996**, *222*, 281.
(282) Buschhaus, C.; Moret, R.; Ravy, S.; Dormann, E. *Synth. Met.* **2000**, *108*, 21.
(283) Pongs, B.; Dormann, E. *J. Phys. Condens. Matter* **2003**, *15*, 5121.
(284) Eichele, H.; Schwoerer, M.; Kröhnke, Ch.; Wegner, G. *Chem. Phys. Lett.* **1981**, *77*, 311.
(285) Enkelmann, V.; Morra, B. S.; Kröhnke, Ch.; Wegner, G.; Heinze, J. *Chem. Phys.* **1982**, *66*, 303.
(286) Hoeptner, W.; Mehring, M.; Von Schütz, J. U.; Wolf, H. C.; Morra, B. S.; Enkelmann, V.; Wegner, G. *Chem. Phys.* **1982**, *73*, 253.
(287) Dormann, E.; Kobler, U. *Solid State Commun.* **1985**, *54*, 1003.
(288) Dormann, E. *Synth. Met.* **1988**, *27*, B529.
(289) Denninger, G. *Mol. Cryst. Liq. Cryst.* **1989**, *171*, 315.
(290) Sachs, G.; Stöcklein, W.; Bail, B.; Dormann, E.; Schwoerer, M. *Chem. Phys. Lett.* **1982**, *89*, 179.
(291) Mueller, E.; Von Schütz, J. U.; Wolf, H. C. *Mol. Cryst. Liq. Cryst.* **1983**, *93*, 407.

(292) Dobbert, O.; Prisner, T.; Dinse, K. P.; Schweitzer, D.; Keller, H. J. *Solid State Commun.* **1987**, *61*, 499.
(293) Ruf, R.; Lossau, H.; Dormann, E. *Synth. Met.* **1995**, *70*, 1215.
(294) Kaplan, N.; Dormann, E.; Ruf, R.; Coy, A.; Callaghan, P. T. *Phys. Rev. B* **1995**, *52*, 16385.
(295) Wokrina, T.; Dormann, E.; Kaplan, N. *Phys. Rev. B* **1996**, *54*, 10492.
(296) Dormann, E.; Wokrina, T. *Synth. Met.* **1997**, *86*, 2183.
(297) Pongs, B.; Dormann, E. *Phys. Rev. B* **2002**, *65*, 144451−1.
(298) Pongs, B.; Wokrina, T.; Matejcek, S.; Buschhaus, C.; Dormann, E. *Euro. Phys. J. B* **2002**, *28*, 289.
(299) Kaiser, A.; Wokrina, T.; Pongs, B.; Dormann, E. *J. Phys.: Condens. Matter* **2003**, *15*, 7085.
(300) Tashma, T.; Feintuch, A.; Grayevsky, A.; Gmeiner, J.; Gabay, A.; Dormann, E.; Kaplan, N. *Synth. Met.* **2003**, *132*, 161.
(301) Sigg, J.; Prisner, Th.; Dinse, K. P.; Brunner, H.; Schweitzer, D.; Hausser, K. H. *Phys. Rev. B* **1983**, *27*, 5366.
(302) Dormann, E.; Sachs, G.; Stöcklein, W.; Bail, B.; Schwoerer, M. *Appl. Phys. A* **1983**, *30*, 227.
(303) Dormann, E.; Denninger, G.; Sachs, G.; Stöcklein, W.; Schwoerer, M. *J. Magn. Magn. Mater.* **1986**, *54*, 1315.
(304) Sanquer, M.; Bouffard, S.; Forró, L. *Mol. Cryst. Liq. Cryst.* **1985**, *120*, 183.
(305) Delrieu, J. M.; Beguin, M.; Sanquer, M. *Synth. Met.* **1987**, *19*, 361.
(306) Mori, T.; Inokuchi, H.; Kobayashi, A.; Kato, R.; Kobayashi, H. *Phys. Rev. B* **1988**, *38*, 5913.
(307) Tomic, S.; Jérome, D.; Aumüller, A.; Erk, P.; Hünig, S.; Von Schütz, J. U. *J. Phys. C* **1988**, *21*, 1203.
(308) Von Schütz, J. U.; Bair, M.; Gross, H. J.; Langohr, U.; Werner, H. P.; Wolf, H. C.; Schmeiber, D.; Graf, K.; Göpel, W.; Erk, P.; Meixner, H.; Hünig, S. *Synth. Met.* **1988**, *27*, B249.
(309) Werner, H. P.; Von Schütz, J. U.; Wolf, H. C.; Kremer, R.; Gehrke, M.; Aumüller, A.; Erk, P.; Hünig, S. *Solid State Commun.* **1988**, *65*, 809.
(310) Langohr, U.; Von Schütz, J. U.; Wolf, H. C.; Meixner, H.; Hünig, S. *Synth. Met.* **1991**, *41*−*43*, 1855.
(311) Von Schütz, J. U.; Bauer, D.; Hünig, S.; Sinzger, K.; Wolf, H. C. *J. Phys. Chem.* **1993**, *97*, 12030.
(312) Bauer, D.; Maier, B.; Schweitzer, D.; Von Schütz, J. U. *Synth. Met.* **1995**, *71*, 1887.
(313) Tega, T.; Nishio, Y.; Kajita, K.; Kato, R.; Kobayashi, H. *Synth. Met.* **1995**, *71*, 1953.
(314) Von Schütz, J. U.; Bauer, D.; Wachtel, H.; Wolf, H. C. *Synth. Met.* **1995**, *71*, 2089.
(315) Von Schütz, J. U.; Bair, M.; Bauer, D.; Bietsch, W.; Krebs, M.; Wolf, H. C.; Hünig, S.; Sinzger, K. *Synth. Met.* **1993**, *55*−*57*, 1809.
(316) Takahashi, T.; Kanoda, K.; Tamura, T.; Hiraki, K.; Ikeda, K.; Kato, R.; Kobayashi, H.; Kobayashi, A. *Synth. Met.* **1993**, *55*−*57*, 2281.
(317) Tamura, M.; Sawa, H.; Kashimura, Y.; Aonuma, S.; Kato, R.; Kinoshita, M.; Kobayashi, H. *Synth. Met.* **1995**, *70*, 1081.
(318) Krebs, M.; Von Schütz, J. U.; Wolf, H. C. *Synth. Met.* **1991**, *41*−*43*, 1851.
(319) Krebs, M.; Bietsch, W.; Von Schütz, J. U.; Wolf, H. C. *Synth. Met.* **1994**, *64*, 187. Bietsch, W.; Von Schütz, J. U.; Wolf, H. C. *Appl. Magn. Reson.* **1994**, *7*, 271.
(320) Hiraki, K.; Kanoda, K. *Synth. Met.* **1997**, *86*, 2111.
(321) Sakurai, T.; Ohta, H.; Okubo, S.; Kanoda, K.; Hiraki, K. *Synth. Met.* **2001**, *120*, 851.
(322) Hiraki, K.; Kanoda, K. *Phys. Rev. B* **1996**, *54*, R17276.
(323) Hiraoka, M.; Sakamoto, H.; Mizoguchi, K.; Kato, R. *Phys. Rev. B* **2002**, *65*, 174413; *Synth. Met.* **2003**, *133*−*134*, 417; *Synth. Met.* **2003**, *135*−*136*, 649; *Physica B* **2003**, *329*−*333*, 1201.
(324) Hiraoka, M.; Sakamoto, H.; Mizoguchi, K.; Kato, T.; Kato, R. *Phys. Rev. Lett.* **2003**, *91*, 056604−1.
(325) Nakagawa, N.; Akioka, K.; Ohta, H.; Okubo, S.; Kanoda, K.; Hiraki, K. *Synth. Met.* **1999**, *103*, 1894.
(326) Sakurai, T.; Nakagawa, N.; Okubo, S.; Ohta, H.; Kanoda, K.; Hiraki, K. *J. Phys. Soc. Jpn.* **2001**, *70*, 1794.
(327) Sakurai, T.; Saruhashi, M.; Inagaki, Y.; Okubo, S.; Ohta, H.; Hiraki, K.; Uwatoko, Y. *Synth. Met.* **2003**, *135*−*136*, 523.
(328) Hiraki, K.; Kanoda, K. *Phys. Rev. Lett.* **1998**, *80*, 4737.
(329) Hiraki, K.; Suzuki, S.; Takahashi, T. *Synth. Met.* **2003**, *133*−*134*, 419.
(330) Heuzé, K.; Fourmigué, M.; Batail, P.; Coulon, C.; Clérac, R.; Canadell, E.; Auban-Senzier, P.; Ravy, S.; Jérome, D. *Adv. Mater.* **2003**, *15*, 1251.
(331) Buntar, V.; Sauerzopf, F. M.; Weber, H. W. *Aust. J. Phys.* **1997**, *50*, 329.
(332) Konarev, D. V.; Lyubovskaya, R. N. *Russ. Chem. Rev.* **1999**, *68*, 19.
(333) Reed, C. A.; Bolskar, R. D. *Chem. Rev.* **2000**, *100*, 1075.
(334) Pénicaud, A. *Fullerene Sci. Technol.* **1998**, *6*, 731.
(335) Allemand, P. M.; Khemani, K. C.; Koch, A.; Wudl, F.; Holczer, K.; Donovan, S.; Grüner, G.; Thompson, J. D. *Science* **1991**, *253*, 301.
(336) Mrzel, A.; Omerzu, A.; Umek, P.; Mihailovic, D.; Zaglicic, Z.; Trontelj, Z. *Chem. Phys. Lett.* **1998**, *298*, 329.
(337) Mrzel, A.; Umek, P.; Cevc, P.; Omerzu, A.; Mihailovic, D. *Carbon* **1998**, *36*, 603.
(338) Tanaka, K.; Zakhidov, A. A.; Yoshizawa, K.; Okahara, K.; Yamabe, T.; Yakushi, K.; Kikuchi, K.; Suzuki, S.; Ikemoto, I.; Achiba, Y. *Phys. Lett. A* **1992**, *164*, 221.
(339) Seshadri, R.; Rastogi, A.; Bhat, S. V.; Ramasesha, S.; Rao, C. N. R. *Solid State Commun.* **1993**, *85*, 971.
(340) Tanaka, K.; Zakhidov, A. A.; Yoshizawa, K.; Okahara, K.; Yamabe, T.; Yakushi, K.; Kikuchi, K.; Suzuki, S.; Ikemoto, I.; Achiba, Y. *Phys. Rev. B* **1993**, *47*, 7554.
(341) Mihailovic, D.; Lutar, K.; Hassanien, A.; Cevc, P.; Venturini, P. *Solid State Commun.* **1994**, *89*, 209.
(342) Tanaka, K.; Sato, T.; Yamabe, T.; Yoshizawa, K.; Okahara, K.; Zakhidov, A. A. *Phys. Rev. B* **1995**, *51*, 990.
(343) Gotschy, B. *Phys. Rev. B* **1995**, *52*, 7378.
(344) Arcon, D.; Blinc, R.; Cevc, P.; Jesenko, T. *Europhys. Lett.* **1996**, *35*, 469.
(345) Maniero, A. L.; Pasimeni, L.; Brunel, L. C.; Pardi, L. A.; Cao, G.; Guertin, R. P. *Solid State Commun.* **1998**, *106*, 727.
(346) Blinc, R.; Pokhodnya, K.; Cevc, P.; Arcon, D.; Omerzu, A.; Mihailovic, D.; Venturini, P.; Golic, L.; Trontelj, Z.; Luznik, J.; Jeglicic, Z.; Pirnat, J. *Phys. Rev. Lett.* **1996**, *76*, 523.
(347) Mihailovic, D.; Pokhodnya, K.; Omerzu, A.; Venturini, P.; Blinc, R.; Cevc, P.; Pratt, F.; Chow, K. H. *Synth. Met.* **1996**, *77*, 281.
(348) Mrzel, A.; Cevc, P.; Omerzu, A.; Mihailovic, D. *Phys. Rev. B* **1996**, *53*, R2922.
(349) Blinc, R.; Arcon, D.; Cevc, P.; Mihailovic, D.; Omerzu, A. *Appl. Magn. Reson.* **1996**, *11*, 203.
(350) Schilder, A.; Bietsch, W.; Schwoerer, M. *New J. Phys.* **1999**, *1*, 51.
(351) Arcon, D.; Blinc, R.; Cevc, P.; Omerzu, A. *Phys. Rev. B* **1999**, *59*, 5247.
(352) Arcon, D.; Blinc, R.; Mihailovic, D.; Omerzu, A.; Cevc, P. *Europhys. Lett.* **1999**, *46*, 667.
(353) Kambe, T.; Nogami, Y.; Oshima, K. *Phys. Rev. B* **2000**, *61*, R862.
(354) Mizoguchi, K.; Machino, M.; Sakamoto, H.; Tokumoto, M.; Kawamoto, T.; Omerzu, A.; Mihailovic, D. *Synth. Met.* **2001**, *121*, 1778. Mizoguchi, K.; Machino, M.; Sakamoto, H.; Kawamoto, T.; Tokumoto, M.; Omerzu, A.; Mihailovic, D. *Phys. Rev. B* **2001**, *63*, 140417−1.
(355) Mizoguchi, K.; Kobayashi, S.; Machino, M.; Sakamoto, H.; Kawamoto, T.; Tokumoto, M.; Kasaka, M.; Tanigaki, K.; Omerzu, A.; Mihailovic, D. *Synth. Met.* **2003**, *133*−*134*, 695.
(356) Kambe, T.; Garaj, S.; Forró, L.; Fujiwara, M.; Oshima, K. *Synth. Met.* **2003**, *133*−*134*, 697.
(357) Garaj, S.; Kambe, T.; Forró, L.; Sienkiewicz, A.; Fujiwara, M.; Oshima, K. *Phys. Rev. B* **2003**, *68*, 144430−1.
(358) Bensebaa, F.; Kevan, L. *J. Phys. Chem.* **1993**, *97*, 5717.
(359) Stankowski, J.; Kevan, L.; Czyzak, B.; Andrzejewski, B. *J. Phys. Chem.* **1993**, *97*, 10430.
(360) Kempinski, W.; Stankowski, J. *Solid State Commun.* **1996**, *97*, 1079.
(361) Kempinski, W.; Scharff, P.; Stankowski, J.; Piekara-Sady, L.; Trybula, Z. *Physica C* **1997**, *274*, 232.
(362) Kempinski, W. *Solid State Commun.* **1999**, *111*, 39.
(363) Kempinski, W.; Piekara-Sady, L.; Katz, E. A.; Shames, A. I.; Shtutina, S. *Solid State Commun.* **2000**, *114*, 173.
(364) Pénicaud, A.; Carreon, O. Y.; Perrier, A.; Watkin, D. J.; Coulon, C. *J. Mater. Chem.* **2002**, *12*, 913.
(365) Stankowski, J.; Byszewski, P.; Kempinski, W.; Trybula, Z.; Zuk, T. *Phys. Stat. Sol. B* **1993**, *178*, 221.
(366) Hwang, Y. L.; Yang, C. C.; Hwang, K. C. *J. Phys. Chem. A* **1997**, *101*, 7971.
(367) Paul, P.; Kim, K.-C.; Sun, D.; Boyd, P. D. W.; Reed, C. A. *J. Am. Chem. Soc.* **2002**, *124*, 4394.
(368) Bensebaa, F.; Xiang, B.; Kevan, L. *J. Phys. Chem.* **1992**, *96*, 10258.
(369) Wong, W. H.; Hanson, M. E.; Clark, W. G.; Grüner, G.; Thompson, J. D.; Whetten, R. L.; Huang, S.-M.; Kaner, R. B.; Diederich, F.; Petit, P.; André, J.-J.; Holczer, K. *Europhys. Lett.* **1992**, *18*, 79.
(370) Jánossy, A.; Chauvet, O.; Pekker, S.; Cooper, J. R.; Forró, L. *Phys. Rev. Lett.* **1993**, *71*, 1091. Kosaka, M.; Tanigaki, K.; Hirosawa, I. *Phys. Rev. Lett.* **1994**, *72*, 3130. Jánossy, A.; Chauvet, O.; Pekker, S.; Cooper, J. R.; Forró, L.; Tegze, M.; Faigel, G. *Phys. Rev. Lett.* **1994**, *72*, 3131.
(371) Chauvet, O.; Forró, L.; Cooper, J. R.; Mihály, G.; Jánossy, A. *Synth. Met.* **1995**, *70*, 1333.
(372) Tanigaki, K.; Kosaka, M.; Manako, T.; Kubo, Y.; Hirozawa, I.; Uchida, K.; Prassides, K. *Chem. Phys. Lett.* **1995**, *240*, 627.
(373) Petit, P.; Robert, J.; Yildirim, T.; Fischer, J. E. *Phys. Rev. B* **1996**, *54*, R3764.
(374) Nemes, N. M.; Fischer, J. E.; Baumgartner, G.; Forró, L.; Fehér, T.; Oszlányi, G.; Simon, F.; Jánossy, A. *Phys. Rev. B* **2000**, *61*, 7118.
(375) Adrian, F. J. *Phys. Rev. B* **1996**, *53*, 2206.

(376) Isawa, Y.; Shimoda, H.; Palstra, T. T. M.; Maniwa, Y.; Zhou, O.; Mitani, T. *Phys. Rev. B* **1996**, *53*, R8836.
(377) Takenobu, T.; Muro, T.; Isawa, Y.; Mitani, T. *Phys. Rev. Lett.* **2000**, *85*, 381.
(378) Iwasa, Y.; Tokenobu, T.; Kitano, H.; Maeda, A. *Physica C* **2003**, *388*−*389*, 615.
(379) Prassides, K.; Tanigaki, K.; Iwasa, Y. *Physica C* **1997**, *282*−*287*, 307.
(380) Arcon, D.; Prassides, K.; Margadonna, S.; Maniero, A.-L.; Brunel, L. C.; Tanigaki, K. *Phys. Rev. B* **1999**, *60*, 3856.
(381) Arcon, D.; Prassides, K.; Maniero, A.-L.; Brunel, L. C. *Phys. Rev. Lett.* **2000**, *84*, 562. Simon, F.; Garaj, S.; Forró, L. *Phys. Rev. Lett.* **2001**, *87*, 129703−1. Arcon, D.; Prassides, K.; Maniero, A.-L.; Brunel, L. C. *Phys. Rev. Lett.* **2001**, *87*, 129704−1.
(382) Kubozono, Y.; Takabayashi, Y.; Fujiki, S.; Kashino, S.; Kambe, T.; Iwasa, T.; Emura, S. *Phys. Rev. B* **1999**, *59*, 15062.
(383) Petit, P.; Robert, J.; Fisher, J. E. *Phys. Rev. B* **1995**, *51*, 11924.
(384) Kosaka, M.; Tanigaki, K.; Tanaka, T.; Atake, T.; Lappas, A.; Prassides, K. *Phys. Rev. B* **1995**, *51*, 12018.
(385) Oszlányi, G.; Bortel, G.; Faigel, G.; Tegze, M.; Granasy, L.; Pekker, S.; Stephens, P. W.; Bendele, G.; Dinnebier, R.; Mihály, G.; Jánossy, A.; Chauvet, O.; Forró, L. *Phys. Rev. B* **1995**, *51*, 12228.
(386) Robert, J.; Petit, P.; Fisher, J. E. *Physica C* **1996**, *262*, 27. Petit, P.; Robert, J.; Fisher, J. E. *Appl. Phys. A* **1997**, *64*, 283.
(387) Bommeli, F.; Degiorgi, L.; Wachter, P.; Legeza, O.; Jánossy, A.; Oszlányi, G.; Chauvet, O.; Forró, L. *Phys. Rev. B* **1995**, *51*, 14794.
(388) Pekker, S.; Jánossy, A.; Mihály, G.; Chauvet, O.; Carrard, M.; Forró, L. *Science* **1994**, *265*, 1077.
(389) Faigel, G.; Bortel, G.; Tegze, M.; Granasy, L.; Pekker, S.; Oszlányi, G.; Chauvet, O.; Baumgartner, G.; Forró, L.; Stephens, P. W.; Mihály, G.; Jánossy, A. *Phys. Rev. B* **1995**, *52*, 3199.
(390) Kinoshita, N.; Grigoryan, L. S.; Kinoshita, T.; Tokumoto, M. *Solid State Commun.* **1997**, *101*, 871.
(391) Robert, J.; Petit, P.; André, J.-J.; Fischer, J. E. *Solid State Commun.* **1995**, *96*, 143.
(392) Atsarkin, V. A.; Demidov, V. V.; Vasneva, G. A. *Phys. Rev. B* **1997**, *56*, 9448.
(393) Sakamoto, H.; Kobayashi, S.; Mizoguchi, K.; Kosaka, M.; Tanigaki, K. *Phys. Rev. B* **2000**, *62*, R7691; *Synth. Met.* **2001**, *121*, 1103.
(394) Coulon, C.; Pénicaud, A.; Clérac, R.; Moret, R.; Launois, P.; Hone, J. *Phys. Rev. Lett.* **2001**, *86*, 4346.
(395) Kittel, C. *Introduction to Solid State Physics*; Wiley and Sons: New York, 1996.
(396) Chaikin, P. M.; Lubensky, T. C. *Principles of Condensed Matter Physics*; Cambridge University Press: New York, 1995.
(397) Kittel, C. *Phys. Rev.* **1948**, *73*, 155.
(398) Note that the γ is traditional notation for the third direction cosine of **M**. It should not be confused with the magnetogyric ratio γ_e previously introduced in eq 2.
(399) Nagamiya, T.; Yosida, K.; Kubo, R. *Adv. Phys.* **1955**, *4*, 1.
(400) Nagamiya, T. *Prog. Theor. Phys.* **1954**, *11*, 309.
(401) De Groot, H. J. M.; De Jongh, L. J. *Physica B* **1986**, *141*, 1.
(402) Keffer, F.; Kittel, C. *Phys. Rev.* **1952**, *85*, 329.
(403) Foner, S. In *Magnetism*; Rado, G. T., Suhl, H., Eds.; Academic Press: New York, 1963; Vol. 1, p 384.
(404) Scott, J. C. *J. Appl. Phys.* **1982**, *53*, 1845.
(405) Roger, M.; Delrieu, J. M.; Wope-Mbougue, E. *Phys. Rev. B* **1986**, *34*, 4952. Delrieu, J. M.; Roger, M.; Coulon, C.; Laversanne, R.; Dupart, E. *Synth. Met.* **1988**, *27*, B35.
(406) Dzyaloshinskii, I. *J. Phys. Chem. Solids* **1958**, *4*, 241.
(407) Moriya, T. *Phys. Rev.* **1960**, *120*, 91.
(408) Pincus, P. *Phys. Rev. Lett.* **1960**, *5*, 13.
(409) Cinader, G. *Phys. Rev.* **1967**, *155*, 453.
(410) Vasilev, A. N.; Marchenko, V. I.; Smirnov, A. I.; Sosin, S. S.; Yamada, H.; Ueda, Y. *Phys. Rev. B* **2001**, *64*, 174403−1.
(411) Rawson, J. M.; Alberola, A.; El-Mkami, H.; Smith, G. M. *J. Phys. Chem. Solids* **2004**, *65*, 727.
(412) Yamauchi, J. *Chem. Lett.* **1974**, *9*, 1031.
(413) Yamauchi, J. *J. Chem. Phys.* **1977**, *67*, 2850.
(414) Yamauchi, J. *Phys. Lett. A* **1979**, *70*, 238.
(415) Scott, J. C.; Pedersen, H. J.; Bechgaard, K. *Phys. Rev. Lett.* **1980**, *45*, 2125.
(416) Torrance, J. B.; Pedersen, H. J.; Bechgaard, K. *Phys. Rev. Lett.* **1982**, *49*, 881.
(417) Walsh, W. M., Jr.; Wudl, F., Jr.; Aharon-Shalom, E.; Rupp, L. W., Jr.; Vandenberg, J. M.; Andres, K.; Torrance, J. B. *Phys. Rev. Lett.* **1982**, *49*, 885. $(TMTSF)_2ClO_4$ salt has in fact a SDW ground state at ambient pressure when the samples are cooled rapidly. Superconductivity is only observed in the "relaxed state" when anions are ordered at low temperature.
(418) Walsh, W. M. J., Jr. *Magn. Magn. Mater.* **1983**, *31*−*34*, 1273.
(419) Parkin, S. S. P.; Scott, J. C.; Torrance, J. B.; Engler, E. M. *Phys. Rev. B* **1982**, *26*, 6319. Parkin, S. S. P.; Scott, J. C.; Torrance, J. B.; Engler, E. M., *J. Phys. Colloq. C3* **1983**, *44*, 1111.
(420) Coulon, C.; Scott, J. C.; Laversanne, R. *Mol. Cryst. Liq. Cryst.* **1985**, *119*, 307.
(421) Coulon, C.; Scott, J. C.; Laversanne, R. *Phys. Rev. B* **1986**, *33*, 6235.
(422) Coulon, C.; Laversanne, R.; Amiell, J. *Physica B* **1986**, *143*, 425.
(423) Coulon, C.; Laversanne, R. In *Low Dimensional Conductors and Superconductors*; Jérome, D., Caron, L. G., Eds.; NATO ASI Series B; Plenum Press: New York, 1987; Vol. 155, p 135.
(424) Vaca, P.; Coulon, C.; Granier, T.; Gallois, B.; Ducasse, L.; Fabre, J. M.; Gouasmia, A. *Synth. Met.* **1988**, *27*, B457.
(425) Dumm, M.; Loidl, A.; Alavi, B.; Starkey, K. P.; Montgomery, L. K.; Dressel, M. *Phys. Rev. B* **2000**, *62*, 6512.
(426) For a review on dynamics of spin-density waves, see: Grüner, G. *Rev. Mod. Phys.* **1994**, *66*, 1.
(427) Takahashi, T.; Maniwa, Y.; Kawamura, H.; Saito, G. *J. Phys. Soc. Jpn.* **1986**, *55*, 1364.
(428) Caron, L. G.; Bourbonnais, C. *J. Phys. Colloq.* **1988**, *C8*, 1419.
(429) Nakamura, T.; Kinami, R.; Takahashi, T.; Saito, G. *Synth. Met.* **1997**, *86*, 2053.
(430) Barthel, E.; Quirion, G.; Wzietek, P.; Jérome, D.; Christensen, J. B.; Jorgensen, M.; Bechgaard, K. *Europhys. Lett.* **1993**, *21*, 87.
(431) Nakamura, T.; Nobutoki, T.; Kobayashi, Y.; Takahashi, T.; Saito, G. *Synth. Met.* **1995**, *70*, 1293.
(432) Klemme, B. J.; Brown, E. E.; Wzietek, P.; Jérome, D.; Fabre, J. M. *J. Phys. I France* **1996**, *6*, 1745. Hasano, M.; Nakamura, T.; Takahashi, T.; Saito, G. *Synth. Met.* **1999**, *103*, 2195.
(433) Welp, U.; Fleshler, S.; Kwok, W. K.; Crabtree, G. W.; Carlson, K. D.; Wang, H. H.; Geiser, U.; Williams, J. M.; Hitsman, V. M. *Phys. Rev. Lett.* **1992**, *69*, 840.
(434) Miyagawa, K.; Kawamoto, A.; Nakazawa, Y.; Kanoda, K. *Phys. Rev. Lett.* **1995**, *75*, 1174.
(435) Ohta, H.; Kimura, S.; Yamamoto, Y.; Azuma, J.; Akioka, K.; Motokawa, M.; Kanoda, K. *Synth. Met.* **1997**, *86*, 2079.
(436) Ohta, H.; Nakagawa, N.; Akioka, K.; Nakashima, Y.; Okubo, S.; Kanoda, K.; Kitamura, N. *Synth. Met.* **1999**, *103*, 1914.
(437) Ito, H.; Kondo, T.; Sasaki, H.; Saito, G.; Ishiguro, T. *Synth. Met.* **1999**, *103*, 1818.
(438) Ito, H.; Ishiguro, T.; Kondo, T.; Saito, G. *Phys. Rev. B* **2000**, *61*, 3243.
(439) Ito, H.; Saito, G.; Ishiguro, T. *J. Phys. Chem. Solids* **2001**, *62*, 109.
(440) Bele, P.; Brunner, H.; Schweitzer, D.; Keller, H. J. *Synth. Met.* **1997**, *89*, 231.
(441) Kremer, R. H.; Kanellakopulos, B.; Bele, P.; Brunner, H.; Neugebauer, F. A. *Chem. Phys. Lett.* **1994**, *230*, 255.
(442) Demishev, S. V.; Semeno, A. V.; Sluchanko, N. E.; Samarin, N. A.; Voskoboinikov, I. B.; Glushkov, V. V.; Singleton, J.; Blundell, S. J.; Hill, S. O.; Hayes, W.; Kartsovnik, M. V.; Kovalev, A. E.; Kurmoo, M.; Day, P.; Kushch, N. D. *Phys. Rev. B* **1996**, *53*, 12794.
(443) Kawamata, S.; Ohsono, K.; Ishida, T.; Sasaki, T. *Synth. Met.* **2003**, *135*−*136*, 559.
(444) Akioka, K.; Ohta, H.; Okubo, S.; Miyagawa, K.; Kanoda, K. *J. Magn. Magn. Mater.* **1998**, *177*−*181*, 746.
(445) Batail, P.; Livage, C.; Parkin, S. S. P.; Coulon, C.; Martin, J. D.; Canadell, E. *Angew. Chem., Int. Ed. Engl.* **1991**, *30*, 1498.
(446) Coulon, C.; Livage, C.; Gonzalvez, L.; Boubekeur, K.; Batail, P. *J. Phys. I France* **1993**, *3*, 1153.
(447) Nakamura, T.; Hiraki, K.; Kobayashi, Y.; Takahashi, T.; Aonuma, S.; Sawa, H.; Kato, R.; Kobayashi, H. *Physica B* **1994**, *194*−*196*, 231. Hiraki, K.; Kobayashi, Y.; Nakamura, T.; Takahashi, T.; Aonuma, S.; Sawa, H.; Kato, R.; Kobayashi, H. *Synth. Met.* **1995**, *70*, 1091.
(448) Brossard, L.; Clérac, R.; Coulon, C.; Tokumoto, M.; Ziman, T.; Petrov, D. K.; Lauklin, V. N.; Naughton, M. J.; Audouard, A.; Goze, F.; Kobayashi, A.; Kobayashi, H.; Cassoux, P. *Eur. Phys. J. B* **1998**, *1*, 439.
(449) Suzuki, T.; Matsui, H.; Tsuchiya, H.; Negishi, E.; Koyama, K.; Toyota, N. *Synth. Met.* **2003**, *135*−*136*, 567; *Phys. Rev. B* **2003**, *67*, 020408−1.
(450) Okubo, S.; Kirita, K.; Inagaki, Y.; Ohta, H.; Enomoto, K.; Miyazaki, A.; Enoki, T. *Synth. Met.* **2003**, *135*−*136*, 589.
(451) Fourmigué, M.; Coulon, C. *Adv. Mater.* **1994**, *6*, 948.
(452) (a) Clérac, R.; Fourmigué, M.; Gaultier, J.; Barrans, Y.; Albouy, P. A.; Coulon, C. *Eur. Phys. J. B* **1999**, *9*, 431. (b) Clérac, R. Ph.D. Thesis, Bordeaux, France, 1997.
(453) Clérac, R.; Fourmigué, M.; Gaultier, J.; Barrans, Y.; Albouy, P. A.; Coulon, C. *Eur. Phys. J. B* **1999**, *9*, 455.
(454) Cevc, P.; Blinc, R.; Erzen, V.; Arcon, D.; Zalar, B.; Mihailovic, D.; Venturini, P. *Solid State Commun.* **1994**, *90*, 543.
(455) Bele, P.; Brunner, H.; Schilder, A.; Gmeiner, J.; Schwoerer, M. *Adv. Mater.* **1997**, *9*, 907.
(456) Arcon, D.; Cevc, P.; Omerzu, A.; Blinc, R. *Phys. Rev. Lett.* **1998**, *80*, 1529.
(457) Arcon, D.; Blinc, R.; Cevc, P.; Chouteau, G.; Barra, A. L. *Phys. Rev. B* **1997**, *56*, 10786.
(458) Blinc, R.; Cevc, P.; Arcon, D.; Omerzu, A.; Mehring, M.; Knorr, S.; Grupp, A.; Barra, A. L.; Chouteau, G. *Phys. Rev. B* **1998**, *58*, 14416.

(459) Simon, F.; Jánossy, A.; Muranyi, F.; Fehér, T.; Shimoda, H.; Isawa, Y.; Forró, L. *Phys. Rev. B* **2000**, *61*, R3826.
(460) Jánossy, A.; Nemes, N.; Fehér, T.; Oszlányi, G.; Baumgartner, G.; Forró, L. *Phys. Rev. Lett.* **1997**, *79*, 2718.
(461) Brouet, V.; Alloul, H.; Yoshinari, Y.; Forró, L. *Phys. Rev. Lett.* **1996**, *76*, 3638.
(462) Simovic, B.; Jérome, D.; Rachdi, F.; Baumgartner, G.; Forró, L. *Phys. Rev. Lett.* **1999**, *82*, 2298.
(463) Simovic, B.; Jérome, D.; Forró, L. *Phys. Rev. B* **2001**, *63*, 125410−1.
(464) Bennati, M.; Griffin, R. G.; Knorr, S.; Grupp, A.; Mehring, M. *Phys. Rev. B* **1998**, *58*, 15603.
(465) Coulon, C.; Duval, J.; Lavergne, C.; Barra, A. L.; Pénicaud, A. *J. Phys. IV France* **2000**, *10*, Pr3−205.
(466) Saito, T.; Akita, Y.; Tanaka, K. *Phys. Rev. B* **2000**, *61*, 16901.
(467) Mizoguchi, K.; Sasano, A.; Sakamoto, H.; Kosaka, M.; Tanigaki, K.; Tanaka, T.; Atake, T. *Synth. Met.* **1999**, *103*, 2395.
(468) Aoi, K.; Swihart, J. C. *Phys. Rev. B* **1970**, *2*, 2555.
(469) Maki, K. *Phys. Rev. B* **1973**, *8*, 191.
(470) Yafet, Y. *Phys. Lett. A* **1983**, *98*, 287.
(471) Blazey, K. W. In *Earlier and Recent Aspects of Superconductivity*; Bednorz, J. G., Muller, K. A., Eds.; Springer Series in Solid-State Sciences; Springer: Berlin, 1990; Vol. 90, p 262.
(472) Khairullin, I. I.; Khabibullaev, P. K.; Sokolov, V. Yu.; Zakhidov, A. A. *Tr. J. Phys.* **1999**, *23*, 1107.
(473) Blazey, K. W.; Muller, K. A.; Bednorz, J. G.; Berlinger, W.; Amoretti, G.; Buluggiu, E.; Vera, A.; Matacotta, F. C. *Phys. Rev. B* **1987**, *36*, 7241.
(474) Khachaturyan, K.; Weber, E. R.; Tejedor, P.; Stacy, A. M.; Portis, A. M. *Phys. Rev. B* **1987**, *36*, 8309.
(475) Pakulis, E. J.; Osada, T. *Phys. Rev. B* **1988**, *37*, 5940.
(476) Durny, R.; Hautala, J.; Ducharme, S.; Lee, B.; Symko, O. G.; Taylor, P. C.; Zheng, D. J. *Phys. Rev. B* **1987**, *36*, 2361.
(477) Blazey, K. W.; Portis, A. M.; Muller, K. A.; Holtzberg, F. H. *Europhys. Lett.* **1988**, *6*, 457.
(478) Delrieu, J. M.; Sullivan, N. S.; Bechgaard, K. *J. Phys. Colloq. C3* **1983**, *44*, 1033.
(479) Haddon, R. C.; Glarum, S. H.; Chichester, S. V.; Ramirez, A. P.; Zimmerman, N. M. *Phys. Rev. B* **1991**, *43*, 2642.
(480) Bohandy, J.; Kim, B. F.; Adrian, F. J.; Moorjani, K.; D'Arcangelis, S.; Cowan, D. O. *Phys. Rev. B* **1991**, *43*, 3724.
(481) Moldenhauer, J.; Wachtel, H.; Schweitzer, D.; Gompf, B.; Eisenmenger, W.; Bele, P.; Brunner, H.; Keller, H. J. *Synth. Met.* **1995**, *70*, 791.
(482) Bele, P.; Brunner, H.; Schweitzer, D.; Keller, H. J. *Solid State Commun.* **1994**, *92*, 189.
(483) Zakhidov, A. A.; Ugawa, A.; Yakushi, K.; Imaeda, K.; Inokuchi, H.; Khairullin, I. I.; Khabibullaev, P. K. *Physica C* **1991**, *185−189*, 2669.
(484) Rosseinsky, M. J.; Ramirez, A. P.; Glarum, S. H.; Murphy, D. W.; Haddon, R. C.; Hebard, A. F.; Palstra, T. T. M.; Kortan, A. R.; Zaburak, S. M.; Makhija, A. V. *Phys. Rev. Lett.* **1991**, *66*, 2830.
(485) Hebard, A. F.; Rosseinsky, M. J.; Haddon, R. C.; Murphy, D. W.; Glarum, S. H.; Palstra, T. T. M.; Ramirez, A. P.; Kortan, A. R. *Nature* **1991**, *350*, 600.
(486) (a) Bensebaa, F.; Xiang, B.; Kevan, L. *J. Phys. Chem.* **1992**, *96*, 6118. (b) Bensabaa, F.; Kevan, L. *J. Phys. Chem.* **1993**, *97*, 5717.
(487) Byszewski, P.; Stankowski, J.; Trybula, Z.; Kempinski, W.; Zuk, T. *J. Mol. Struct.* **1992**, *269*, 175.
(488) Imaeda, K.; Khairullin, I. I.; Yakushi, K.; Nagata, M.; Mizutani, N.; Kitagawa, H.; Inokuchi, H. *Solid State Commun.* **1993**, *87*, 375.
(489) Khairullin, I. I.; Imaeda, K.; Yakushi, K.; Inokuchi, H. *Physica C* **1994**, *231*, 26; *Synth. Met.* **1995**, *70*, 1369.
(490) Yamasaki, N.; Araki, H.; Zakhidov, A. A.; Mizobuchi, H.; Yakushi, K.; Yoshino, K. *Physica C* **1996**, *259*, 265.
(491) Yoshino, K.; Zakhidov, A. A.; Kajii, H.; Araki, H.; Tada, K.; Noguchi, T.; Ohnishi, T.; Yakushi, K. *Physica C* **1996**, *264*, 161.
(492) Kajii, H.; Araki, H.; Zakhidov, A. A.; Yakushi, K.; Yoshino, K. *Synth. Met.* **1997**, *86*, 2351.
(493) Zakhidov, A. A.; Ugawa, A.; Imaeda, K.; Yakushi, K.; Inokuchi, H. *Solid State Commun.* **1991**, *79*, 939.
(494) Zakhidov, A. A.; Imaeda, K.; Ugawa, A.; Yakushi, K.; Inokuchi, H.; Iqbal, Z.; Baughman, R. H.; Ramakrishna, B. I.; Achiba, Y. *Physica C* **1991**, *185−189*, 411.
(495) Zakhidov, A. A.; Yakushi, K.; Imaeda, K.; Inokuchi, H.; Kikuchi, K.; Suzuki, S.; Ikemoto, I.; Achiba, Y. *Mol. Cryt. Liq. Cryst.* **1992**, *218*, 299.
(496) Sugawara, K.; Ohya, N.; Arai, N.; Ichimura, S.; Yamamoto, K.; Hirose, H. *Modern Phys. Lett. B* **1999**, *13*, 59.
(497) Zakhidov, A. A.; Khairullin, I. I.; Khabibullaev, P. K.; Sokolov, V. Yu.; Imaeda, K.; Yakushi, K.; Inokuchi, H.; Achiba, Y. *Synth. Met.* **1993**, *55−57*, 2967.
(498) Zakhidov, A. A.; Imaeda, K.; Petty, D. M.; Yakushi, K.; Inokuchi, H.; Kikuchi, K.; Ikemoto, I.; Suzuki, S.; Achiba, Y. *Phys. Lett. A* **1992**, *164*, 355.
(499) Glarum, S. H.; Duclos, S. J.; Haddon, R. C. *J. Am. Chem. Soc.* **1992**, *114*, 1996.
(500) Metzger, R. M.; Wang, P.; Wu, X.-L.; Tormos, G. V.; Lorcy, D.; Shcherbakova, I.; Lakshmikantham, M. V.; Cava, M. P. *Synth. Met.* **1995**, *70*, 1435.
(501) Rakvin, B.; Pozek, M.; Dulcic, A. *Solid State Commun.* **1989**, *72*, 199.
(502) Shvachko, Yu. N.; Wang, H.-H.; Williams, J. M. *Synth. Met.* **2003**, *137*, 1325.

CR030639W